DIEGO GÖTZ (CEA SACLAY-IRFU/DÉPARTEMENT D'ASTROPHYSIQUE)

# SVOM FOLLOW-UP FROM SPACE

With Inputs from the SVOM team, and in particular J. Palmiero & Y. Qiu for the VT

cea irfu

# FOLLOWING UP GAMMA-RAY BURSTS IN THE X-RAYS WITH MXT

- Why and what do we observe in X-rays?
- How do we observe X-rays?
- The  Microchannel X-ray Telescope on board SVOM

# FOLLOWING UP GAMMA-RAY BURSTS IN THE OPTICAL BAND WITH THE VT

# WHAT CAN BE OBSERVED IN X-RAYS?

- X-ray astronomy is now more than 60 years old
- Almost all sky objects emit in X-rays
  - stars (including the Sun)
  - galaxies and AGNs
  - galaxy clusters
  - SN and their remnants
  - compact objects (INSs, Binaries, GRBs)
  - ISM gas
- The power of X-ray astronomy is that is can inform us both on thermal and non-thermal processes that are on going at the sources

- X-ray data (spectroscopy) are unique because they allow to access the abundances of the freshly synthesized elements (in a hot plasma of a few keV), namely the so-called alpha elements (O, Ne, Mg, Si, S, Ar, Ca) and the iron-group elements (mainly Fe, Ni)
- All these elements present relatively strong emission lines in the 0.2-10 keV range
- Shock physics can also be addressed through X-rays: lines provide information about the temperature and ionisation state of the shocked plasma, but direct observation of synchrotron continuum can also be performed.
- The size of the synchrotron emitting regions can be used to infer magnetic field strength, and more generally the properties of the emitting electron population

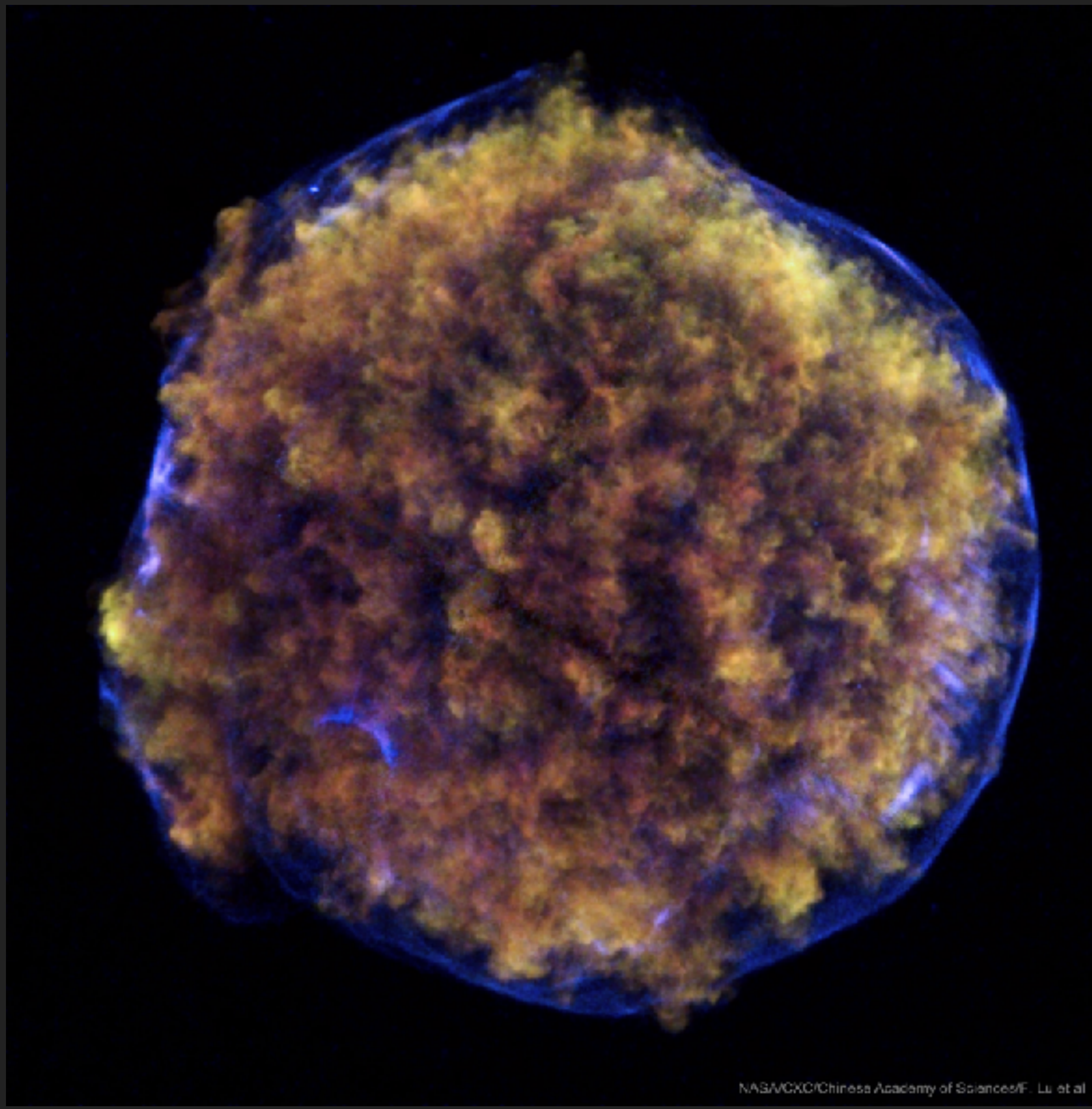

- Nucleosynthesis can be observed also at hard X-rays

- $^{44}$Ti decay lines have been observed by INTEGRAL and Nustar (Cas A, SN 1987A)

- Nustar could prove the asymmetry of the Ti ejecta ruling out symmetrical SN explosions (not correlated to e.g. Fe)

- These observations prove the power of precise imaging at hard X-rays

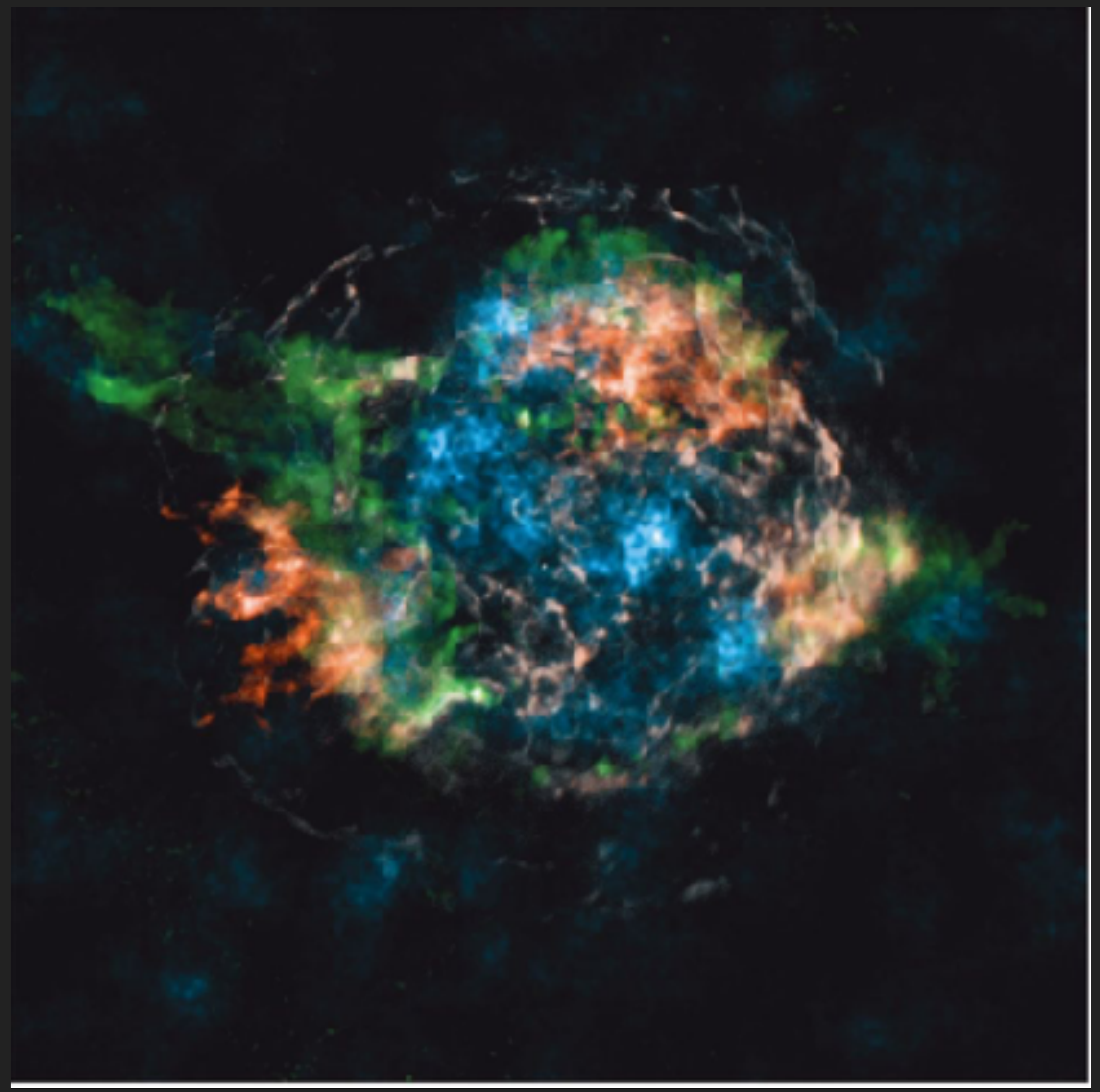

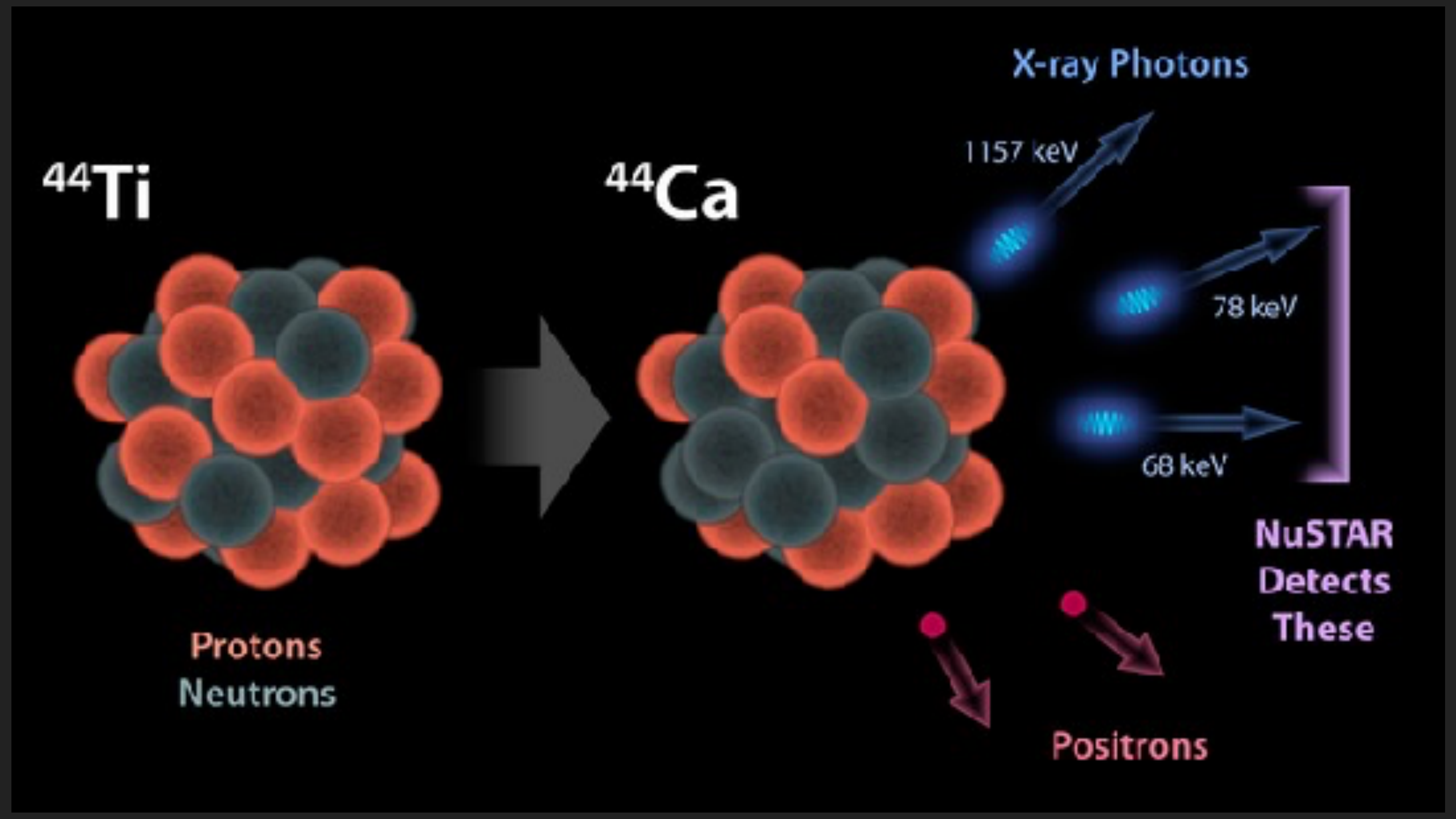


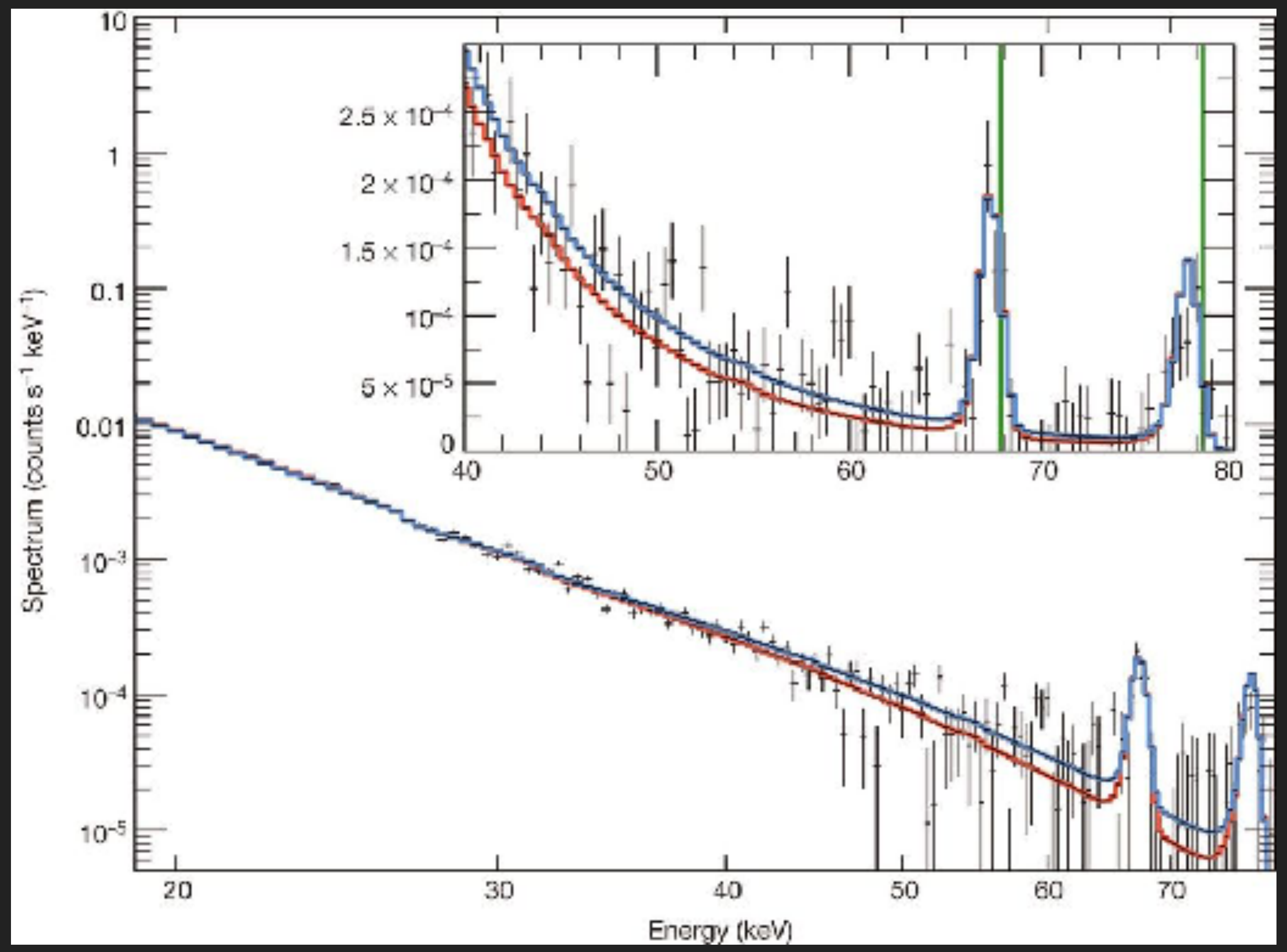


Grefenstette+14

- Rotation powered (radio) pulsars are the most common form of isolated neutron stars (INSs)
- However some INSs are X-ray emitters, in particular the youngest and most energetic (like the Crab pulsar), or old nearby like XDINs and CCOs
- The origin of the X-ray emission can be internal heat, rotational energy, and magnetic field decay (magnetars)
- INSs can have internal temperatures of $10^{11}$ K at birth and then rapidly drop to $10^{9}$ K. For the following $10^{5\text{-}6}$ years the main cooling mechanism i neutrino emission from the star core. This leads to surface temperatures of $10^{5\text{-}6}$ K with thermal emission peaking in the soft X-ray band. Temperature gradients on the surface produce observable modulations.
- Board-band non-thermal emission can originate from charged particles accelerated in the NS magnetosphere, producing strongly variable emission patterns (X-ray pulsations). These particles will eventually feed X-ray nebulae, called PWN (pulsar wind nebulae)

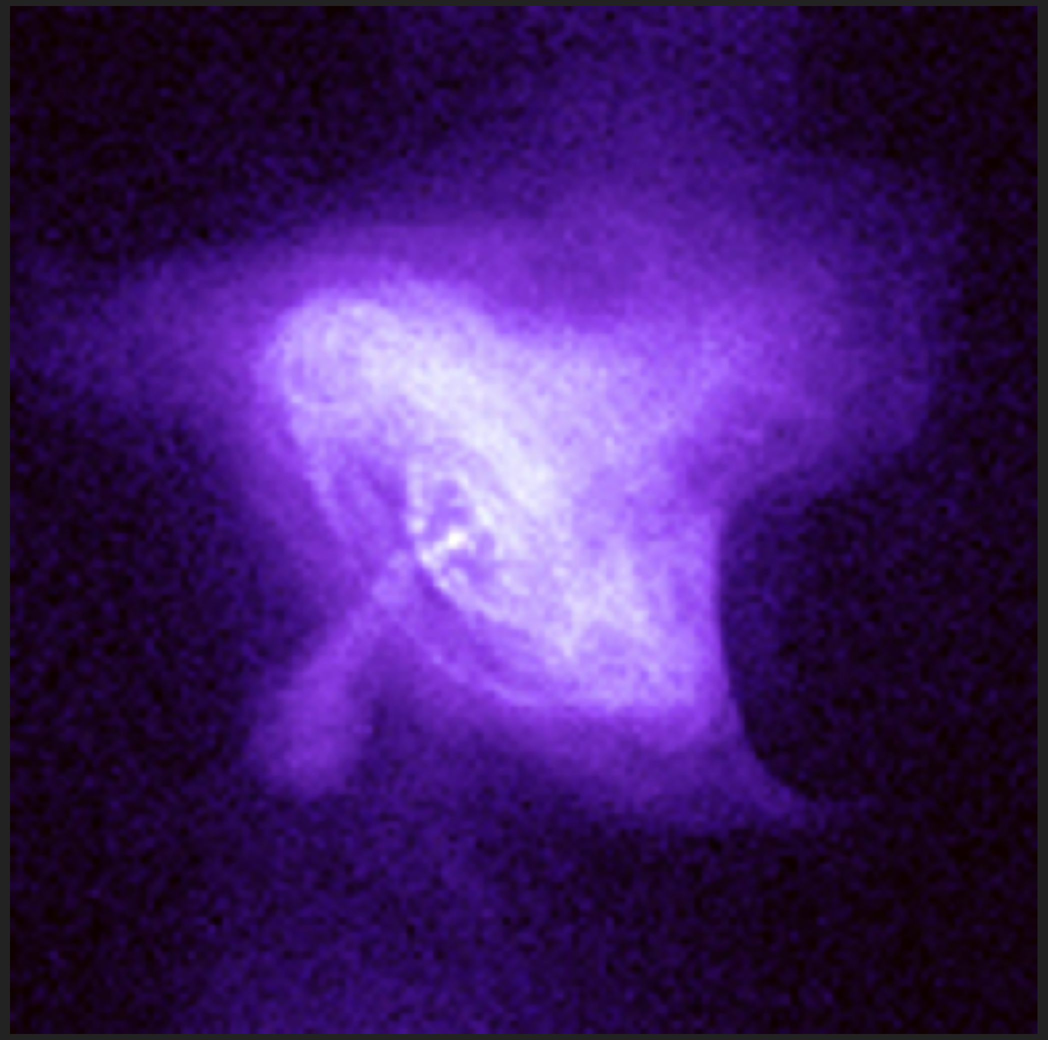

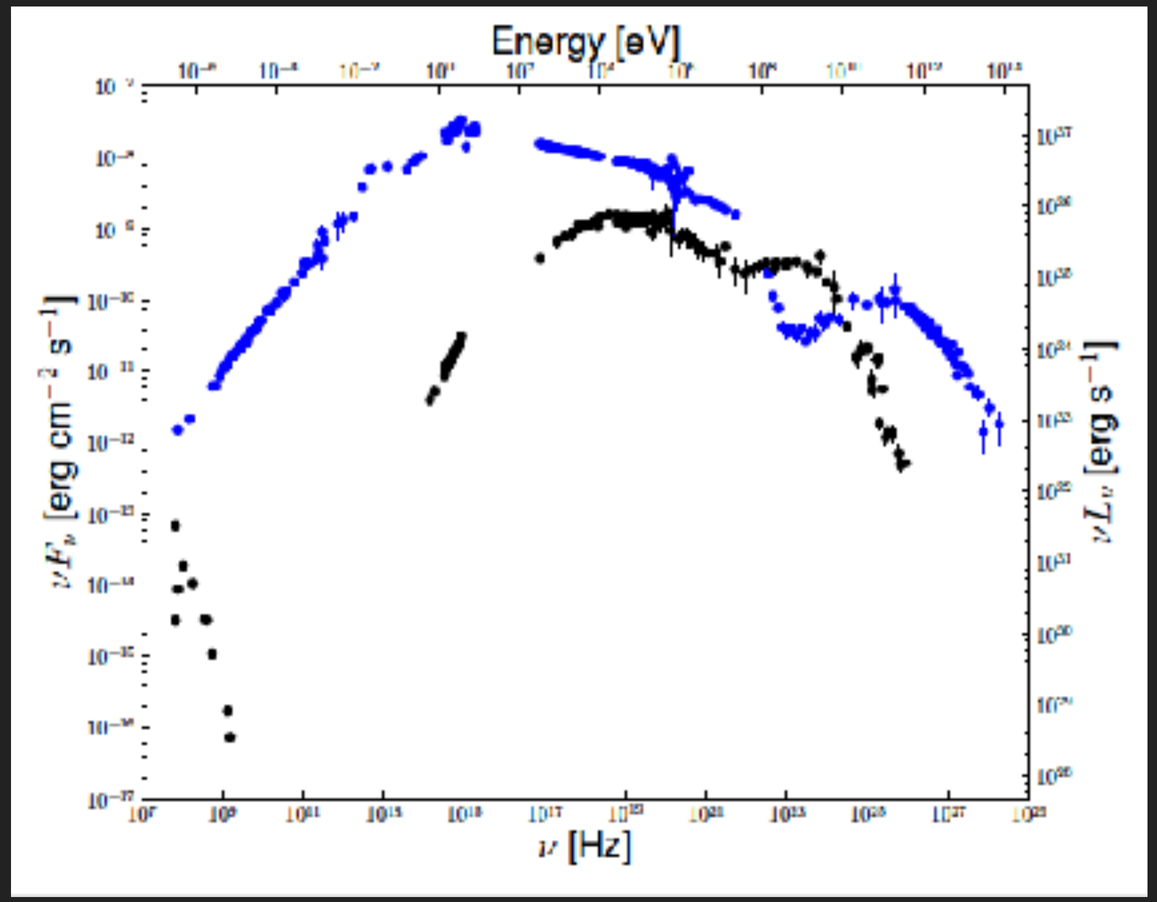

- Magnetars (AXPs & SGRs) are a peculiar class of INSs, whose source of energy is believed to be a huge magnetic field B~$10^{13\text{-}15}$ G
- They are extremely variable sources on different time scales
    - short bursts (~0.1 s) with thermal spectra (kT~25 keV), can be emitted individually or in bunches
    - intermediate bursts lasting a few seconds
    - giant flares, lasting several hundred of seconds
    - outbursts: the persistent X-ray flux increases of a few orders of magnitude and decays over hundreds of days
- The Magnetars phenomenology can be explained by a magnetic field which is highly twisted, and the energy released indicates moments or re-arrangement of the magnetic field configuration towards a more simple dipole

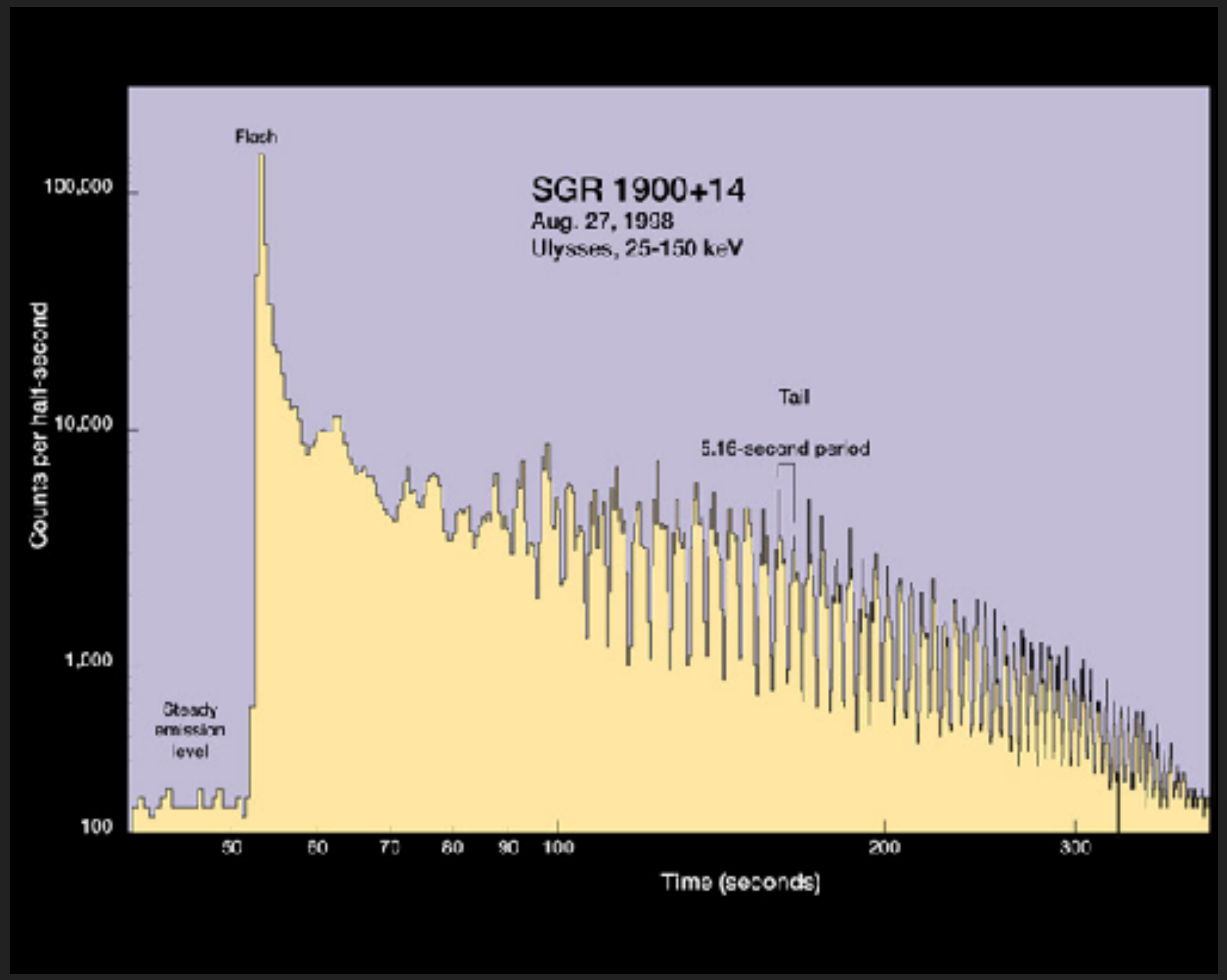


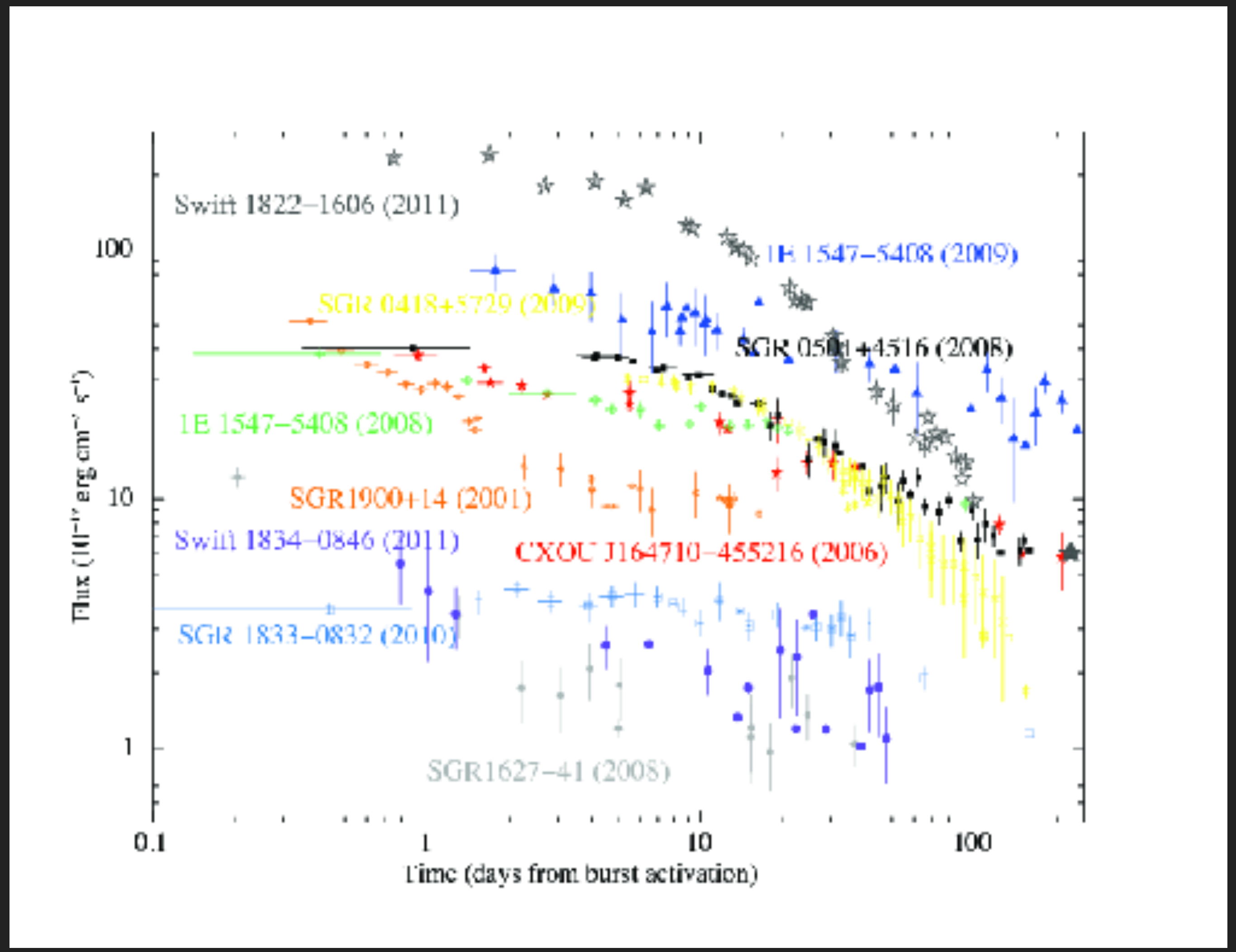

- Magnetars used as an example of diversity
- Their pulse periods span 2-12 s and they have significant period derivatives ($10^{-13}$-$10^{-11}$ s $s^{-1}$)
- Pulsed fraction as well as pulse profile are variable (also as a function of the source flux)
- The measured period and its derivative change over time -> glitches
- These data provide inputs for the modeling of the magnetosphere and returning currents (hot spots on the NS surface)

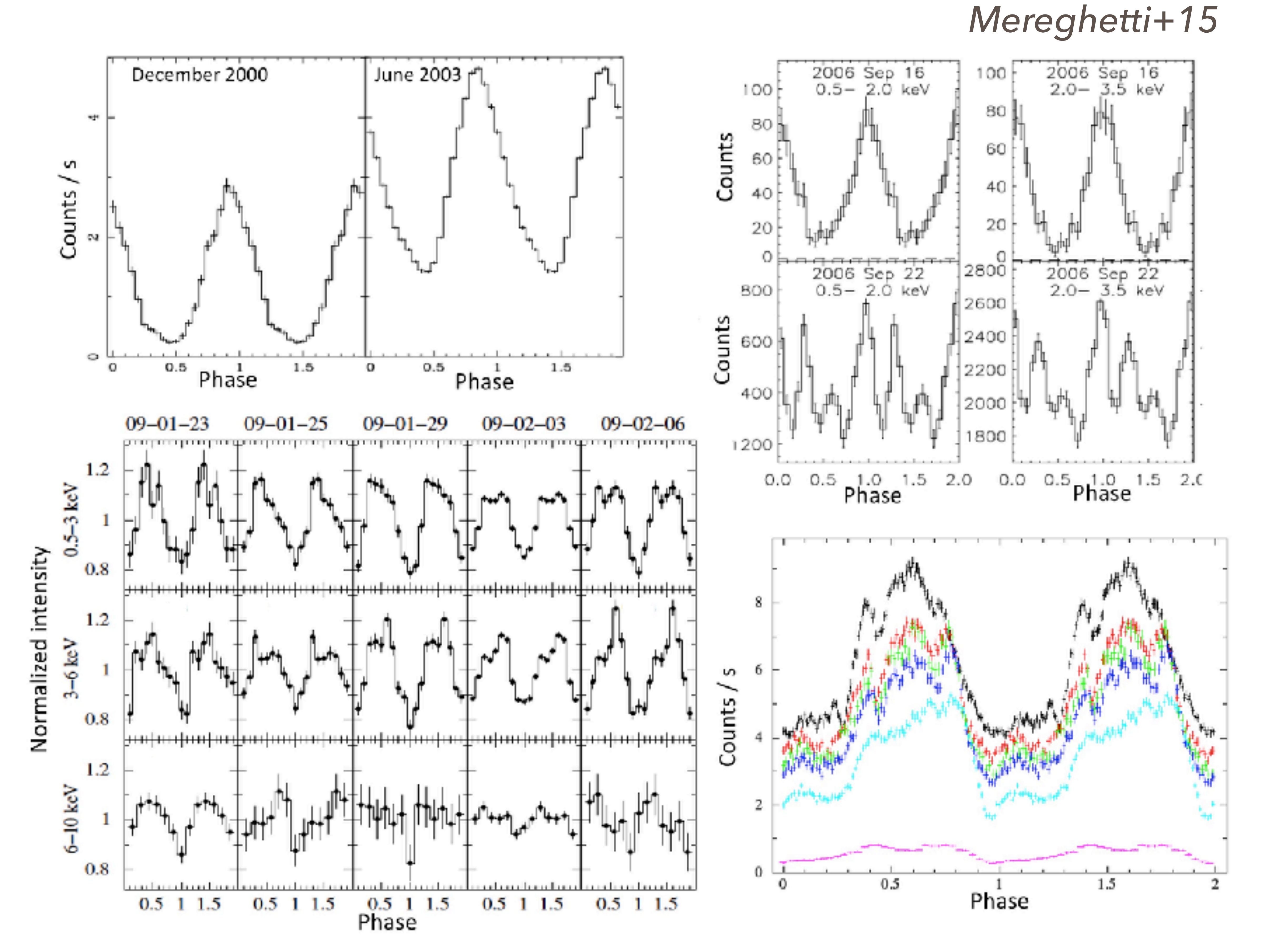

- A tool to derive preliminary **characteristic age** and **magnetic field** values for pulsars

$$\tau = \frac{P}{2\dot{P}}$$

$$B > \left(\frac{3c^3 I}{8\pi^2 R^6}\right)^{1/2} (P\dot{P})^{1/2}$$

$$\frac{B}{Gauss} > 3.2 \times 10^{19} \frac{(P\dot{P})^{1/2}}{s}$$

*assuming canonical values for NS moment of inertia I and NS radius*

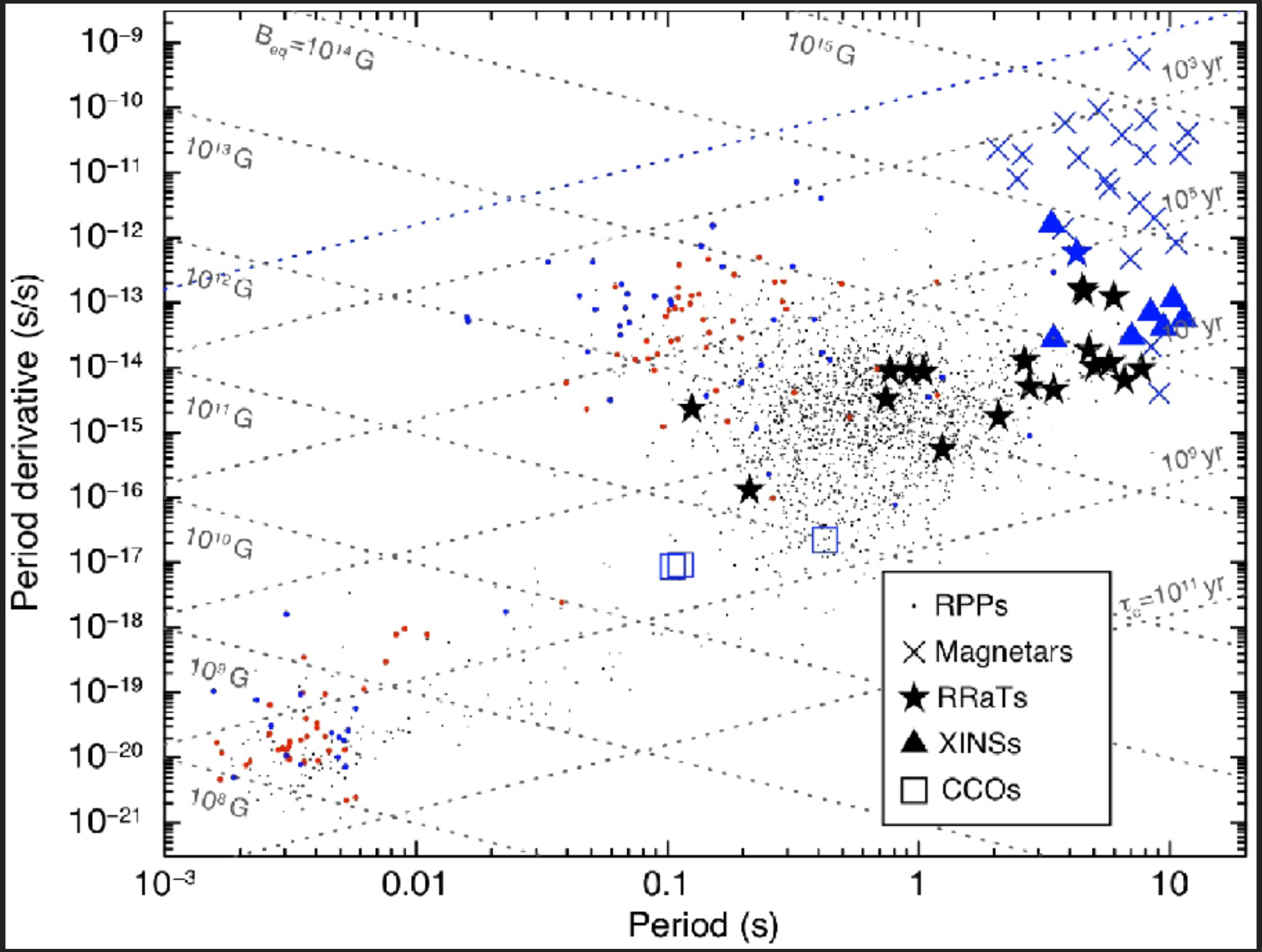

- Relativistic doppler shifts, gravitational redshift, photon bending and beaming affect the spectral shape and the flux observed from each point in the accretion disk flow, leading to a variety of quantifiable distortions of the Fe line profile.

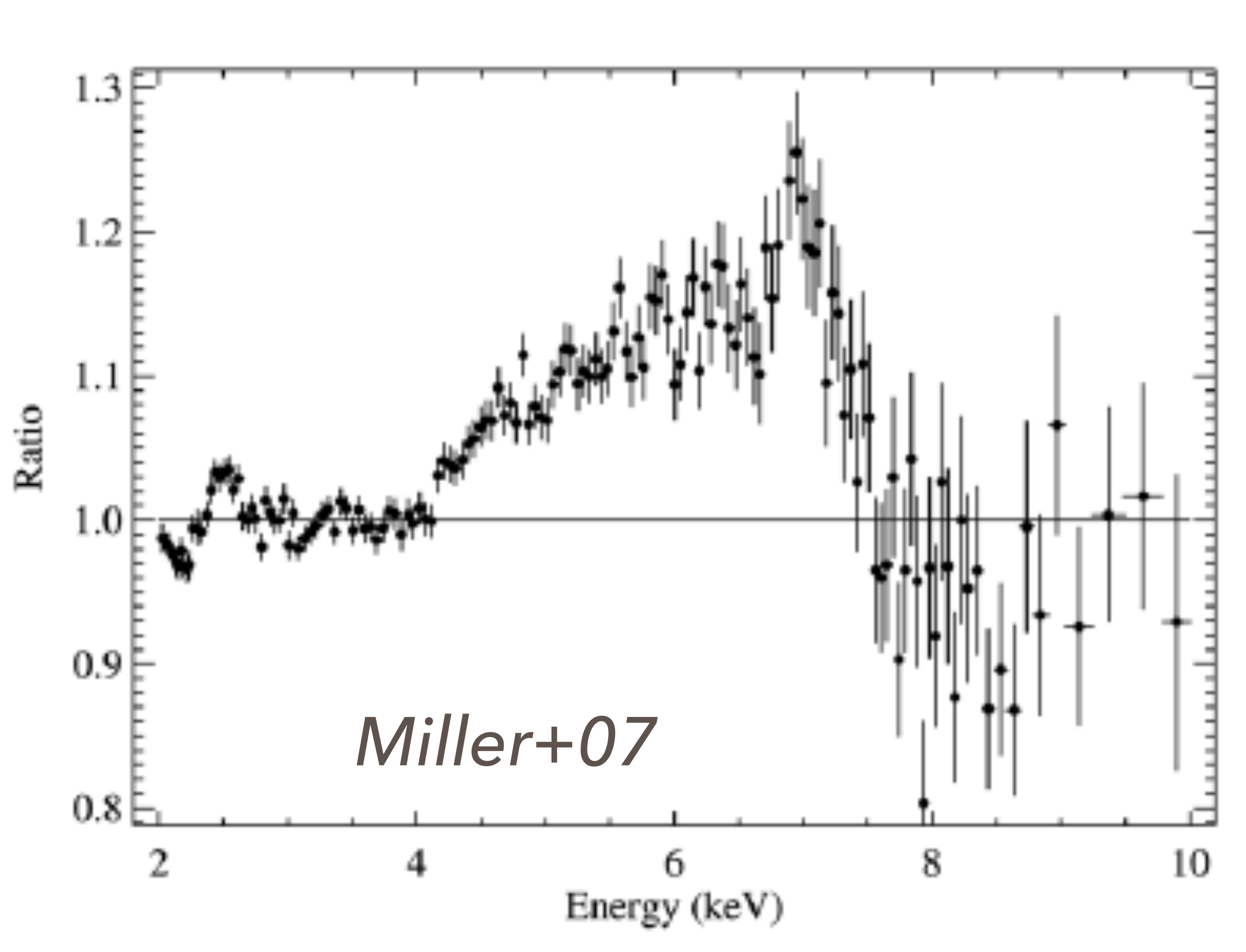


- Redshift z from a point on the disk at radius r and azimuthal angle φ is given in Schwarzschild geometry by

$$1 + z = \frac{1 + (b r_g^{\frac{3}{2}} / r^{\frac{3}{2}}) \sin i \sin \phi}{\sqrt{1 - 3 r_g / r}}$$

*where i is the disk inclination and b the impact parameter at infinity of the photon relative to the BH. An equivalent calculation can be done for a Kerr BH*

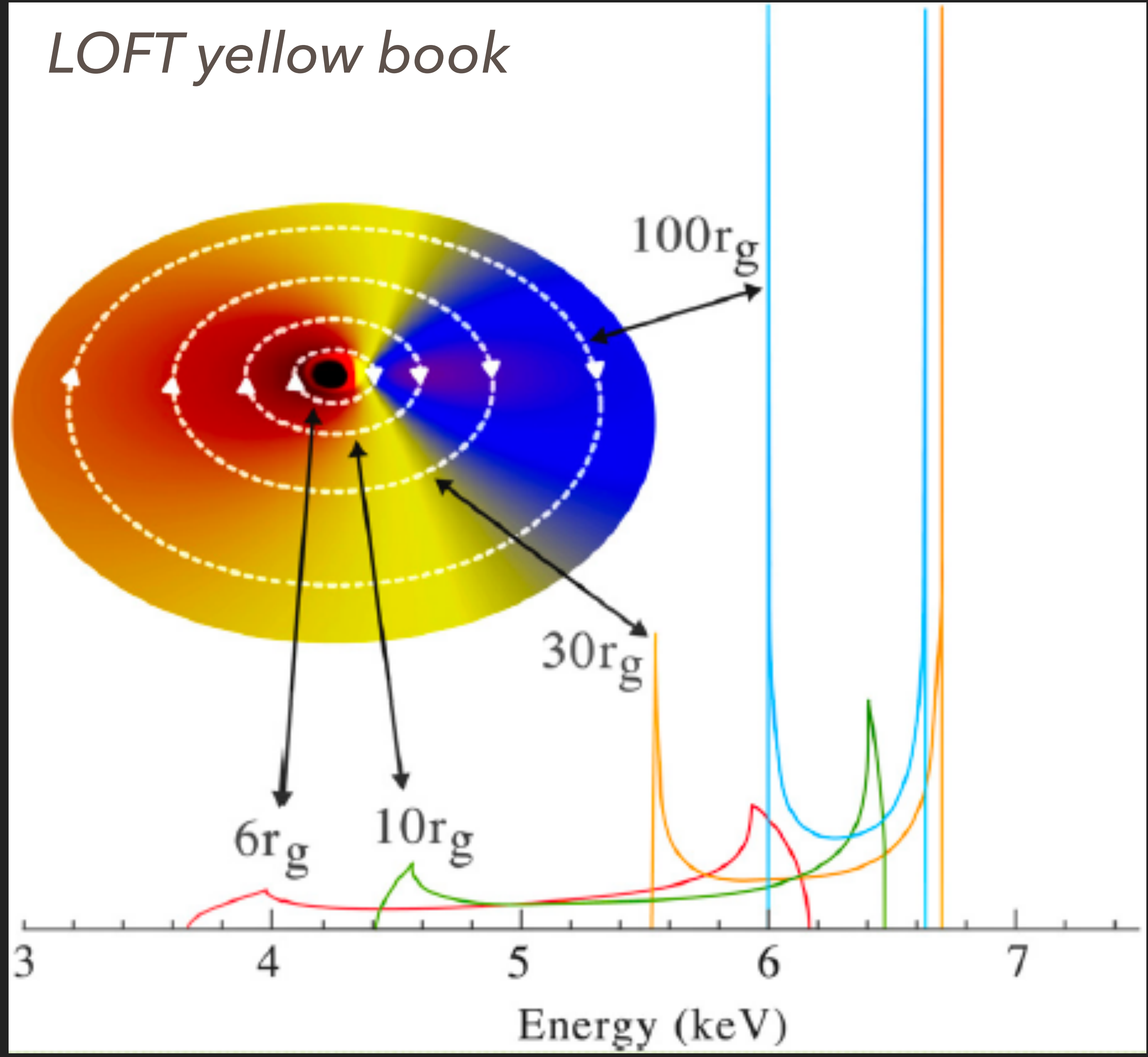


- Measurements of Fe line profile can constrain BH spin

- Supernovae are routinely discovered by optical surveys, but usually days to weeks after the actual explosion
- In 2008 Swift UVOT was monitoring a SN (2007uy) in NGC 2770 when another SN when off (2008D, type Ib/c)
- A luminous X-ray transient ($L_X \sim 10^{44}$ erg $s^{-1}$) was detected by XRT lasting just a few minutes. Interpreted as the shock breakout i.e. when the shocked material becomes optically thin. Can be used to infer the properties of the SN progenitor: in this case a Wolf-Rayet star
- No contemporaneous flash was recorded by the UVOT until two hours later
- Coupled analysis of radio and X-ray data allowed to constraint the speed of the ejected material (0.25 c) and its energy of $10^{48}$ erg (0.1% of the total explosion energy)

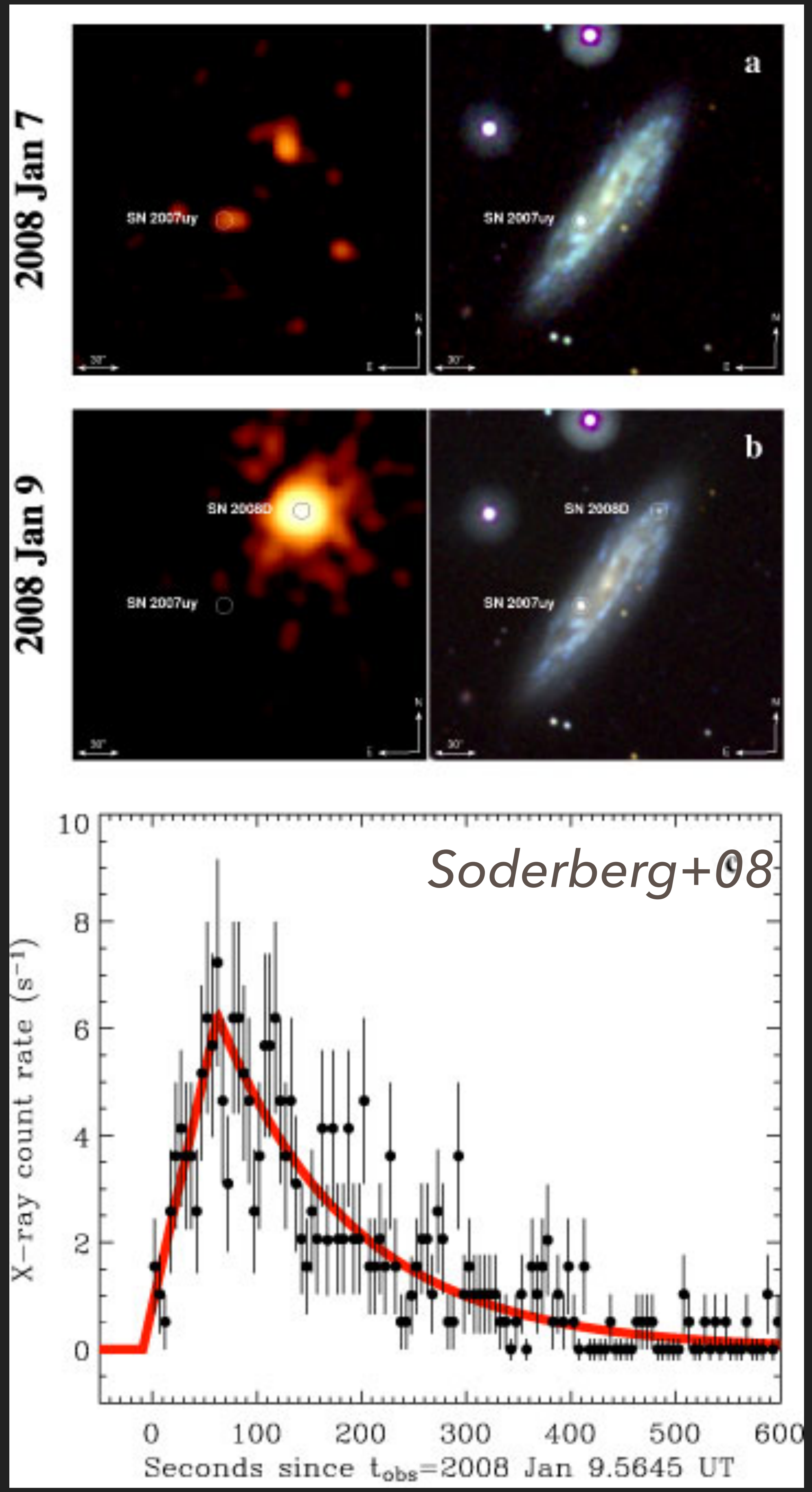

- The detection of GW170817 (binary neutron star merger) and its association with a short GRB detected by Fermi/GBM and INTEGRAL/ACS marked the beginning of a new era for multi-messenger astrophysics

- First direct link between NS mergers and short GRBs!

- A kilonova was associated to this event and was observed by many telescopes in different wavelengths from radio to X-rays

- The nature of the observed prompt radiation was unclear (jet or cocoon or both?). Difficult to conclude based on gamma-ray data only

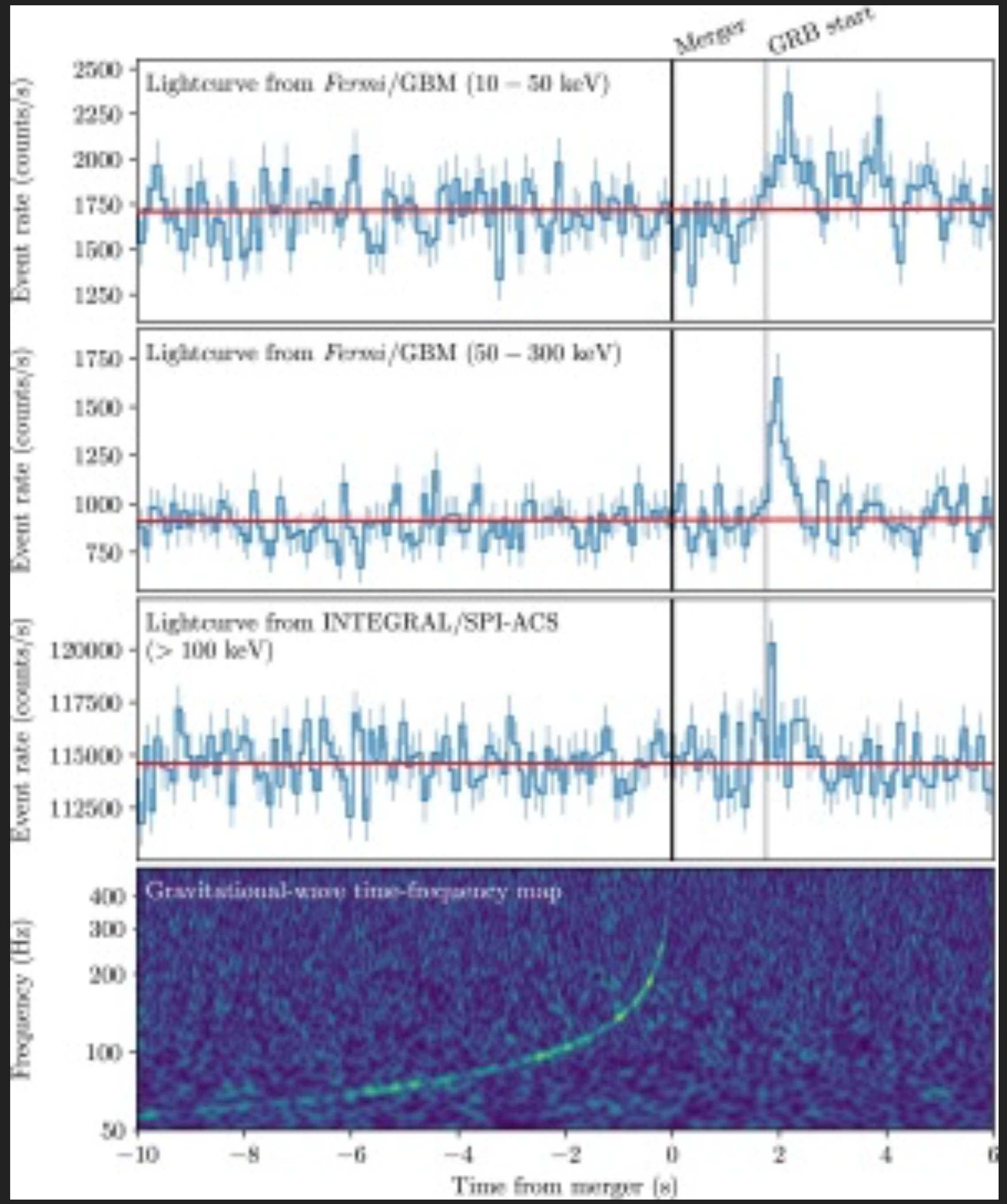


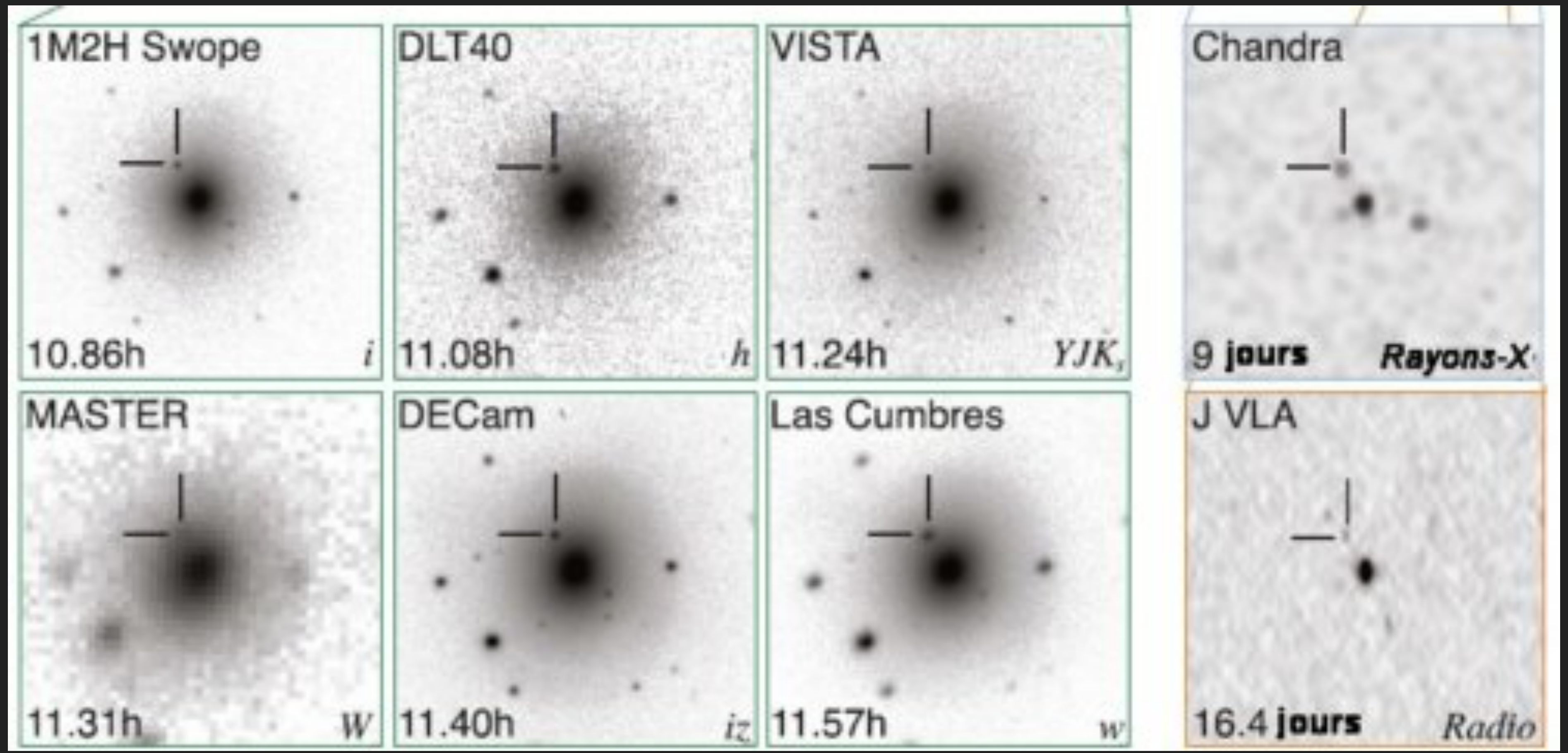

An off-axis GRB afterglow:

structured jet models are favored from X-ray observations, and confirmed by radio observations (Ghirlanda+19).

*9 days* *108 days* *260 days*

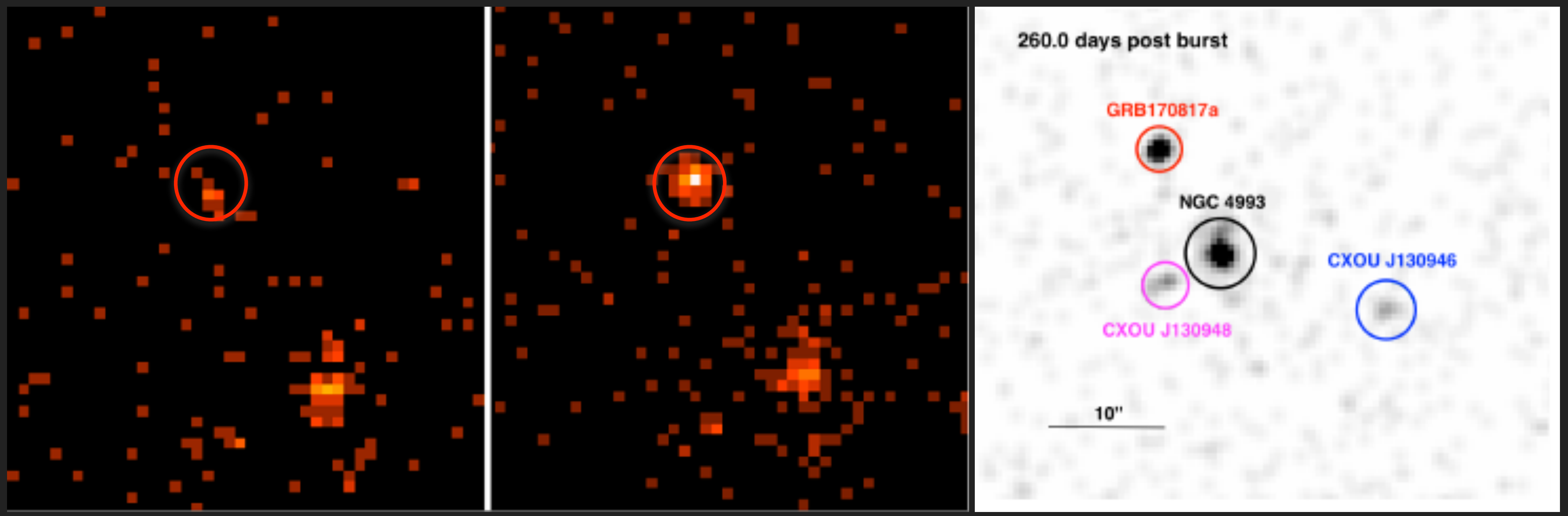


*Troja+18* *Nyka+18*

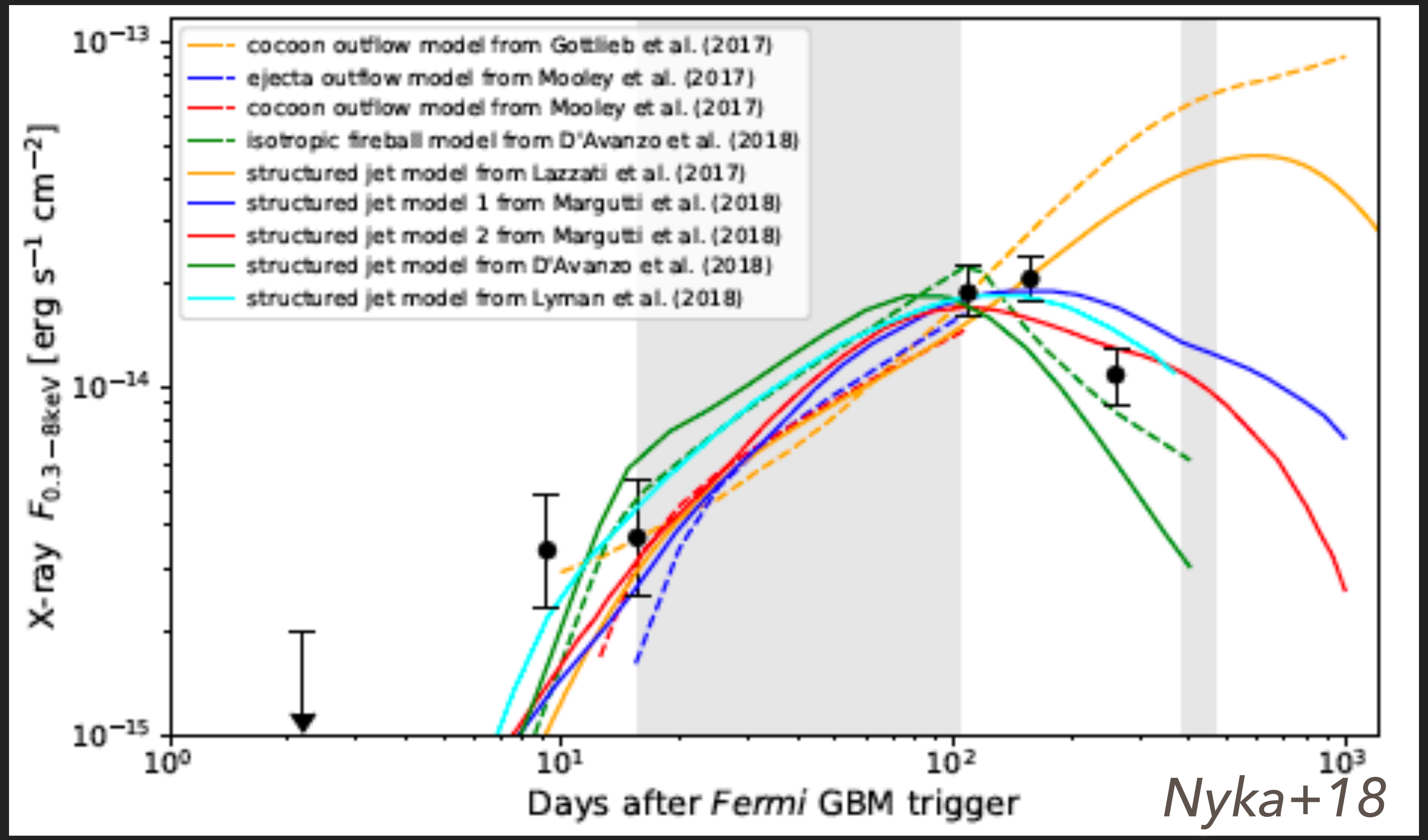


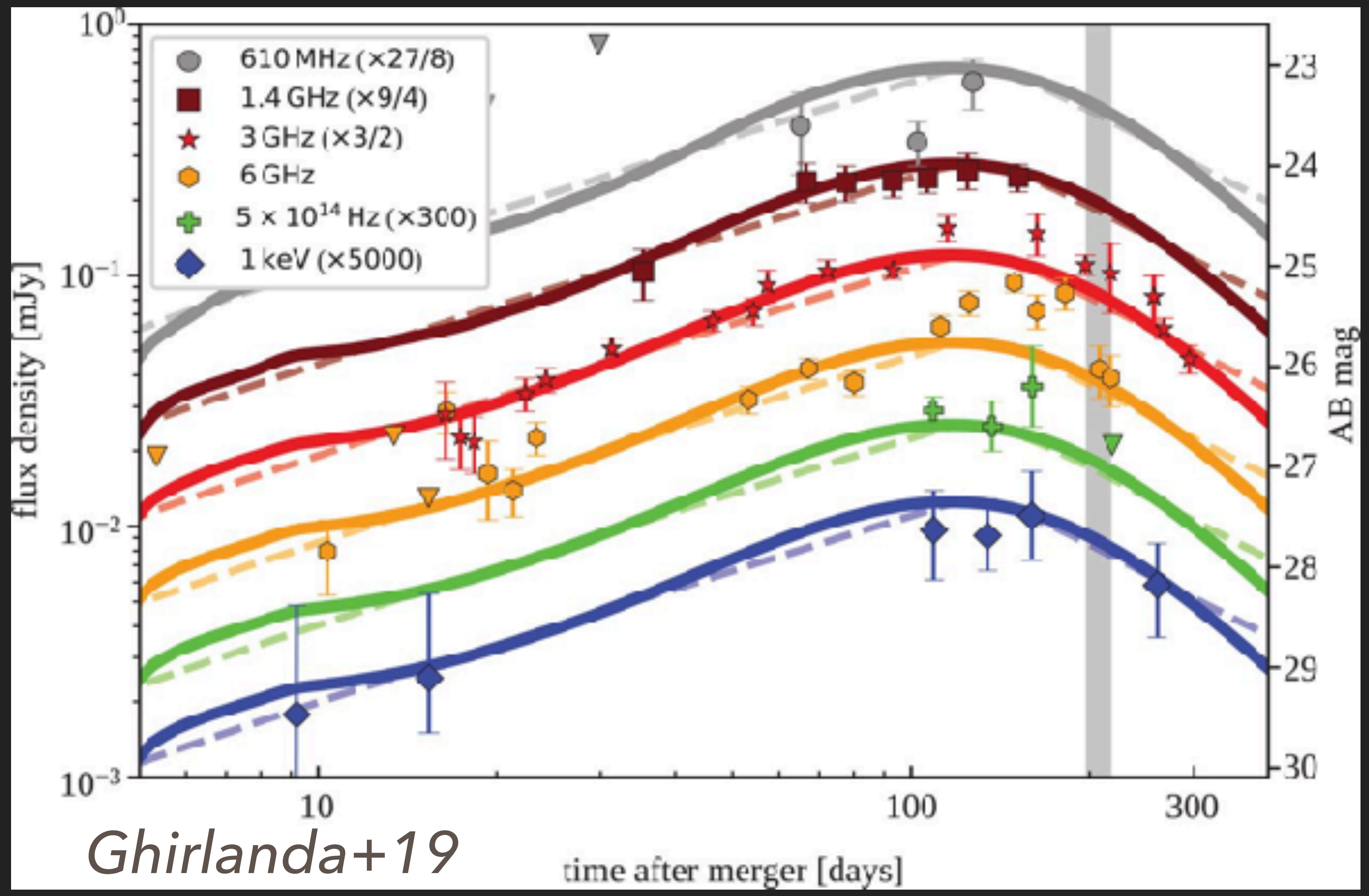

- A major contribution from X-ray measurement of GRB afterglows is, in the first place, the ability of producing precise images (which is much more complex in gamma-rays).

- Indeed thanks to *BeppoSAX* data a GRB afterglow could be localized at the arc minute scale (GRB 970228) for the first time, which in turn allowed optical astronomers to follow-up the event from the ground and determine its distance and energy content -> GRBs are cosmological!

- X-ray spectroscopy can be used to investigate the shock accelerated electrons emission properties, as well as the intervening matter density ($N_H$ absorption) and hence the GRB environment

- X-ray light curves present different morphologies and can provide information about the geometry of the relativistic outflow and on the progenitors of GRBs

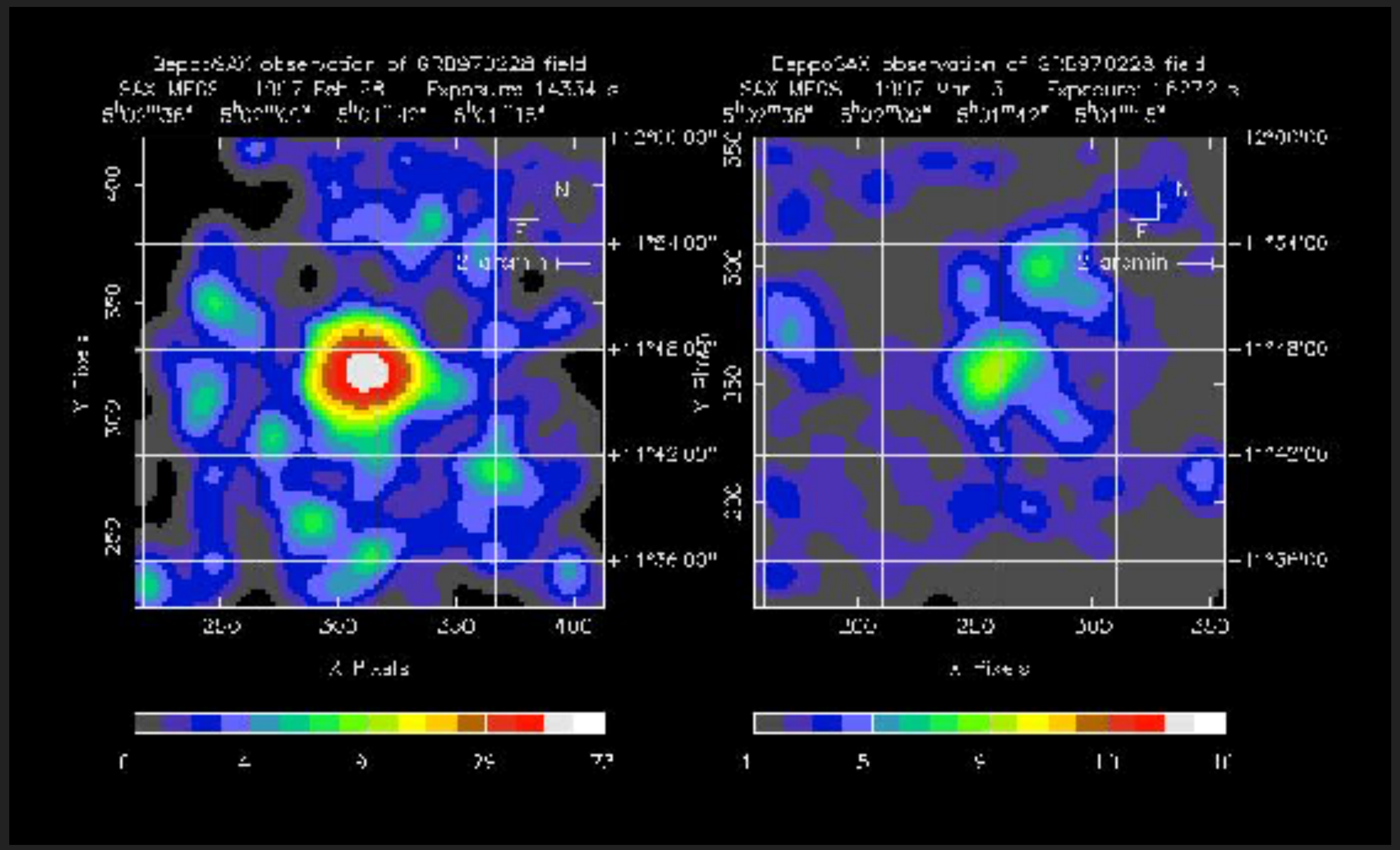

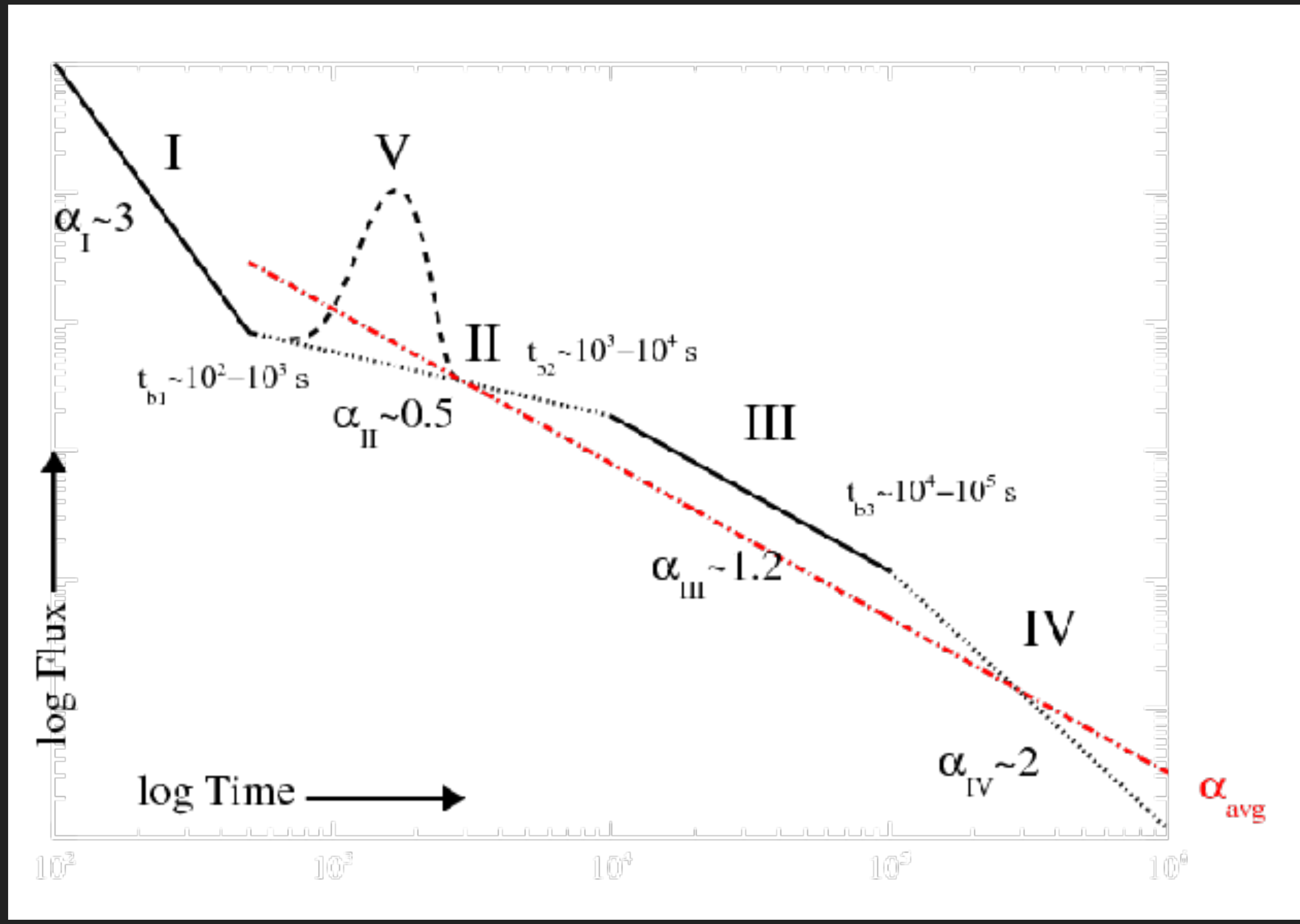

# HOW DO WE OBSERVE X-RAYS?

- X-ray astronomy can be performed only at very high altitude due to absorption by the Earth atmosphere
- Thus it was only after rockets were available to lift payloads above the atmosphere that X-ray astronomy coud be fully developed

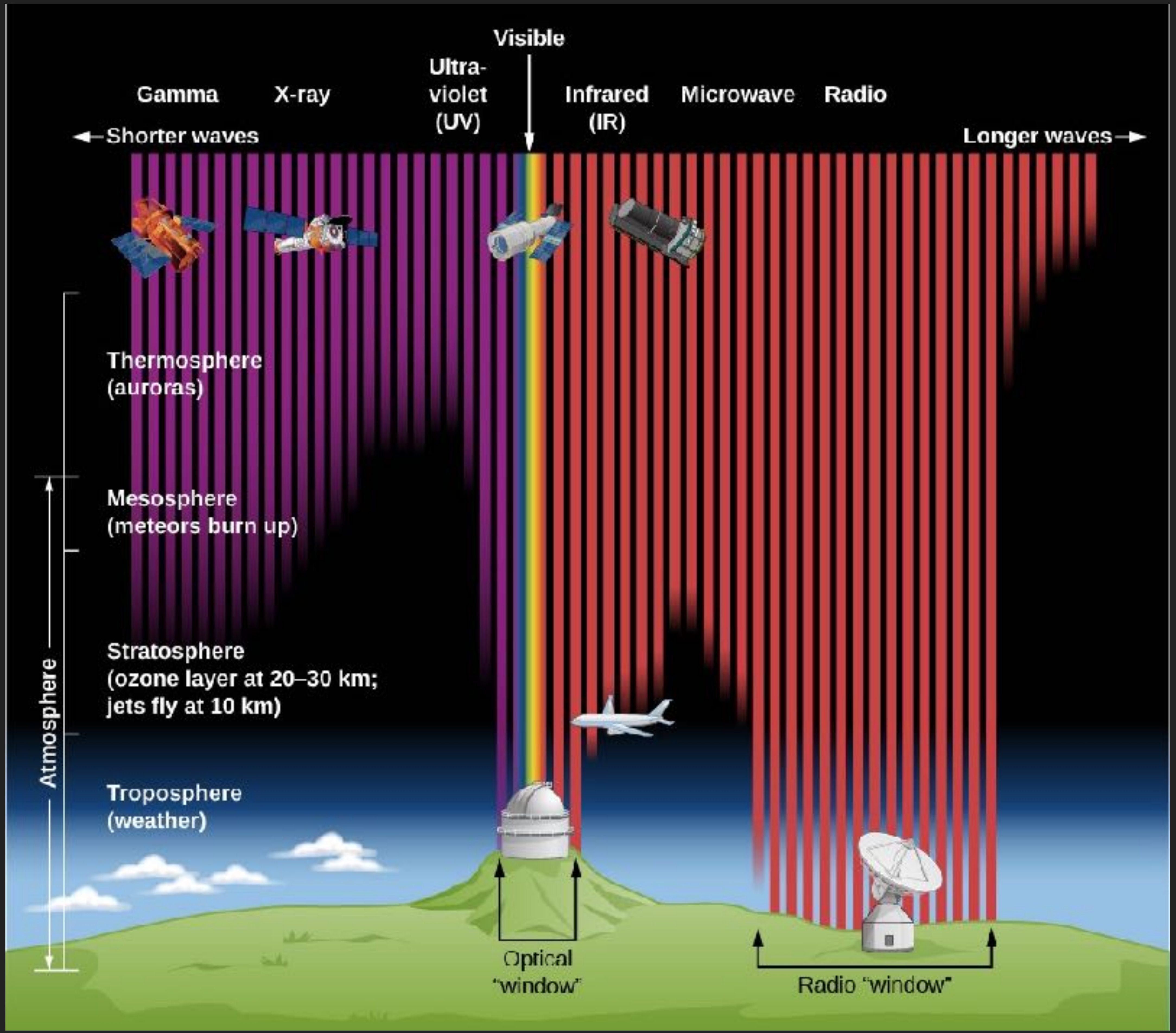

- Already after the first rocket flights in 1962 and 1963 lasting just a few minutes it was clear that the sky was full of X-ray sources
  - The team lead by the Nobel Prize winner Riccardo Giacconi (1931-2018) discovered the brightest X-ray source, Sco X-1, while looking for fluorescence X-rays from the Moon surface.
- The first all-sky map in X-rays has been performed using the data from the UHURU satellite
- X-ray allow to test thermal and non-thermal emission processes, both in compact objects (binaries, isolated NS, GRBs,…) and diffuse environments (SNRs, Galaxy Clusters,…)
- X-ray spectroscopy allows e.g. to determine the elemental composition of the observed plasmas

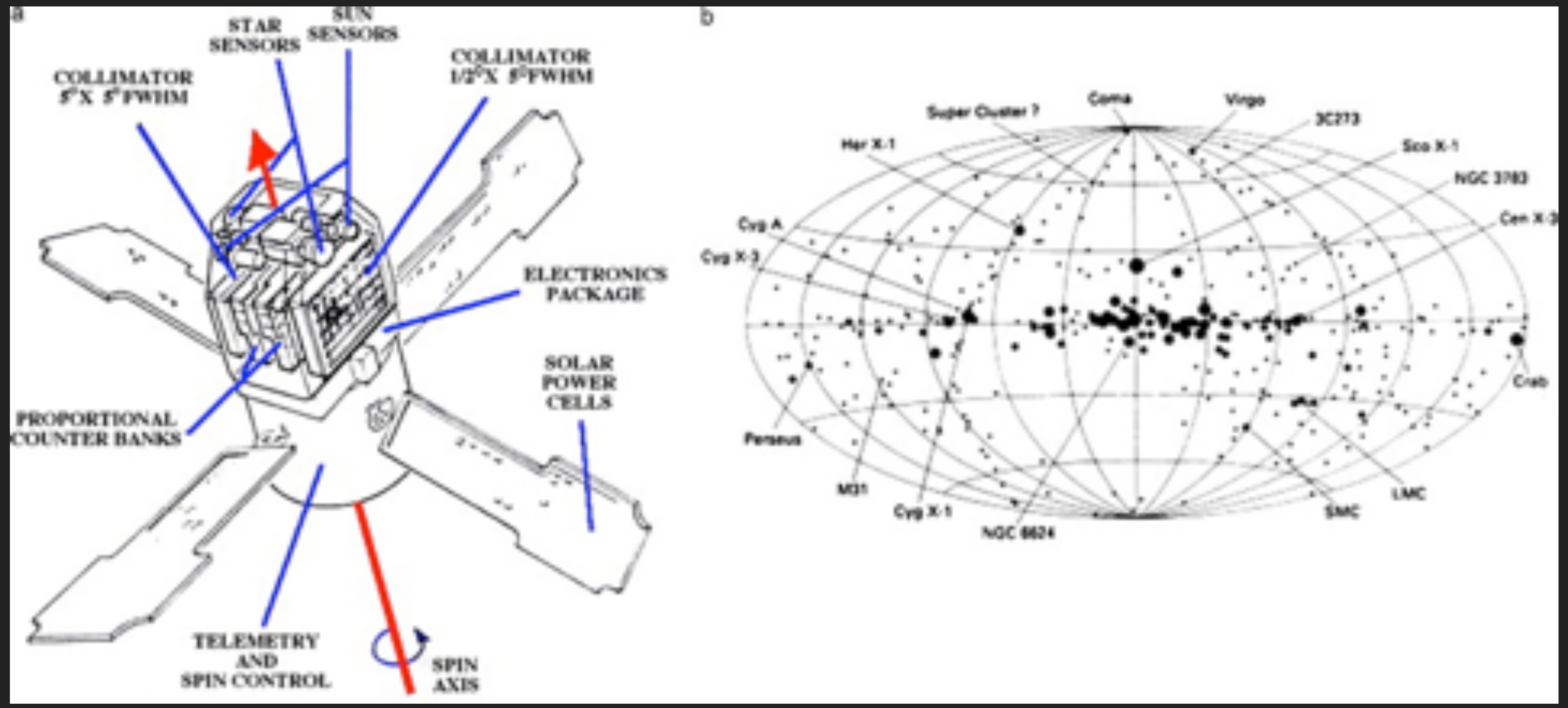


At X-ray energies imaging is only possible for small incidence (grazing) angles

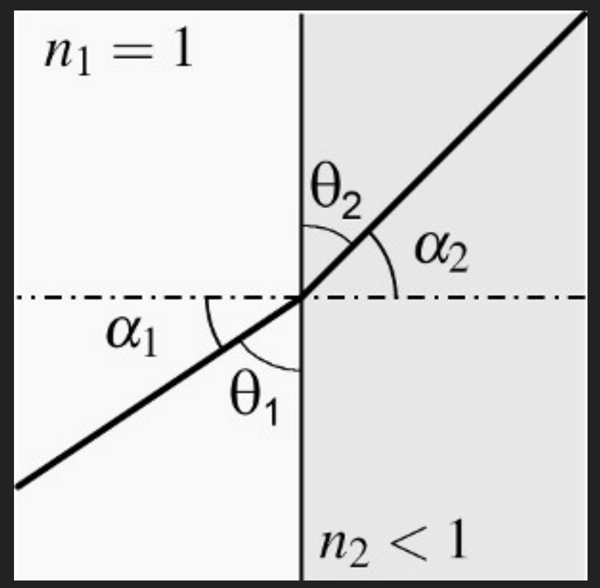


*Reflection of X-rays (Snell's law)*

$$\frac{\sin \alpha_1}{\sin \alpha_2} = \frac{n_2}{n_1}$$

If $\alpha_2$ reaches 90° we have a reflection. So if we assume $n_1=1$, the critical angle to have a reflection is

$$\alpha_{critical} = \arcsin n_2$$

As $n_2$ is slightly below 1 in the X-rays regime (for example for Au for photon energies of 12.4 keV, $n_2 = 1-1.88 \cdot 10^{-5}$), the maximum angle for total external reflection to occur is close to 90° (for gold at 12.4 keV $\alpha_{critical}$ = 89.65° = 90°-0.351°).

For X-rays total external reflection occurs only under grazing incidence. So the reflection angles α are always close to 90°.

Normally the reflection angles are measured as angles $\theta$ between the incoming ray and the mirrors surface. The critical angle $\theta_{critical}$ is then expressed as

$$\cos \theta_{critical} = n_2$$

For example $\theta_{critical}$ is ~ 1° for 3 keV photons on metals such as Nickel or Gold

- In 1978 the Einstein X-ray Telescope was launched
- In provided the first high resolution X-ray images of many sources, thanks to the grazing incidence reflection technique (in a Wolter I configuration)

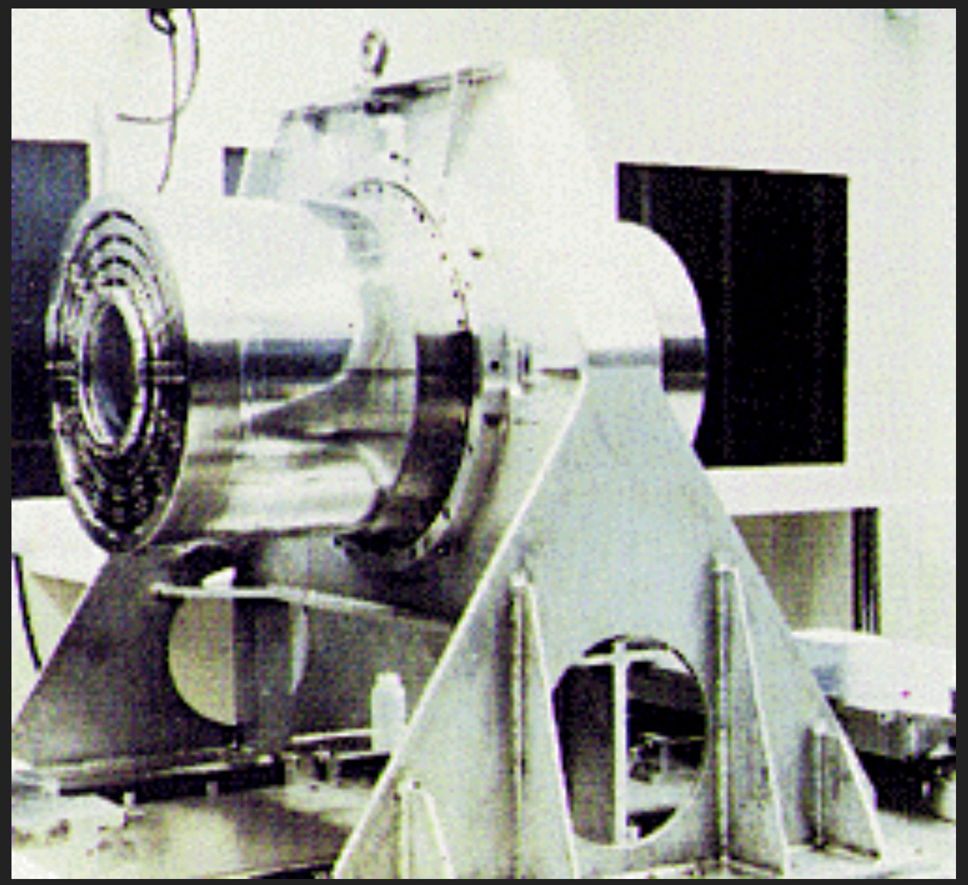

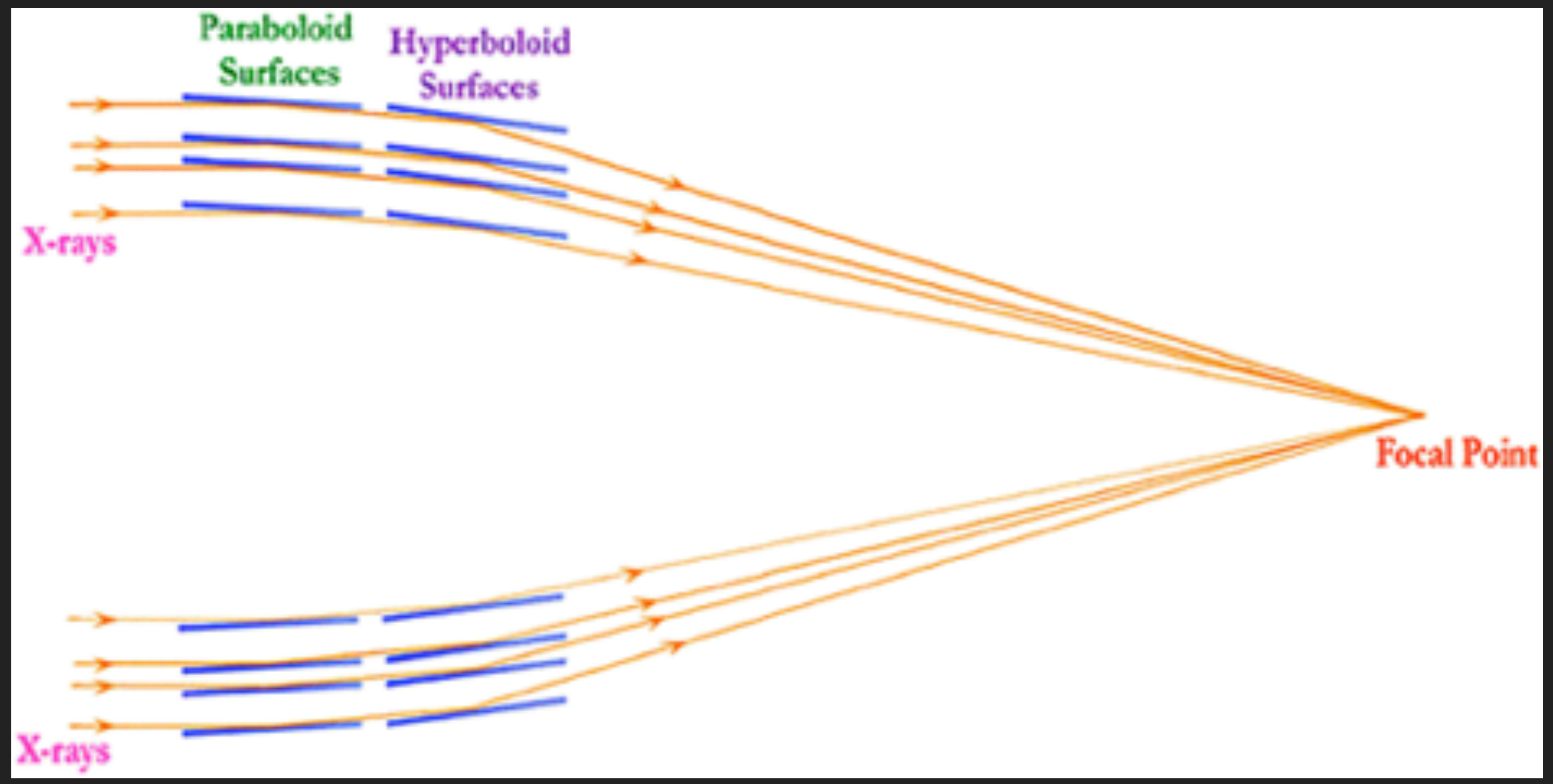

- The sky background radiation was largely reduced wrt UHURU
- This allowed for the first time to image faint and extended sources
- Main result: all the celestial objects are X-ray emitters (stars, galaxies, AGNs, clusters, etc.)

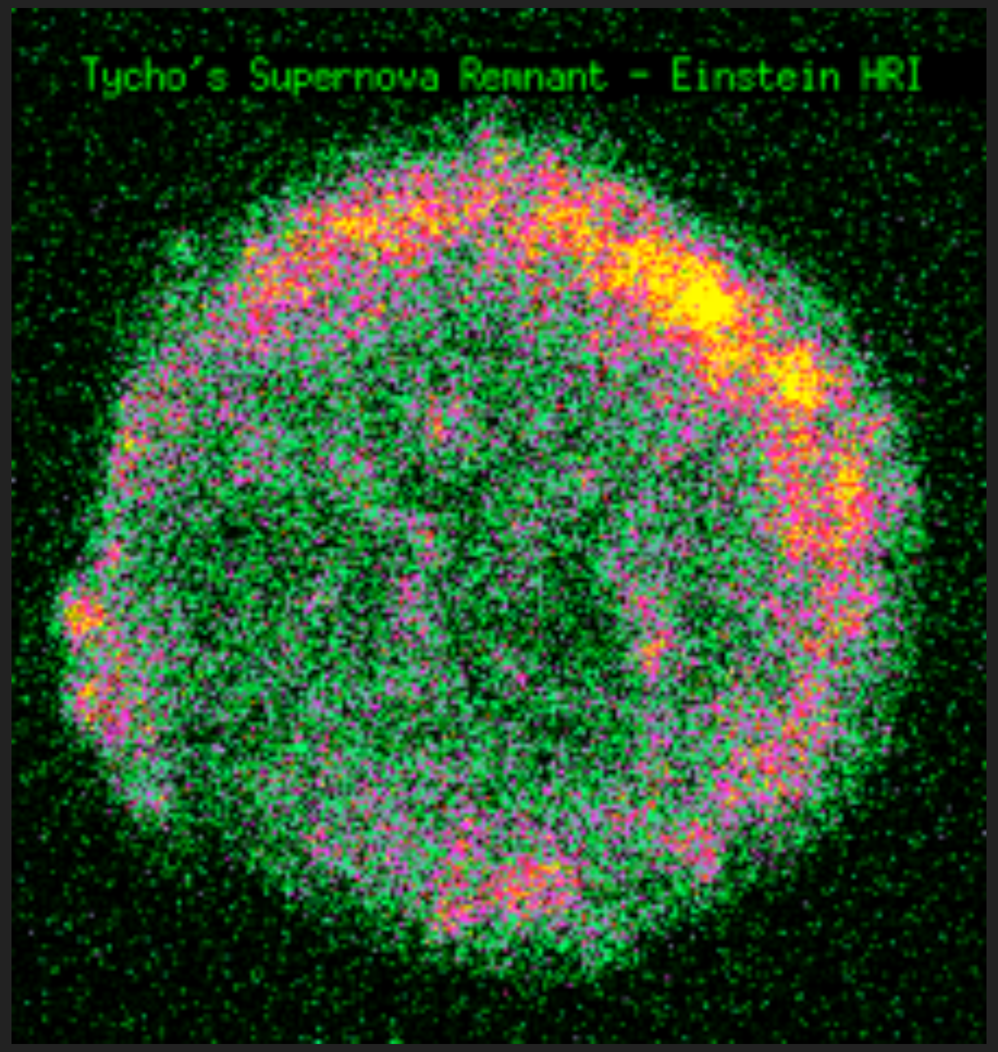


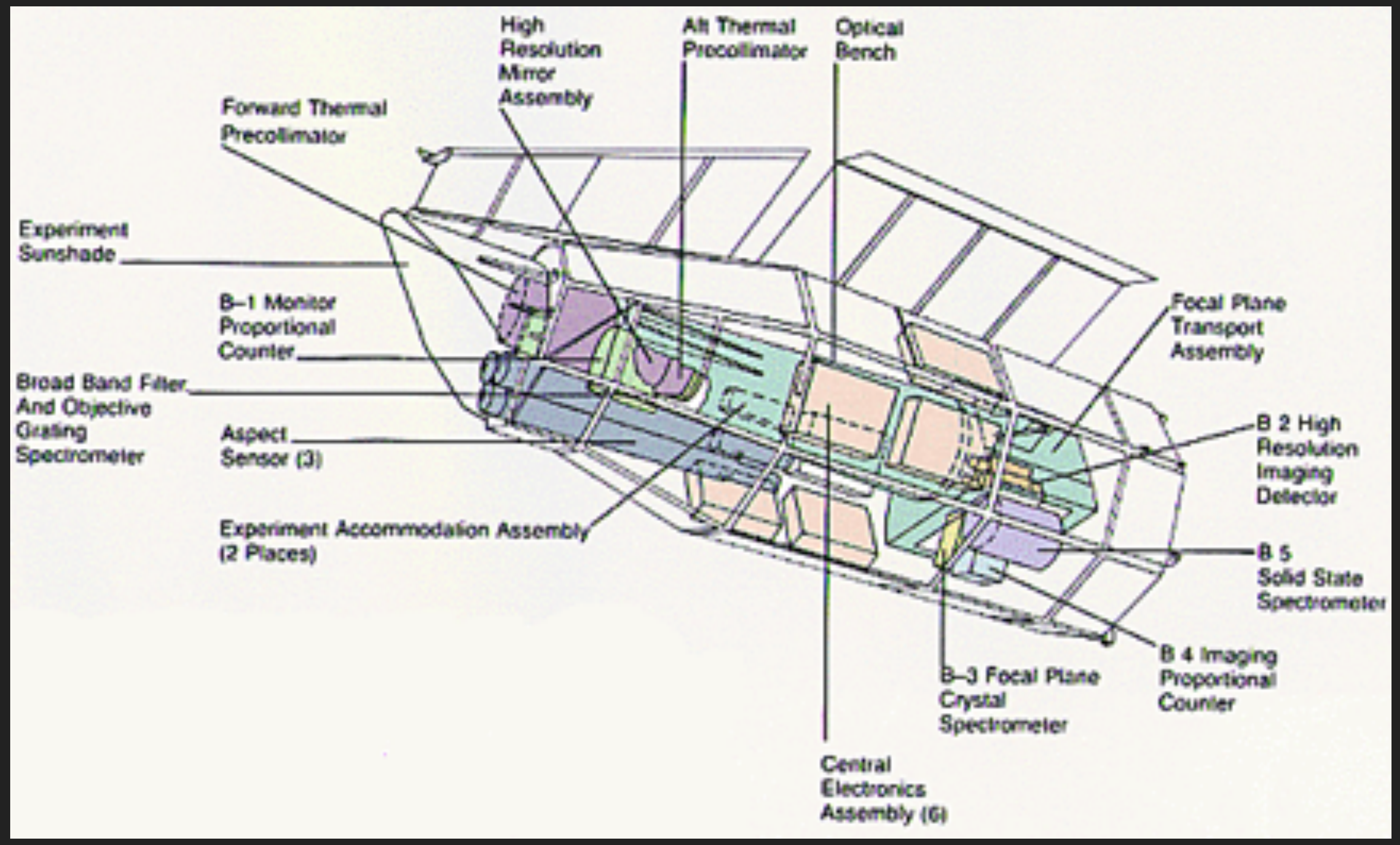

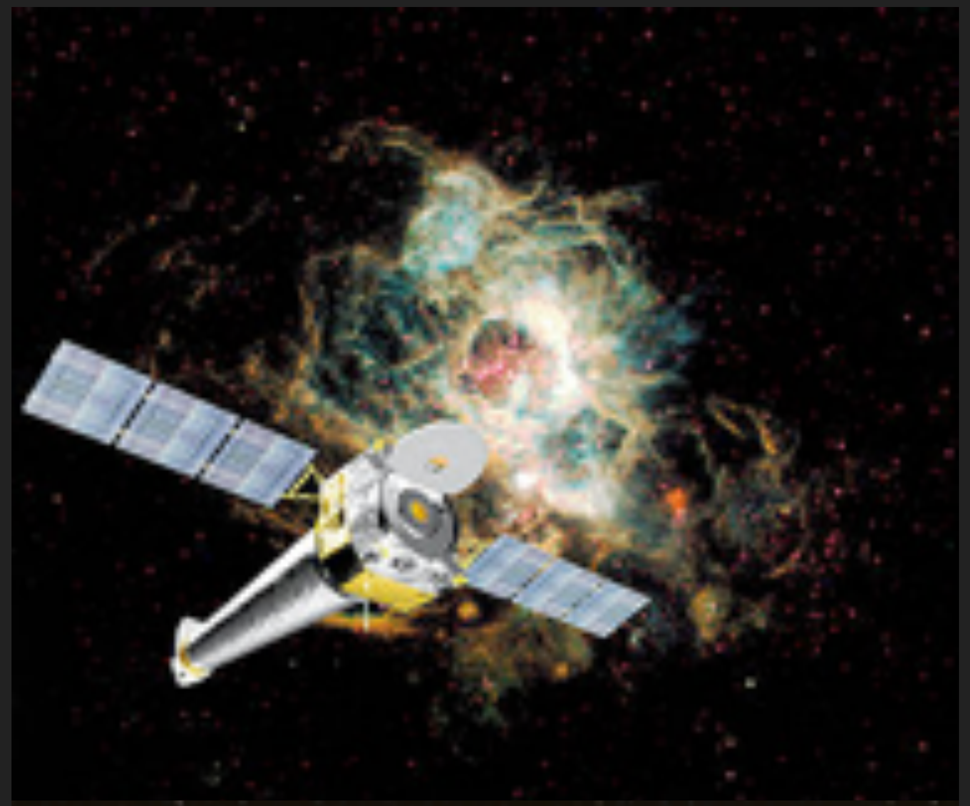

Chandra X-ray Observatory
launched in 1999 by NASA
10 m focal length, 0.1-10 keV
600 cm$^2$ @ 1.5 keV, PSF: 0.5 arc sec

ESA XMM Newton, launched in 2000
7.5 m focal, length 0.1-12 keV
1500 cm$^2$ @ 1 keV, PSF: 6 arc sec

Nustar, launched in 2012 by NASA
10.15 m focal, length 6-79 keV
849 cm$^2$ @ 9 keV, 60 cm$^2$ @ 78 keV
PSF: 9.5 arc sec

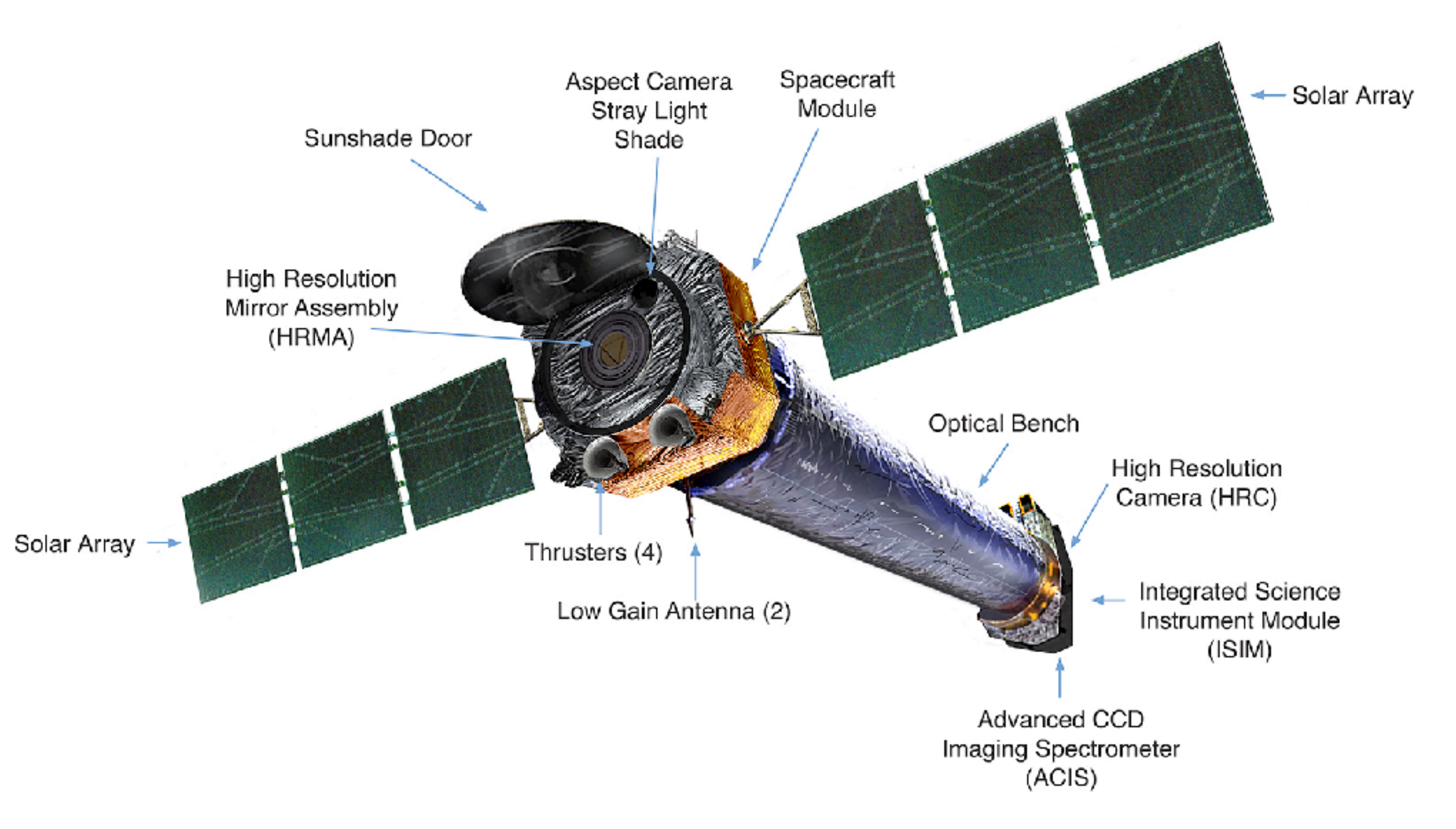


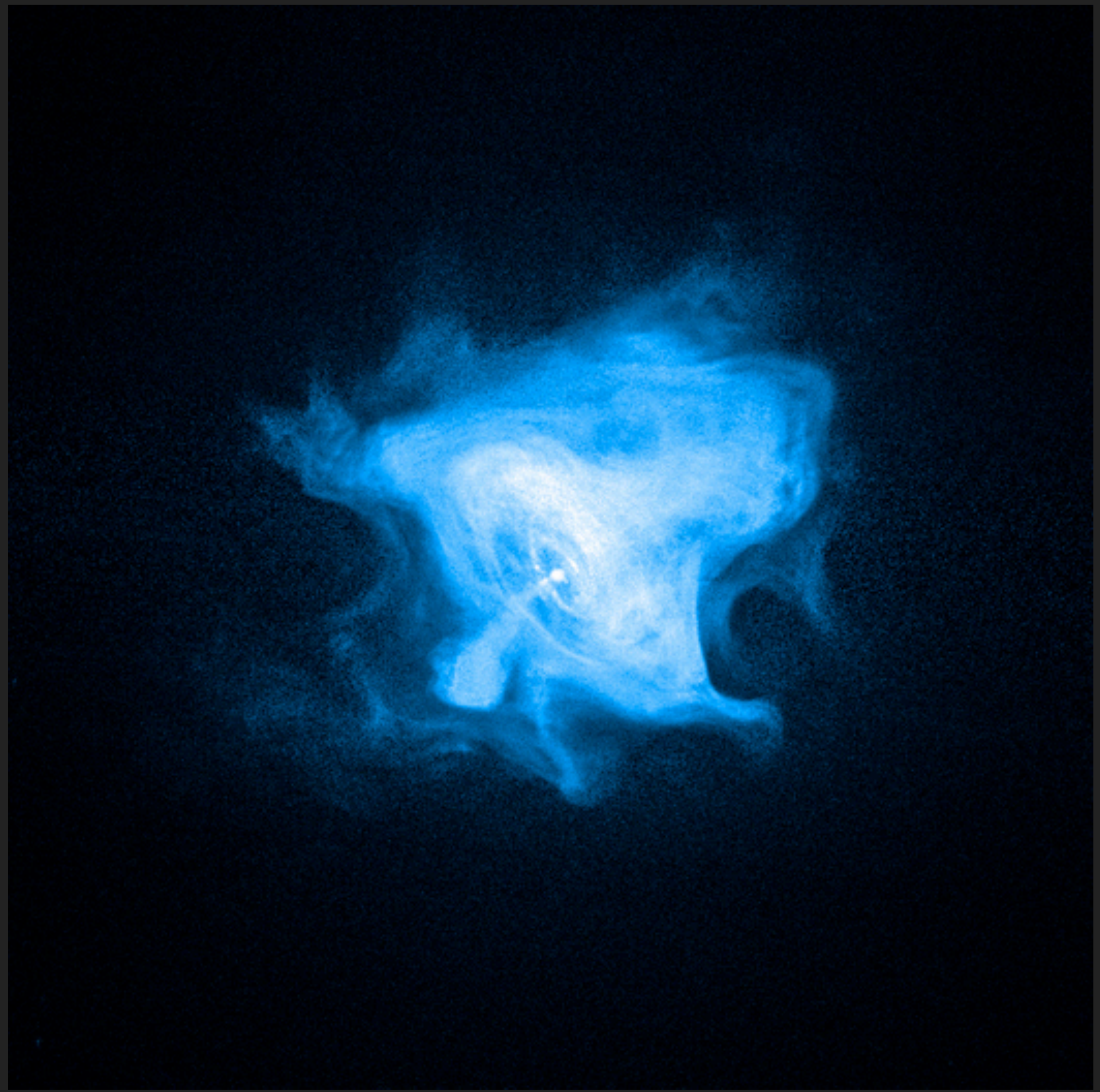

The Crab Nebula observed by Chandra

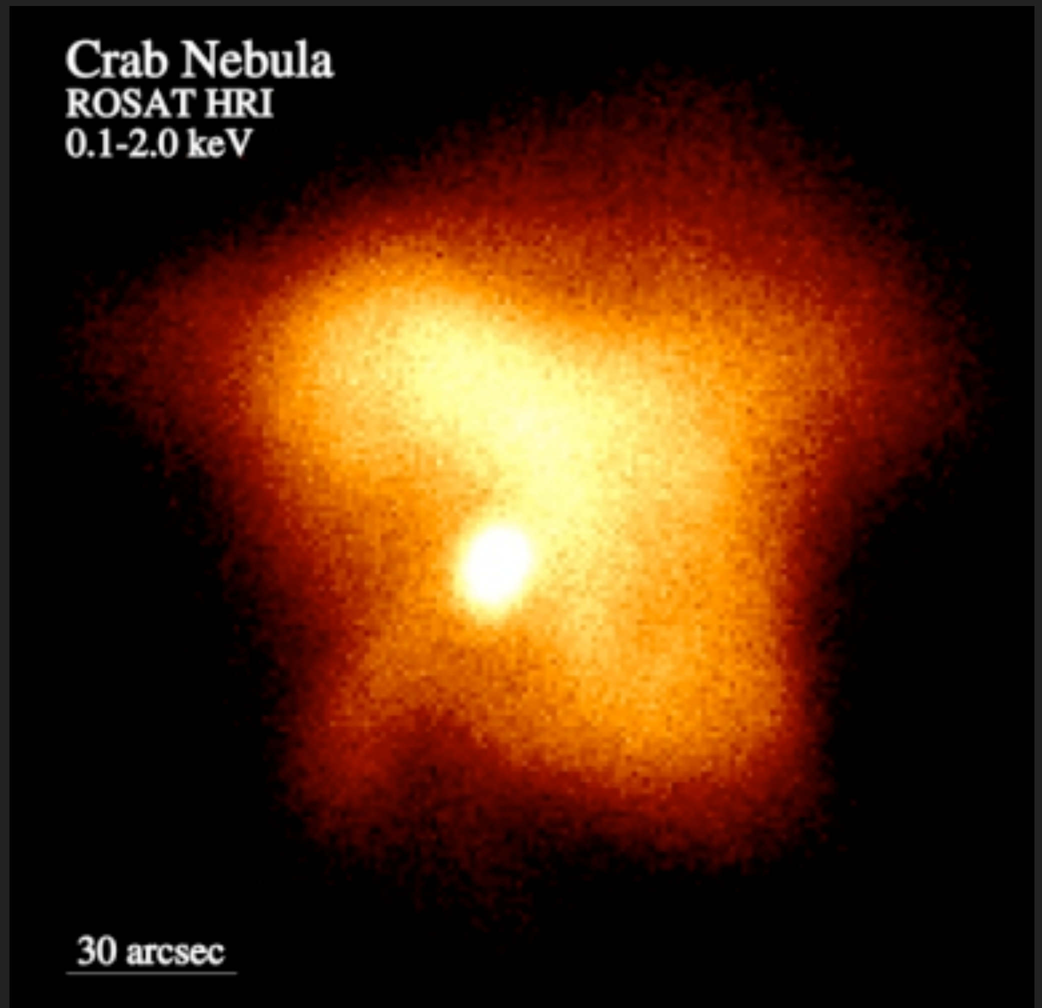


High Resolution Camera: two Micro-Channel Plates (MCP), each consist of a 10-cm square cluster of 69 million tiny lead-oxide glass tubes that are about 10 micrometers in diameter (1/8 the thickness of a human hair) and 1.2 millimeters long. The tubes have a special coating that causes electrons to be released when the tubes are struck by X-rays. These electrons are accelerated down the tube by a high voltage, releasing more electrons as they bounce off the sides of the tube. A crossed grid of wires detects this electronic signal and allows the position of the original X-ray to be determined with high precision.

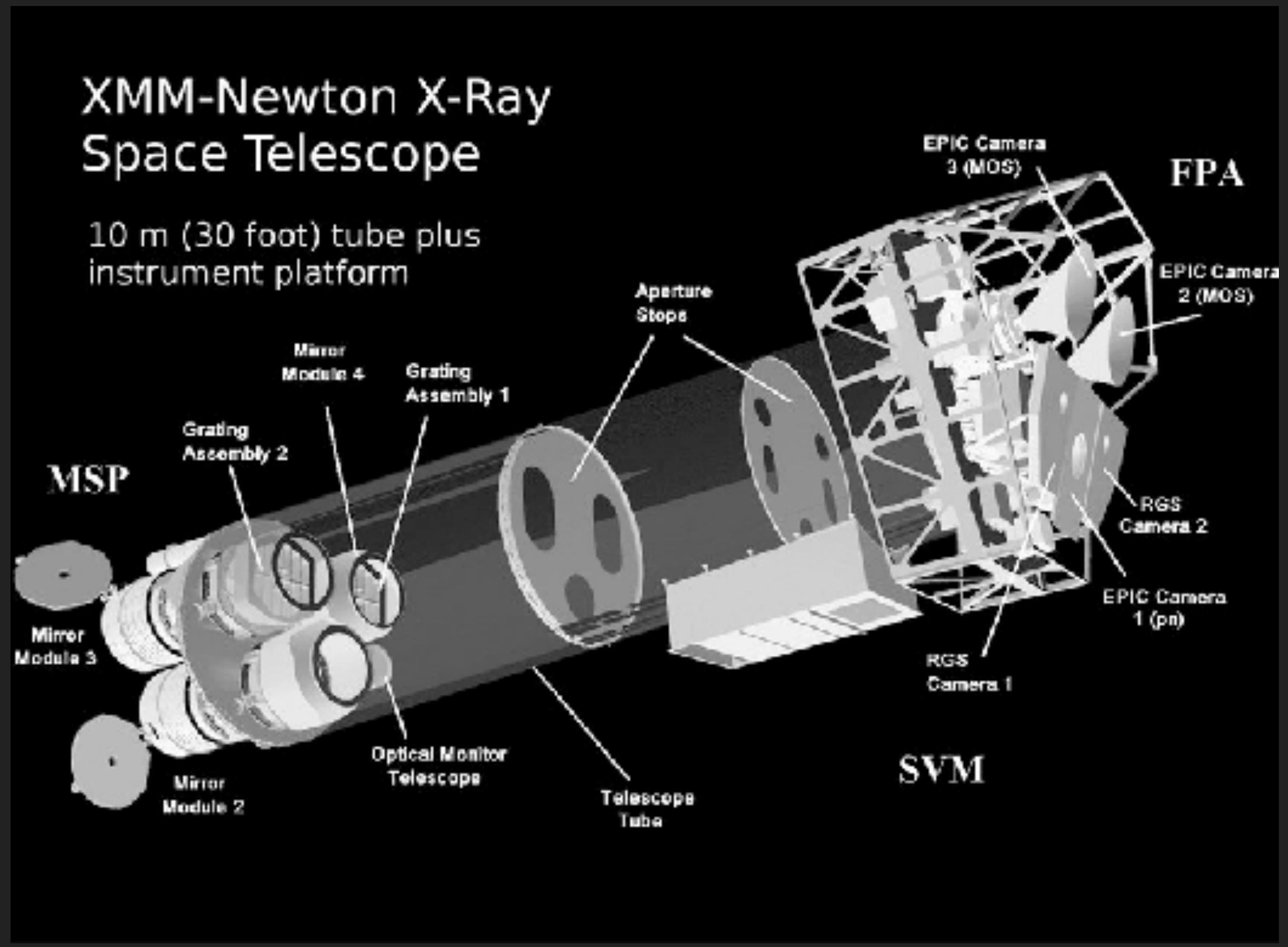


EPIC: state of the art CCDs coupled with powerful mirrors in terms of photon collecting capabilities

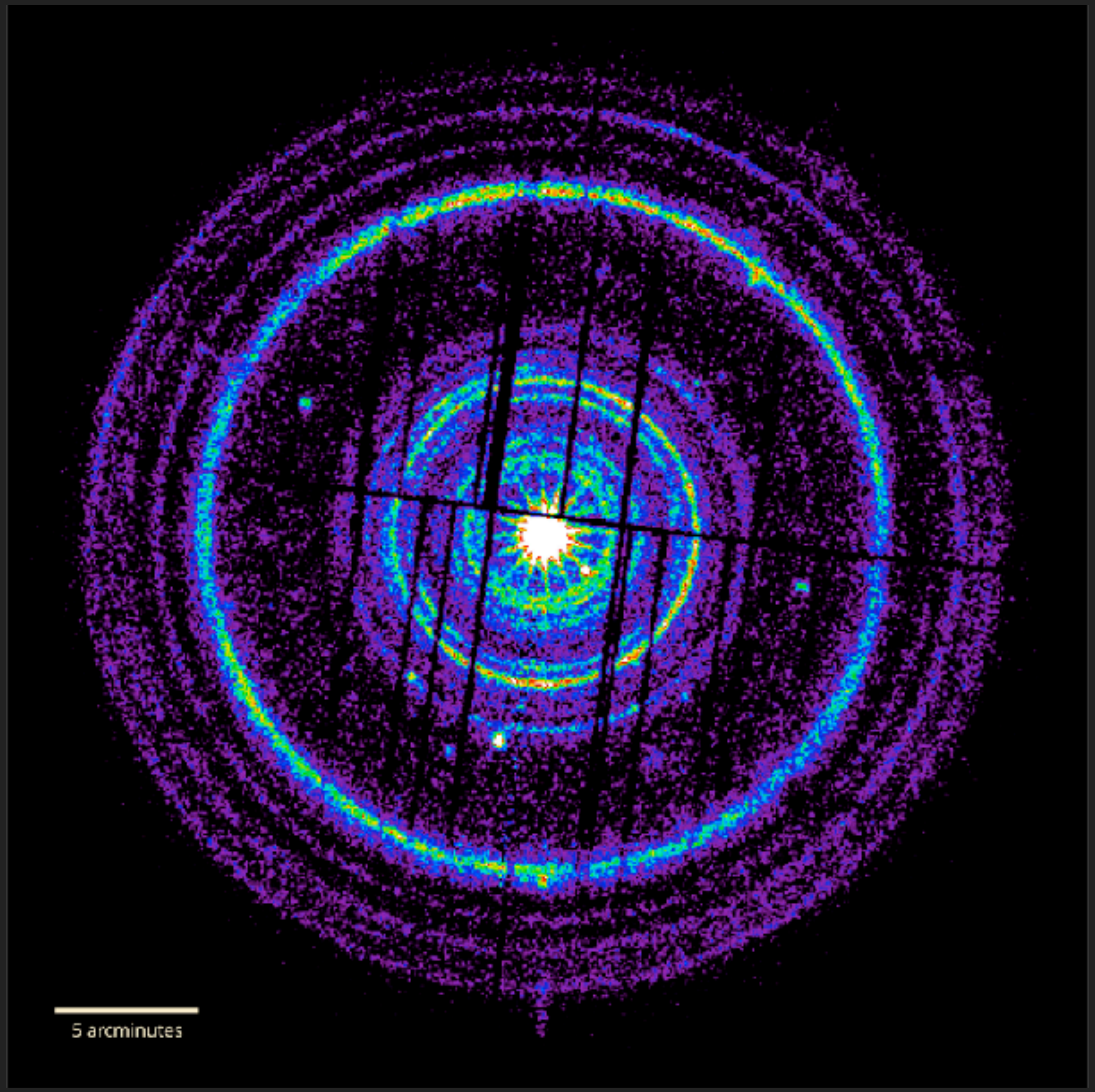


GRB221009A dust rings see with EPIC

https://www.esa.int/Science_Exploration/Space_Science/Brightest_gamma-ray_burst_illuminates_our_galaxy_as_never_before

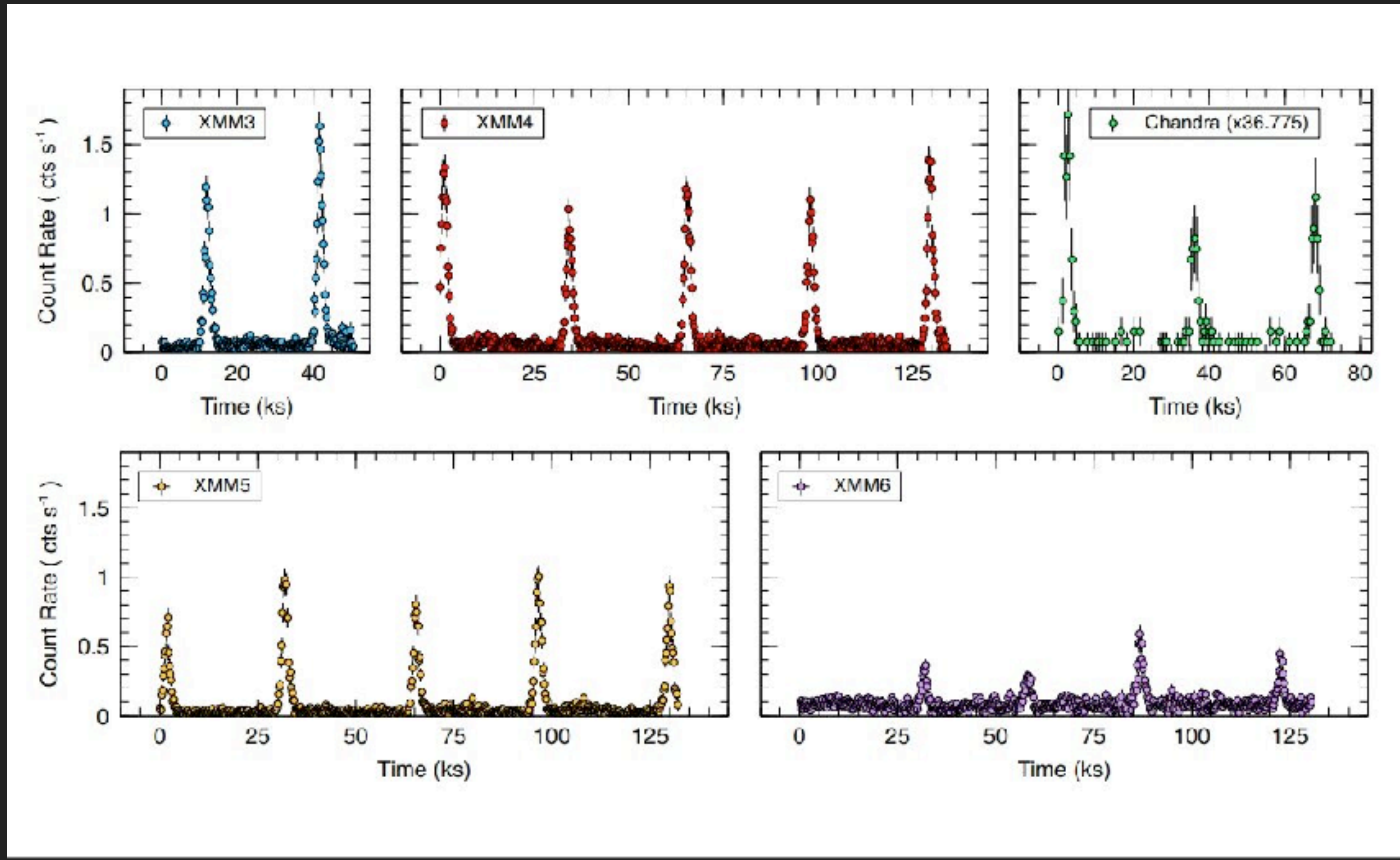


Quasi Periodic Eruptions in GSN 069 hosting a SMBH

https://phys.org/news/2022-07-astronomers-behavior-quasi-periodic-eruptions-galaxy.html

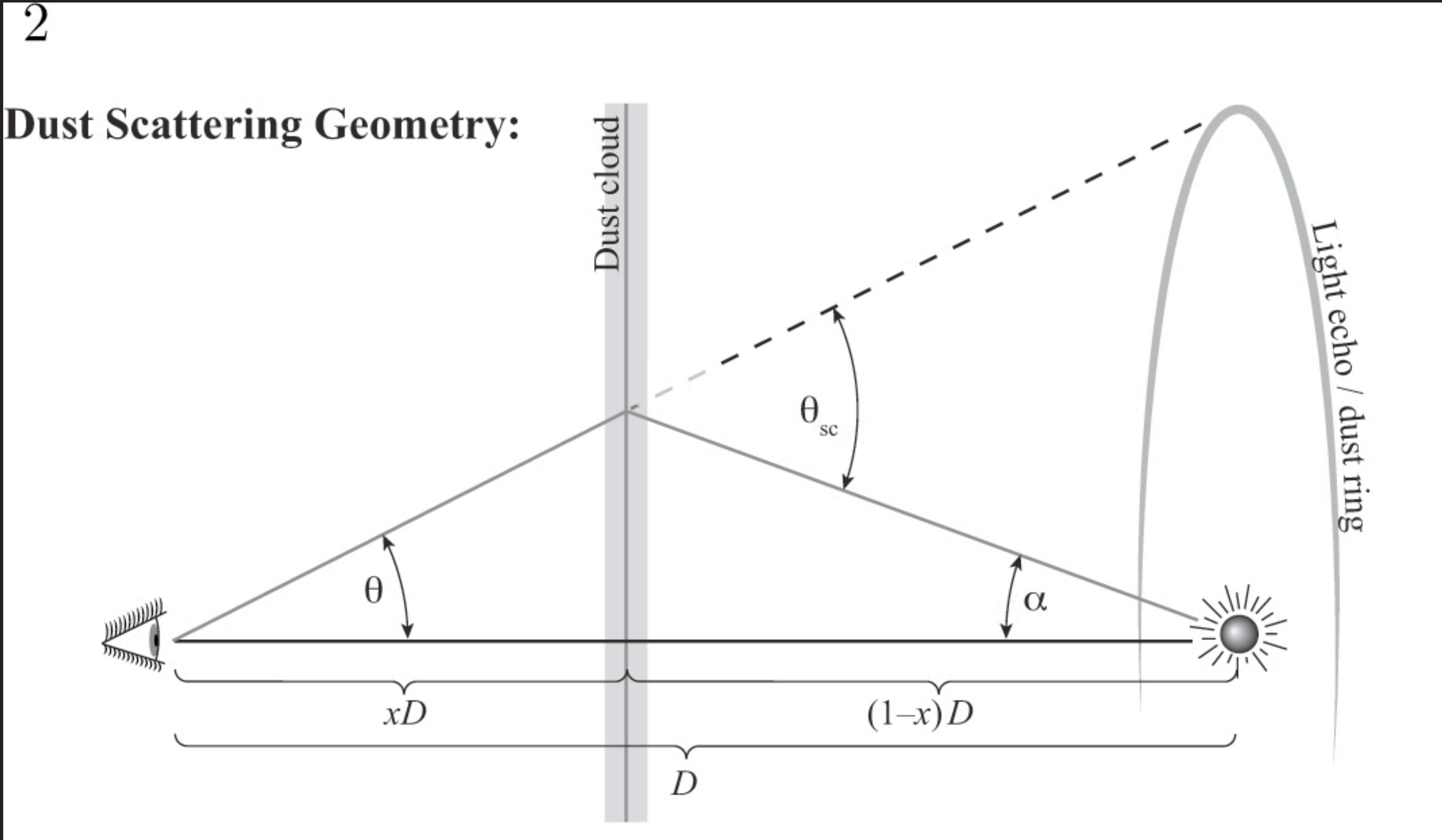
2
Dust Scattering Geometry:
Dust cloud
Light echo / dust ring
θ
θ_sc
α
xD
(1–x) D
D

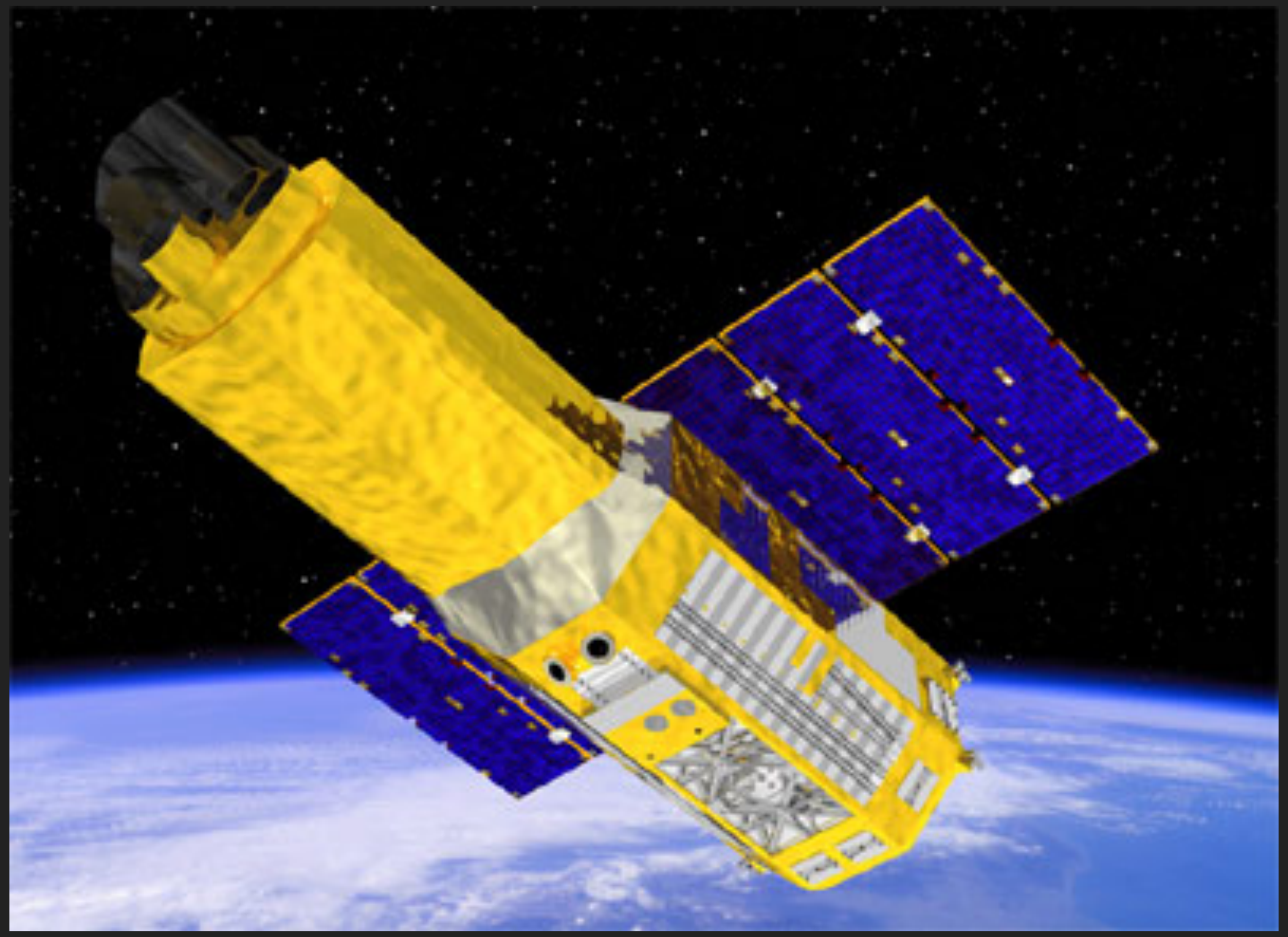

Suzaku (JAXA)
2005-2015
7.3 m focal length, ~400 $cm^2$@1.5 keV
Micro-calorimeter (failed soon after launch, cooling)
Non-imaging Hard X-ray detector

*JAXA launched Astro-H (Hitomi) in 2016 carrying also a micro-calorimeter but the satellite failed 1.5 months after launch (attitude control)*

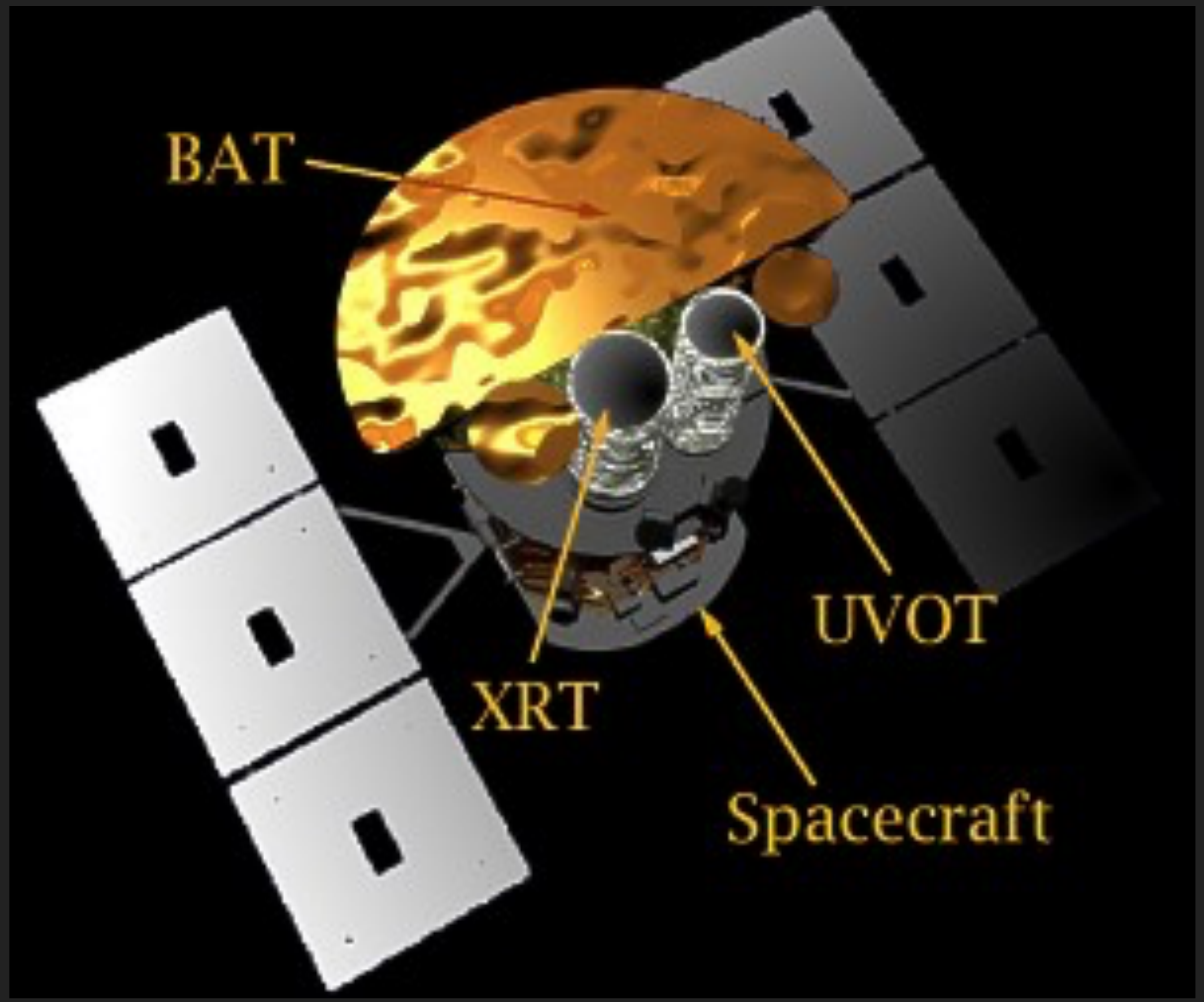


Swift/XRT (NASA)
launched in 2004
3.5 m focal length, ~110 $cm^2$@1.5 keV
0.2-10 keV
Very versatile, adapted for fast ToO

+ *MAXI, NICER, RXTE, ASCA, BeppoSAX…*

NASA Explorer mission launched in 2021

Can measure polarization and provide images at the same time!

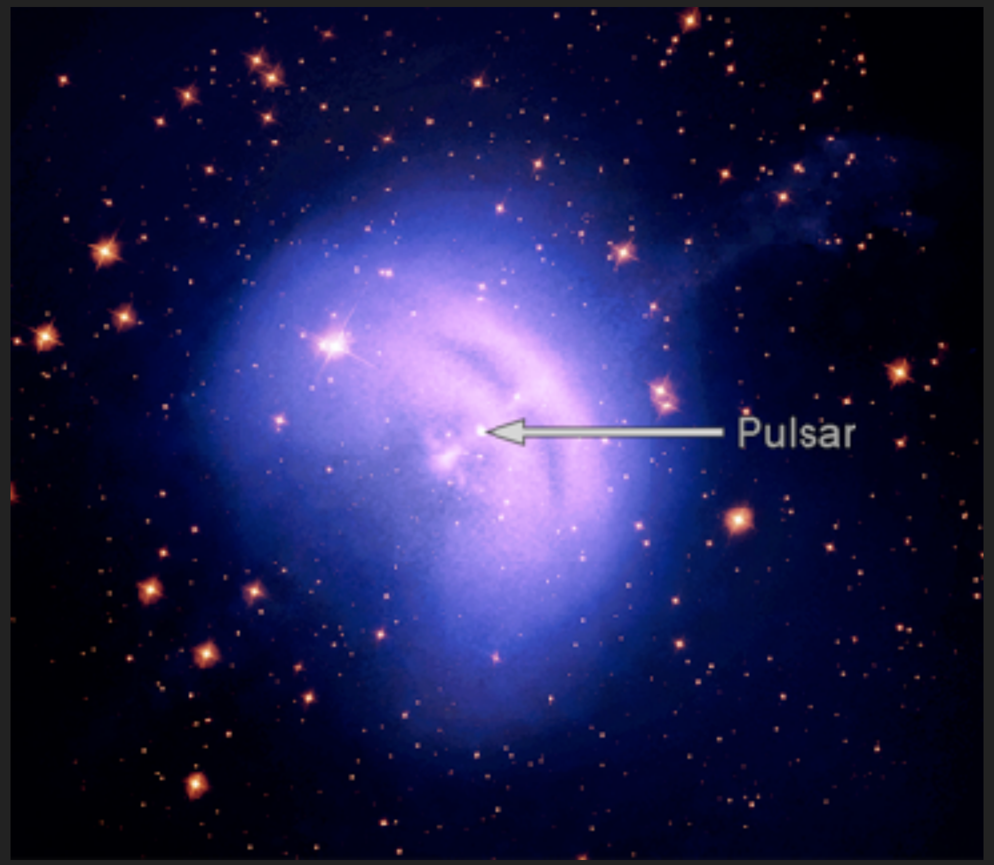


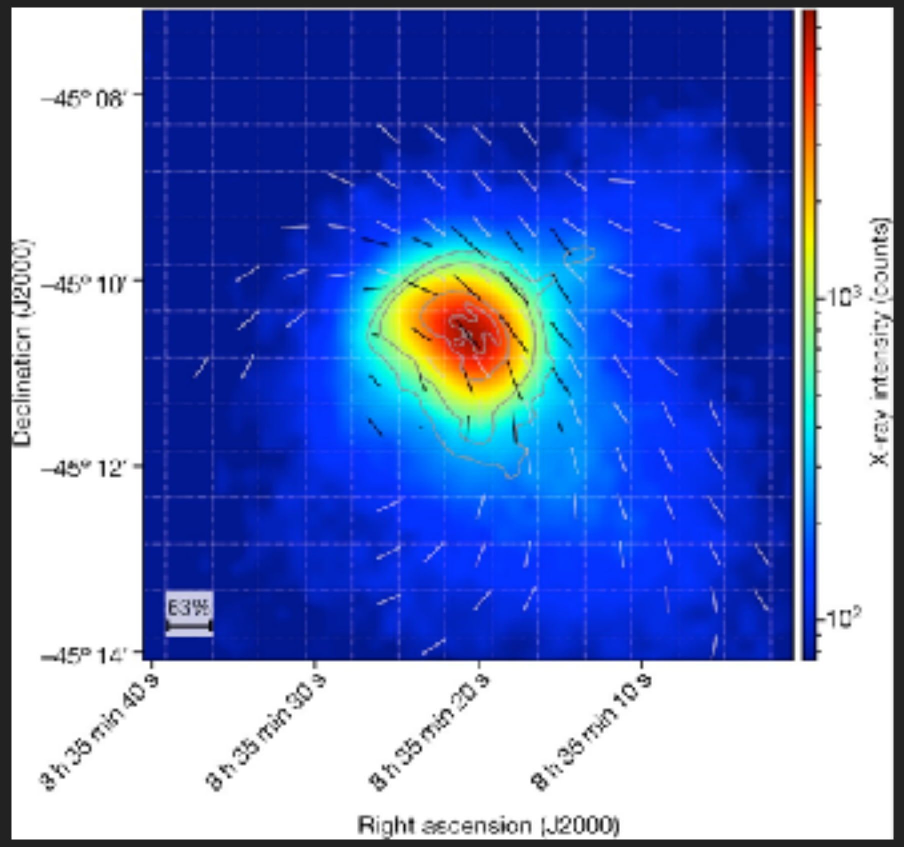


*Combined Chandra (pink), HST (magenta) and IXPE (blue) image of the Vela pulsar and nebula*

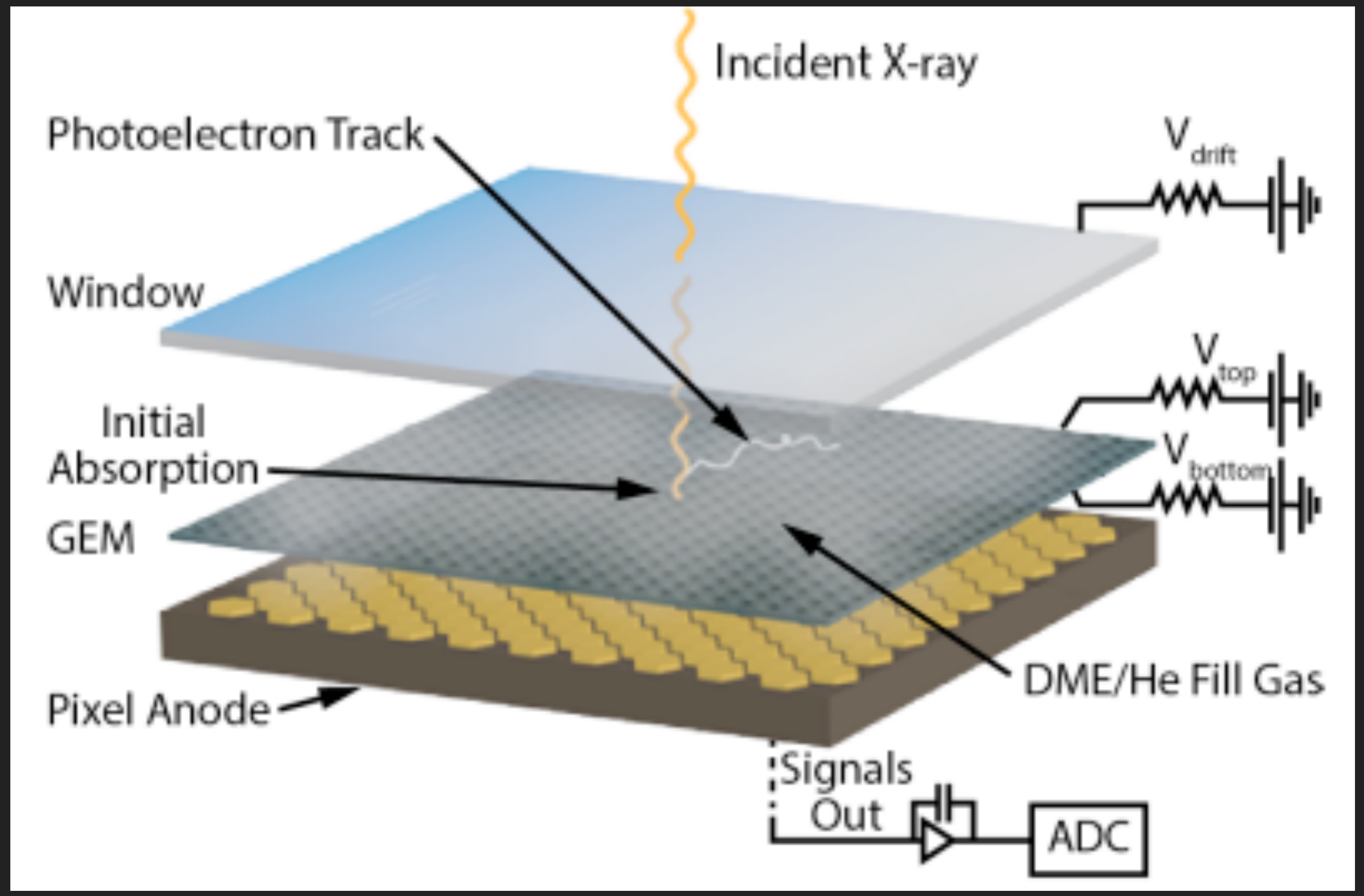


Polarized X rays interacting with a gaseous medium create photoelectons that are preferentially emitted in the polarization direction.

Photoelectron tracks mark the path of the photoelectron from the position of the initial X-ray interaction to its stopping point.

Analysis of the distribution of the initial directions of the tracks gives the degree of polarization and the position angle from the incident X ray.

In passing through a medium, photons will traverse a certain distance unaffected, until depositing its energy either by

a) Photoelectric absorption

b) Compton scattering

c) Pair production

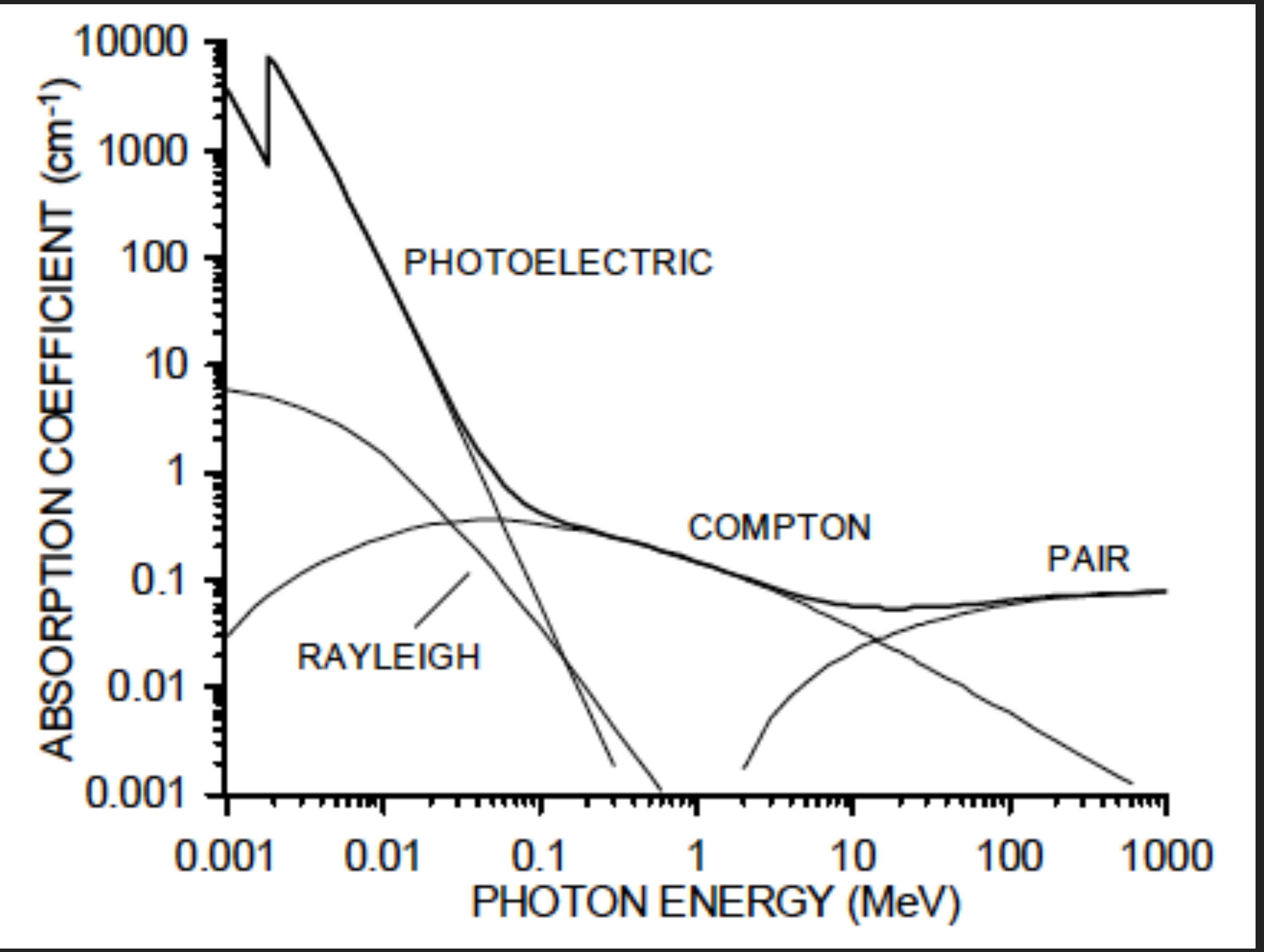


The probability of undergoing an interaction is an exponential function of distance. The fraction of photons that suffered any interaction after traversing a distance x is $f=1-\exp(-\mu x)$, where $\mu$ is the total absorption coefficient expressed in $cm^{-2}$.

We will focus on Photoelectric Absorption

An electron is emitted with the energy $E_{PE}=E_X-E_b$, where $E_b$ is the binding energy of the photo electron and $E_X$ the incident photon energy.

- Generally speaking X-ray detectors are based on the conversion of X-ray photons into electrical charge through the photoelectric effect

- In the early times gas proportional counters were used to convert X-rays in electrical signals. These detectors had the advantage to be simple in operation, but the drawback of the possibility of leakage and that a relatively large volume of gas is needed to de efficient in the detection. Spectral resolution is moderate

- Microchannel plates (MCPs) are compact electron multipliers of high gain. Channels can be as small as 2 μ providing excellent imaging properties (Chandra HRC). Energy resolution is poor.

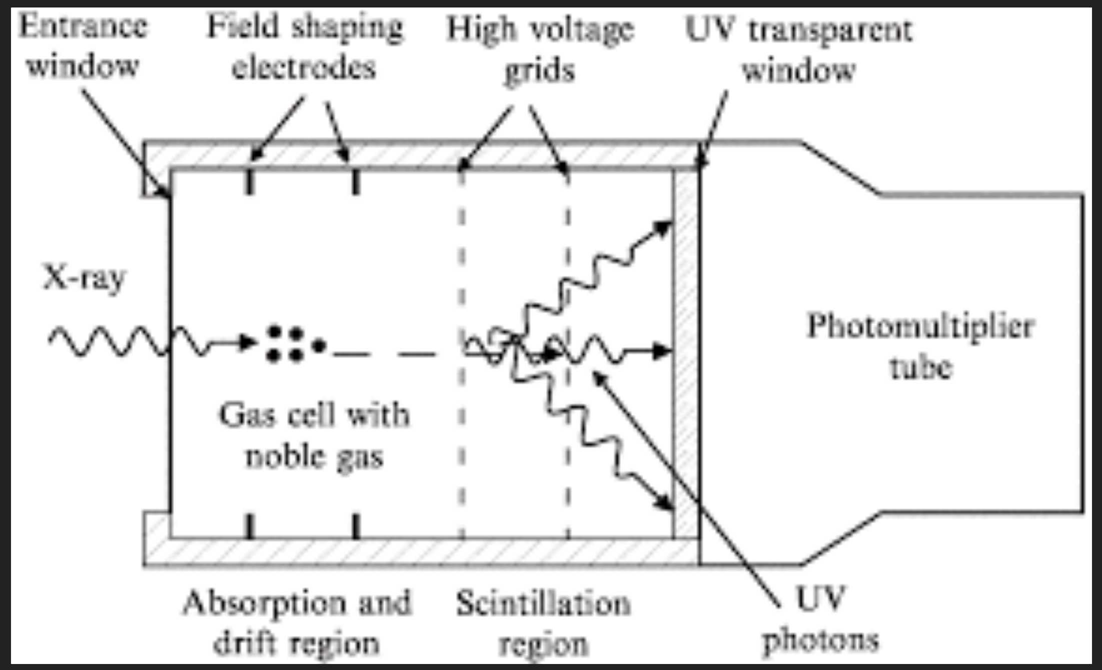


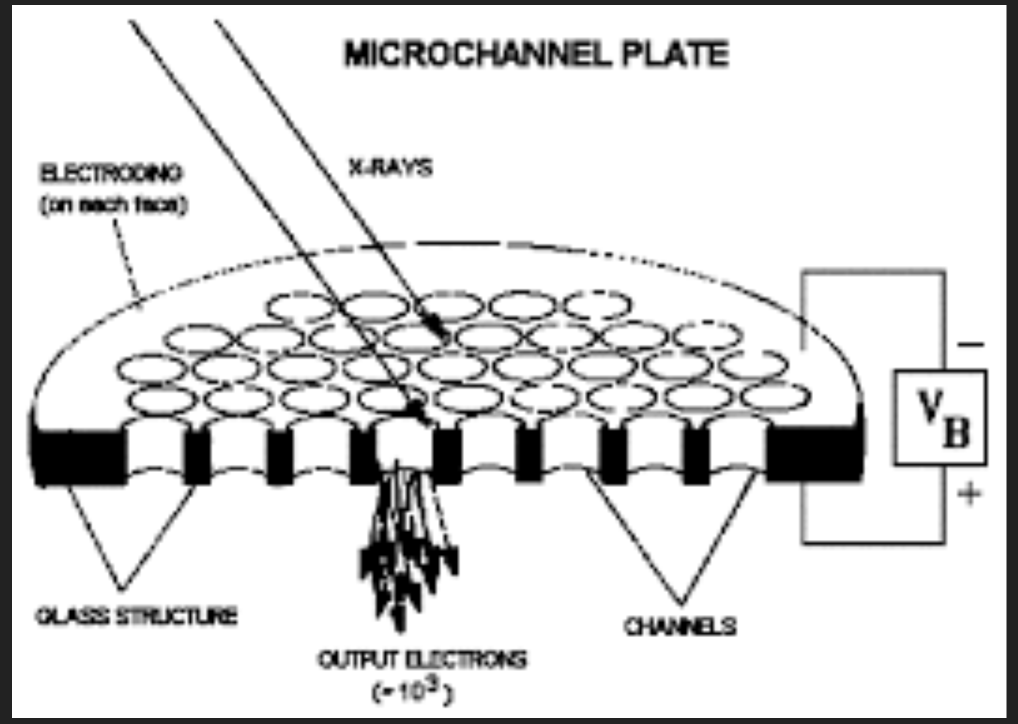

- The most used detectors those days in X-ray astronomy are the ones based on semiconductors (Si, Ge, CdTe,…).
- Such devices are the solid state analogues of gas-filled ionisation chambers, in the sense that there is no multiplication of the charge within the detecting material, and the generated charges/holes (collected after drifting within the semiconductor) are proportional to the energy of the incident particle. Advantage: can be in principle manufactured in any shape, is more dense than gas -> higher efficiency
- In order to have the best performances in terms of spectroscopy these detectors need to be cooled well beyond room temperature (to reduce thermal noise), but they are much more compact then gas filled detectors (which is a huge advantage in space applications)
- In X-ray astronomy Si based CCDs are implemented in all current space missions: they allow for low readout noise and hence good energy resolution (~100 eV) and at the same time they provide a high quantum efficiency.
- The minimum energy required to create a pair/hole is only 3.66 eV

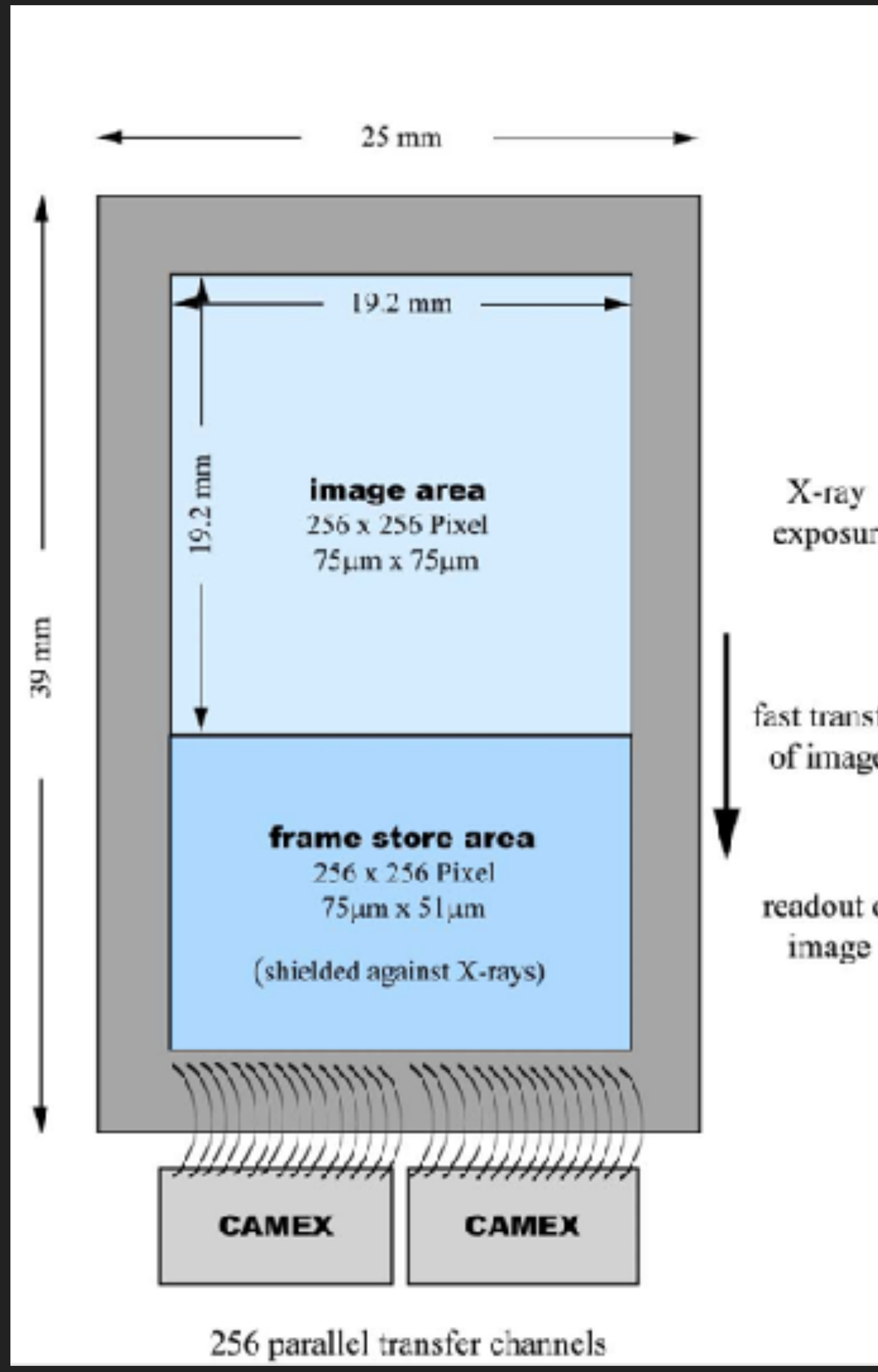


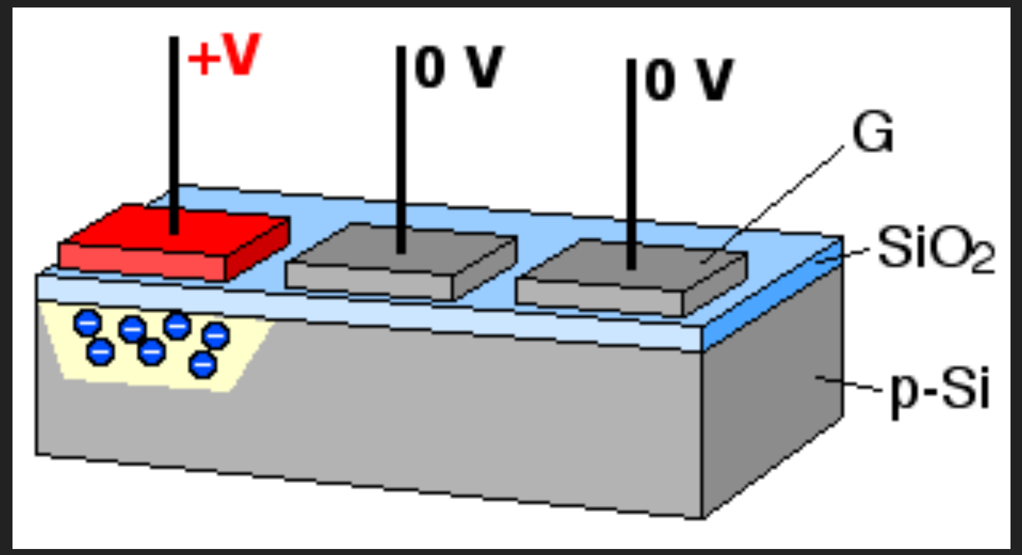

- The future of X-ray detection is nowadays represented by single photon calorimeters in which X-rays are detected via temperature pulses they induce in small absorbers, cooled to a fraction of a degree kelvin.
- Advantage: excellent energy resolution (few eV). Drawback: limited spatial resolution, complex thermal system
- Will be flying on XRISM (JAXA) and NewATHENA (ESA), see J. Wilms lecture

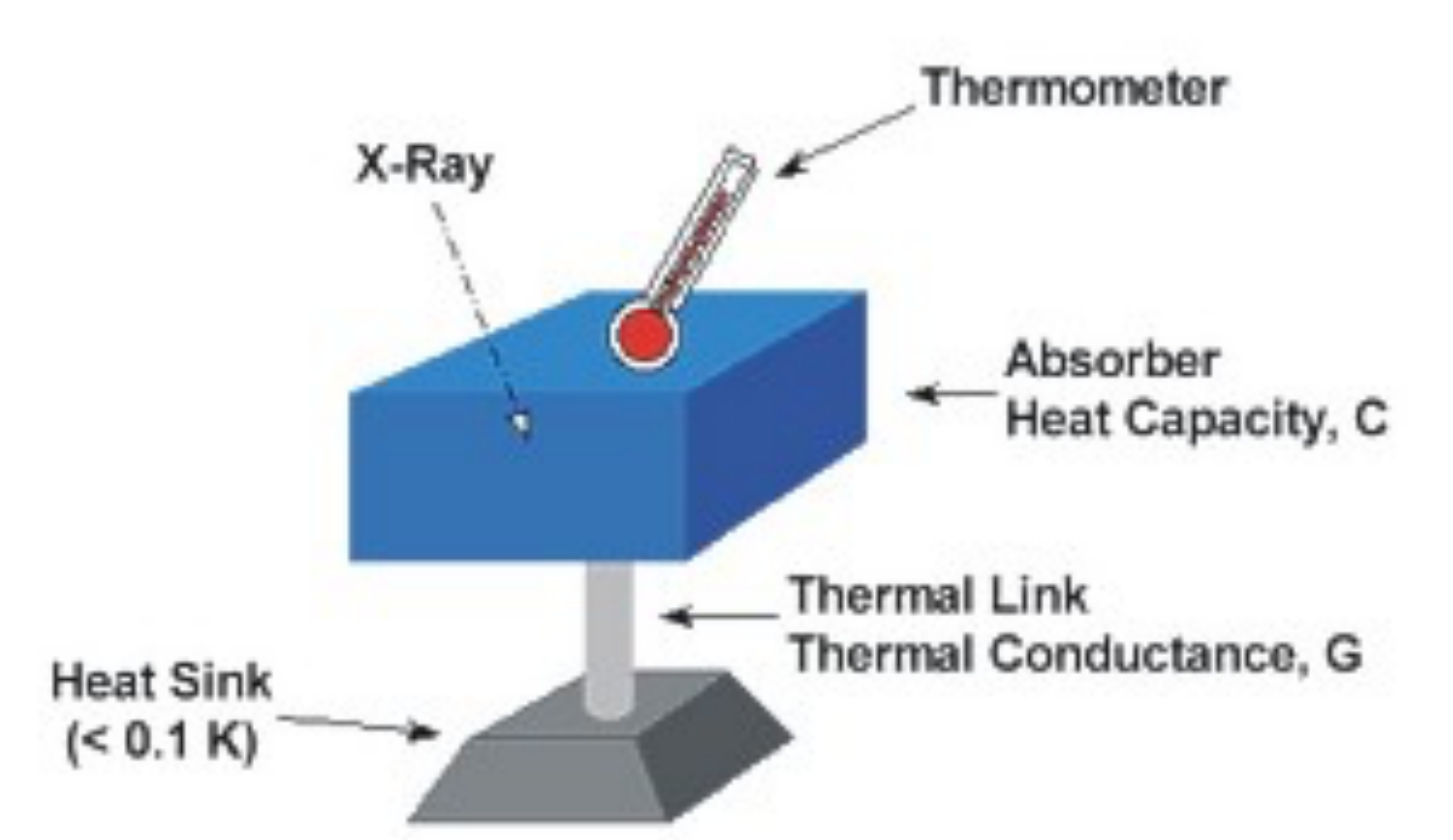

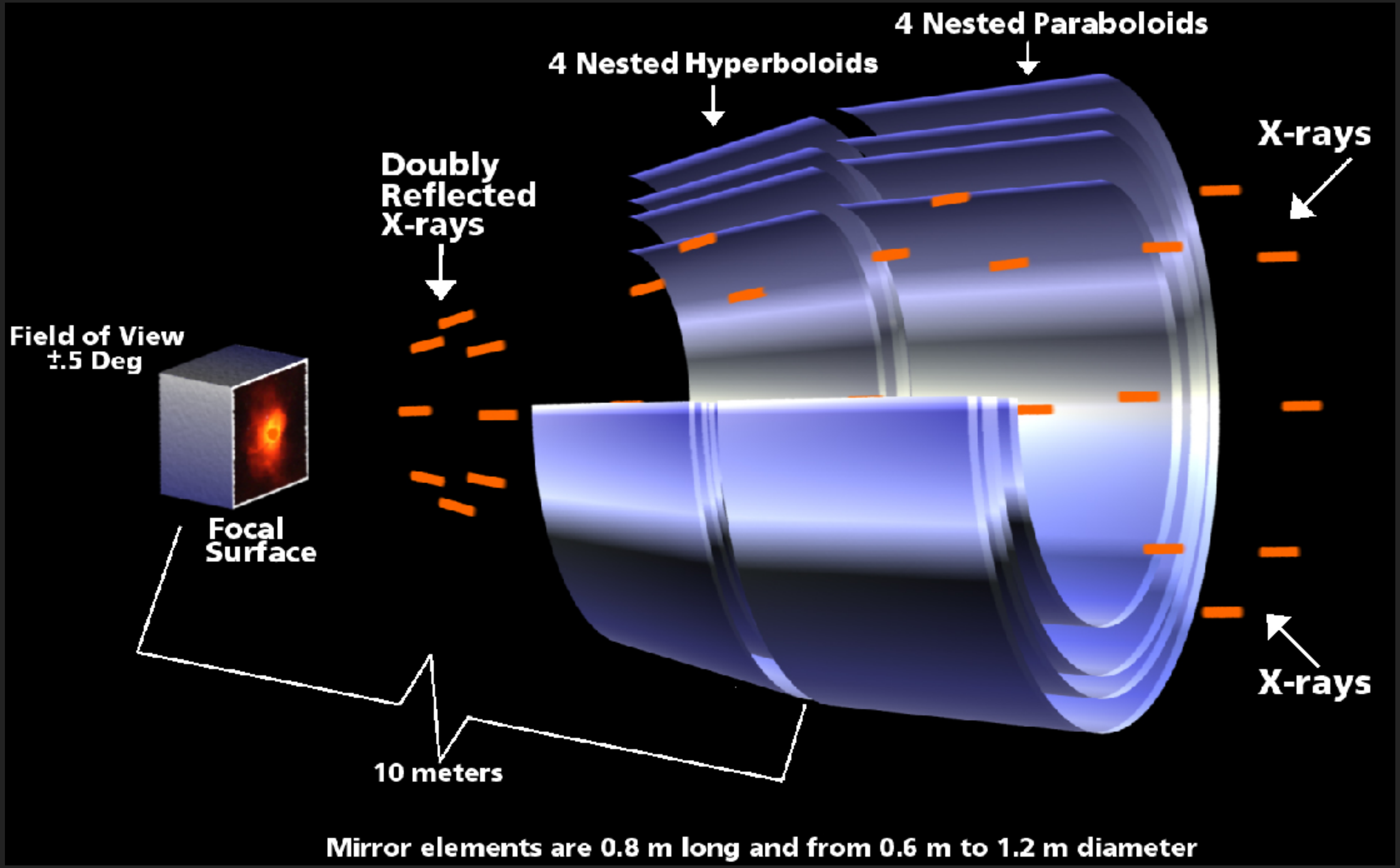
4 Nested Paraboloids
4 Nested Hyperboloids
Doubly Reflected X-rays
X-rays
Field of View ±.5 Deg
Focal Surface
X-rays
10 meters
Mirror elements are 0.8 m long and from 0.6 m to 1.2 m diameter

- The observation of a weak point source of X-ray flux $F$ (photons/cm2/s/keV) is always made in the presence of unwanted background $B$ (counts/cm$^2$/s/keV)
- $B$ is the sum of an intrinsic detector background $B_i$ (arising mainly from the interaction of cosmic rays and the detection medium) and the diffuse X-ray sky background $B_d$, called CXB, discovered at the same time of Sco X-1.
- If the quantum efficiency of the detector is $Q$ counts/photon and its aperture is $\Omega$ in steradians
    - $B_d = Q\,\Omega j_d$ where $j_d$ is the diffuse background flux (ph/cm$^2$/s/keV/sr)
- If all quantities are constant over the observation time $t$, then statistical fluctuations in the background $B$ determine the sensitivity of the instrument
- The minimum detectable flux $F_{min}$ for a given signal-to-noise ratio $S$ is that flux that produces a count $S$ standard deviations above $B$
- Assuming the bandwidth of the instrument $\delta E$, the geometric area for the collection of source photons (and diffuse X-ray background) is $A_s$ and $A_b$ the equivalent detector background area then
    - $F_{min} = (S/QA_s)\,[B_iA_b + Q\,\Omega j_d\, A_s)/t\delta E]^{1/2}$


Lobsters and other kind of decapods are a rare example in Nature where the vision is obtained by reflection and not by refraction. This kind of vision is adapted for low-background wide vision (like the dark deep sea).

Can be adapted to X-rays (Angel, 1979)!

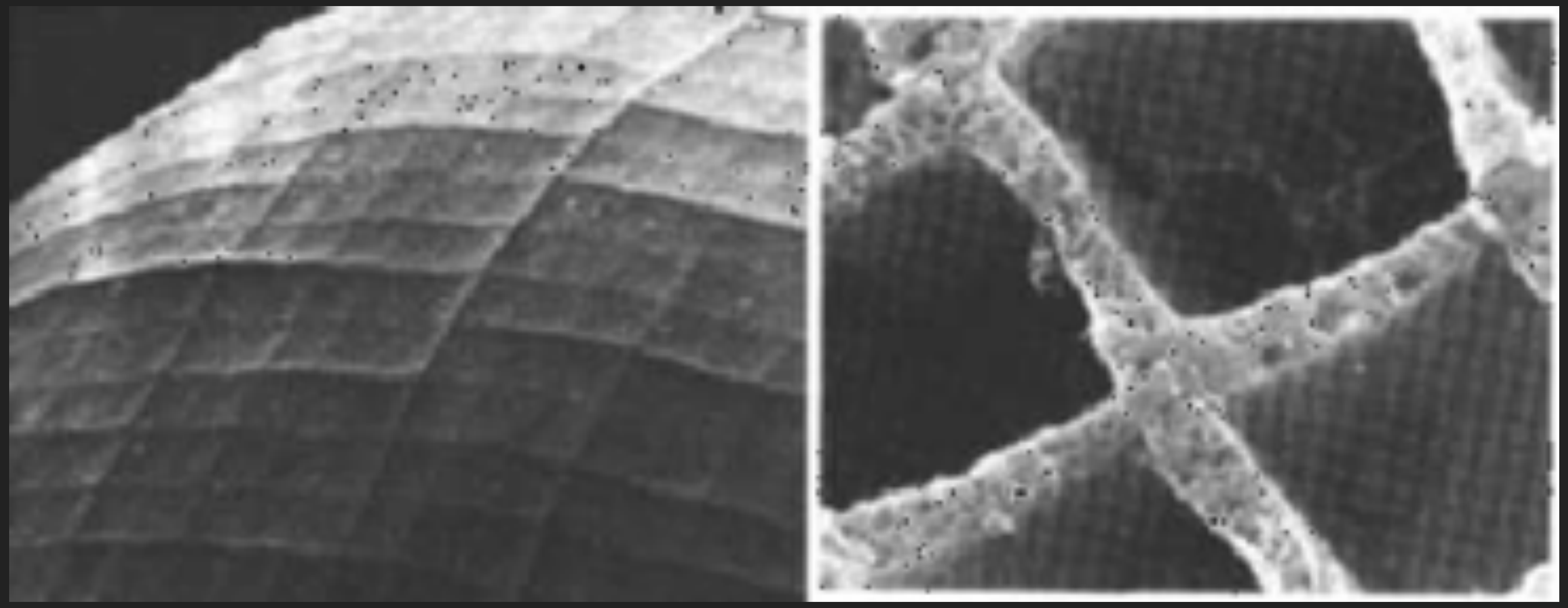

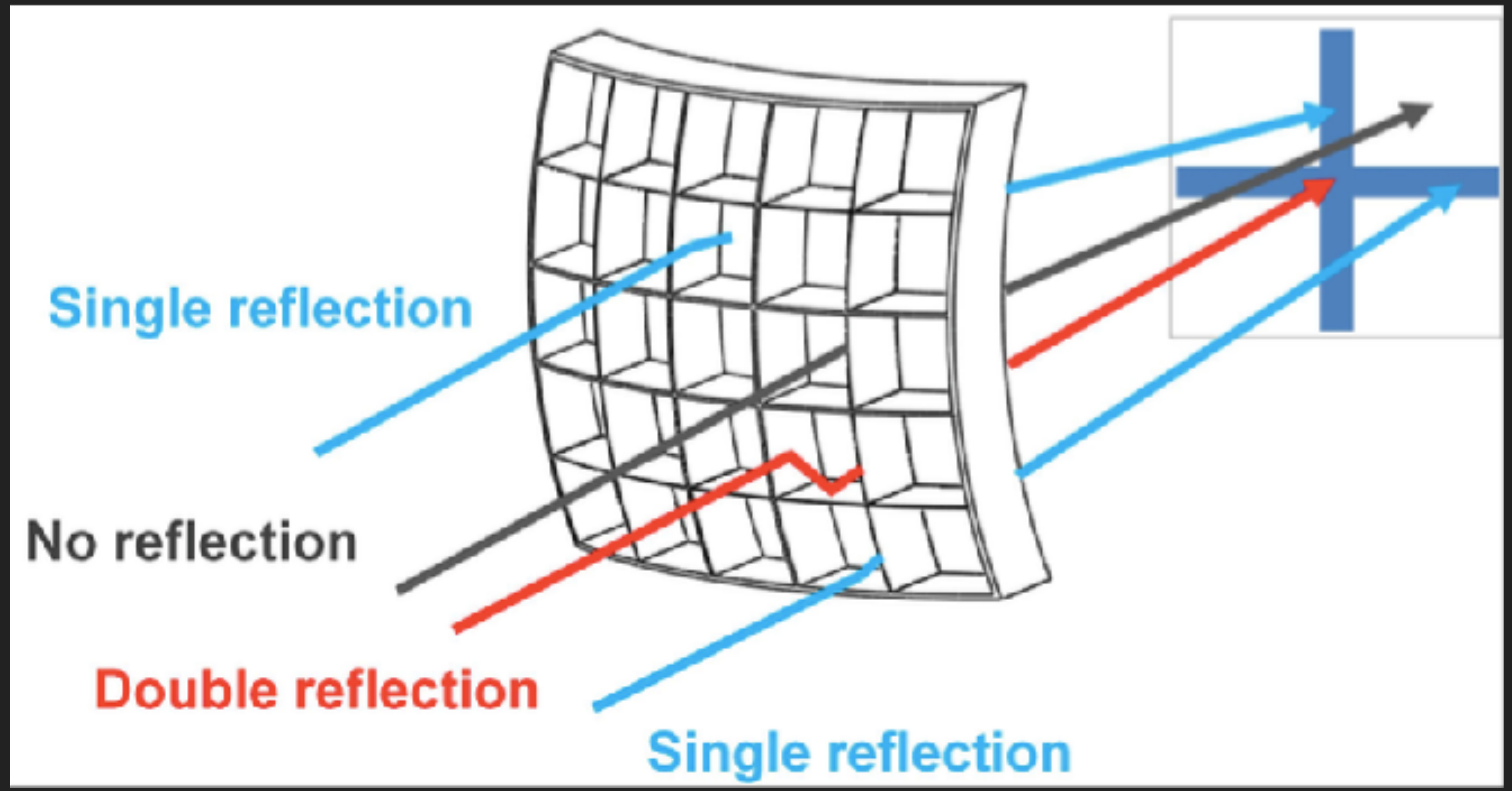


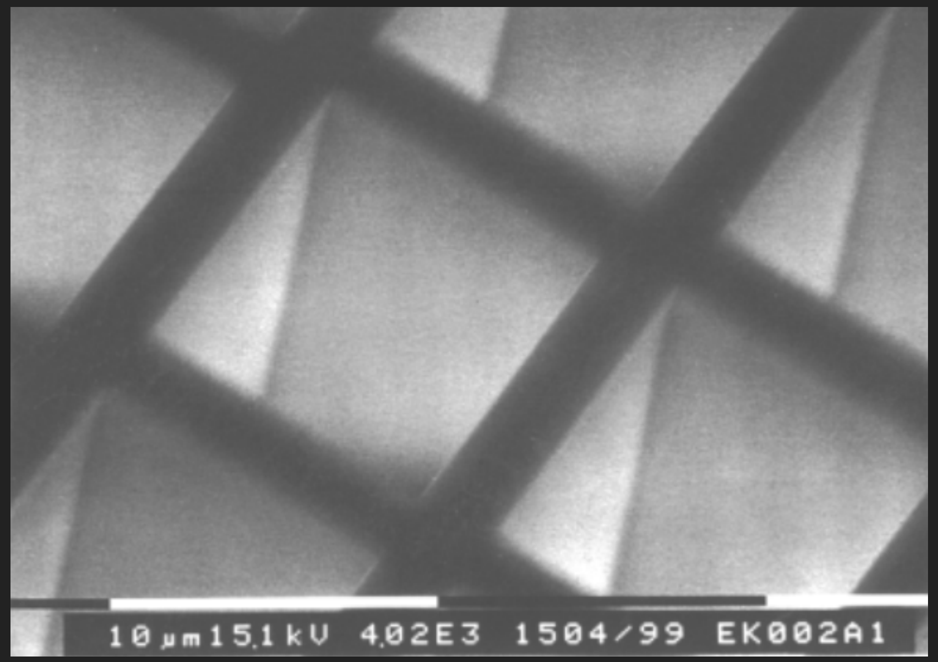

*40 microns pitch lead glass MPOs (micro-pore optics) produced by Photonis*

- « Lobster Eyes » are very light (few kg vs. several tens of kg for traditional X-ray optics)
- Hence they are adapted for relatively small missions like SVOM (total mass ~1000 kg) or SMILE  and Einstein Probe (small mission developed jointly by ESA and CAS). TEIA (EP pathfinder) has already produced encouraging results.
- They have a peculiar Point Spread Function (The one of MXT is shown, small FOV version, to be flown on SVOM)
  - 50% of the flux in the central peak, 22% in each arm, the rest in a diffuse patch, lead glass MPOs
- But micropore optics in general can be used also in a Wolter-I approximation (single peaked PSF, small FOV) as foreseen for the next major X-ray observatory NewATHENA (based on Si)

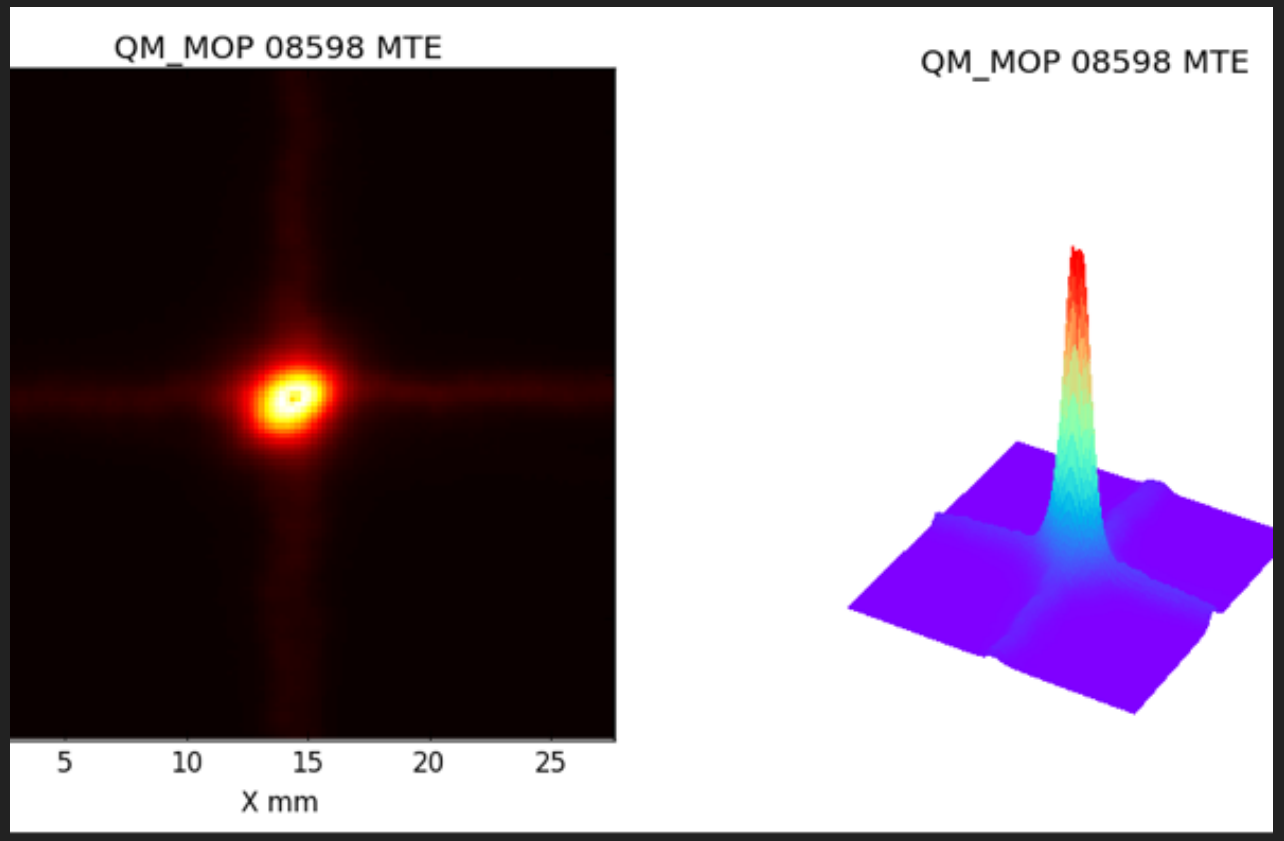


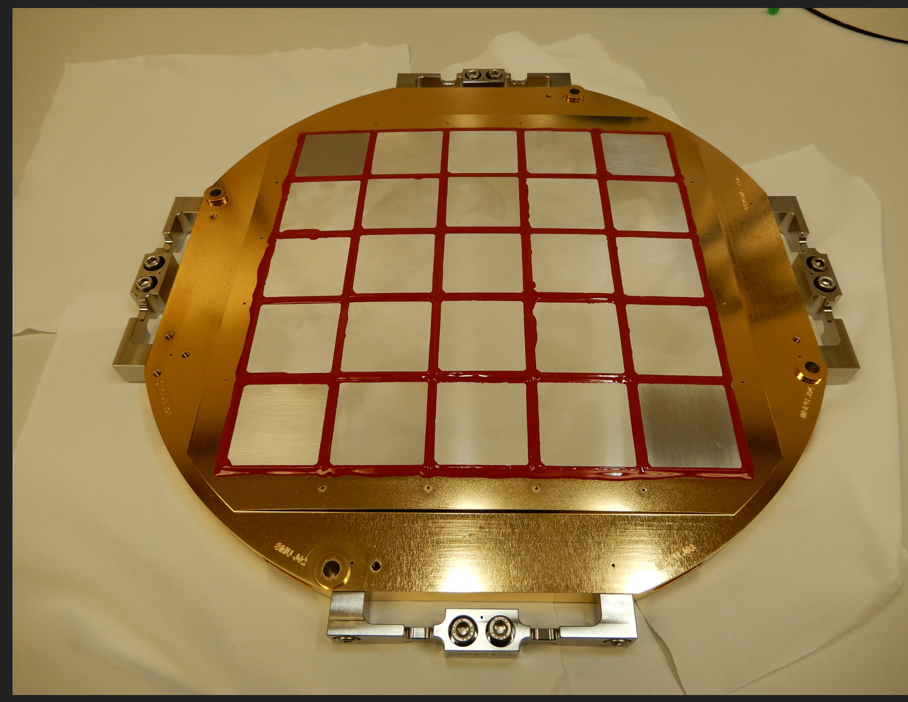

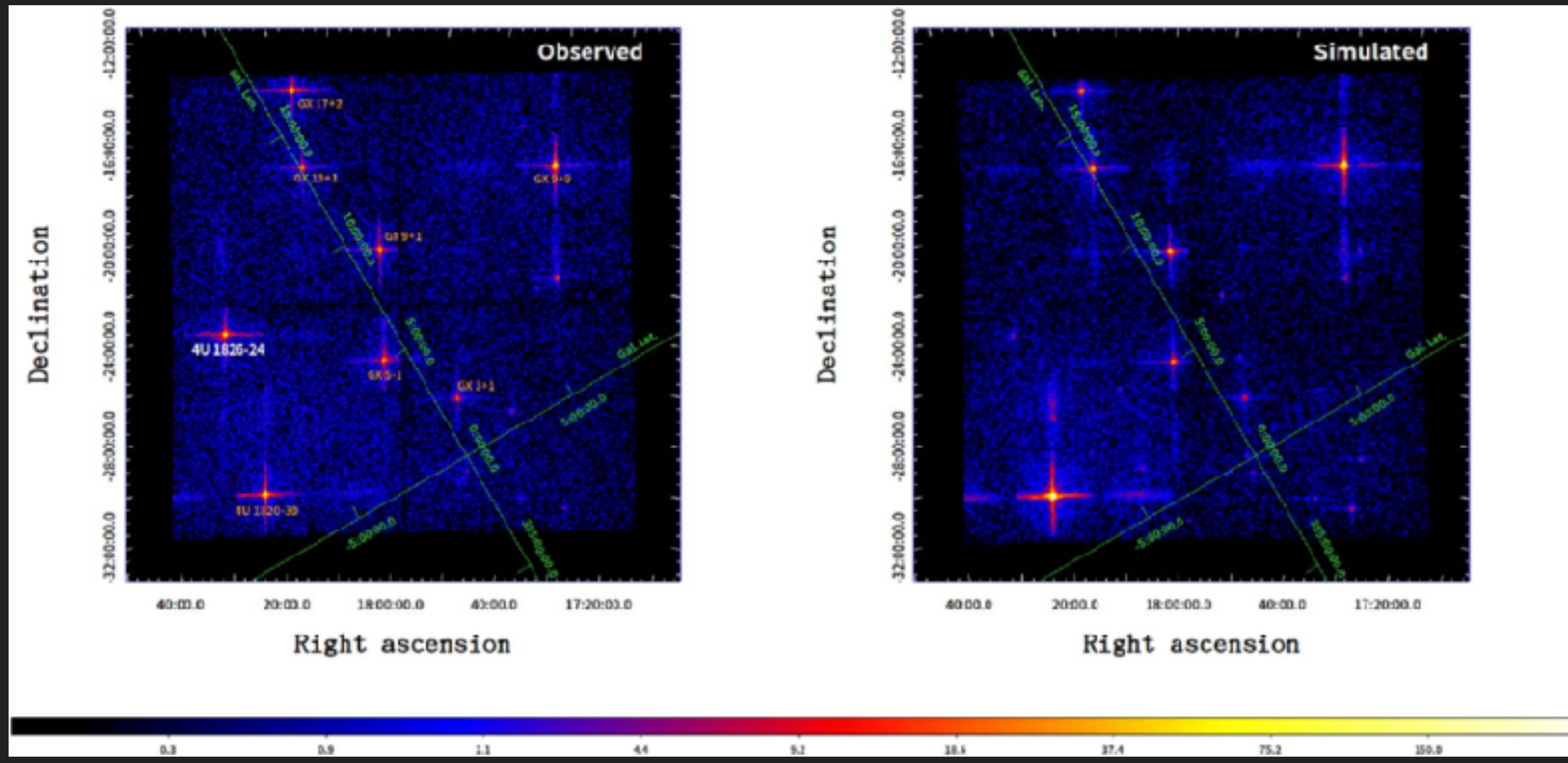

# GRB FOLLOW-UP WITH THE MXT

**Space Variable Object Monitor**



SPACE

ECLAIRS

MXT

VT

GRM

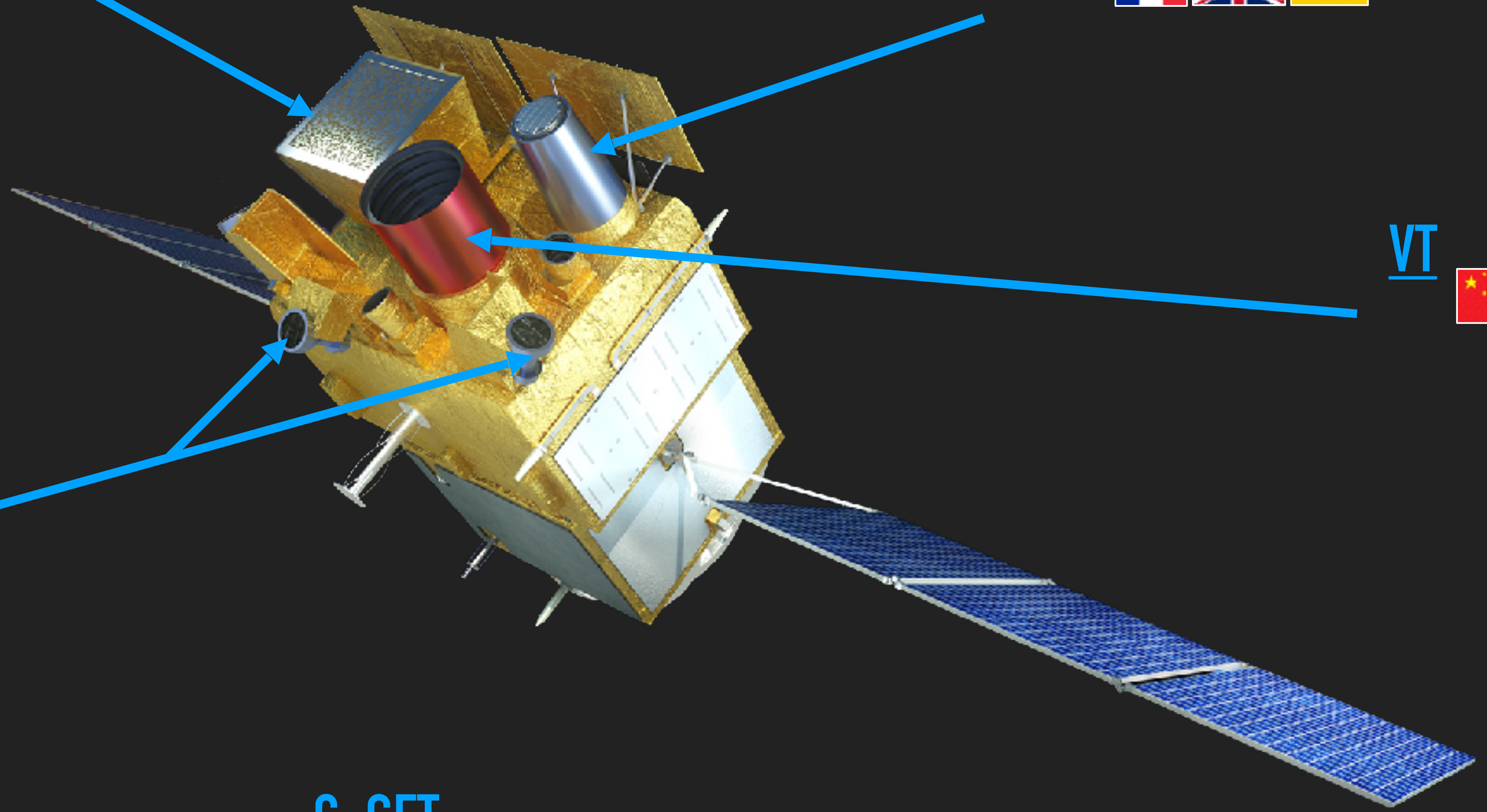

GROUND

GWAC

C-GFT

F-GFT (COLIBRI)

- Detection of all types of GRBs, with special focus on *high z events*
- Provide fast, reliable and accurate GRB positions
- Measure the temporal and spectral GRB properties *from visible to MeV*
- Quickly identify the SVOM GRB afterglows and provide (sub-)arc sec positions
- Quickly provide redshift indicators for SVOM GRBs

- Major discovery (GRB 970228) by the Italian-Dutch BeppoSAX satellite: GRBs are followed by long term declining X-ray emission; well localized (~ arcmin)
- This led to the discovery of optical afterglows and finally of GRB host galaxies
- Measured (spectroscopic and photometric) redshifts between ~0.1 and ~9.4
- $E_{ISO}$~$10^{50}$-$10^{54}$ erg
- GRBs are powerful cosmic explosions
- Fast reaction is the key!

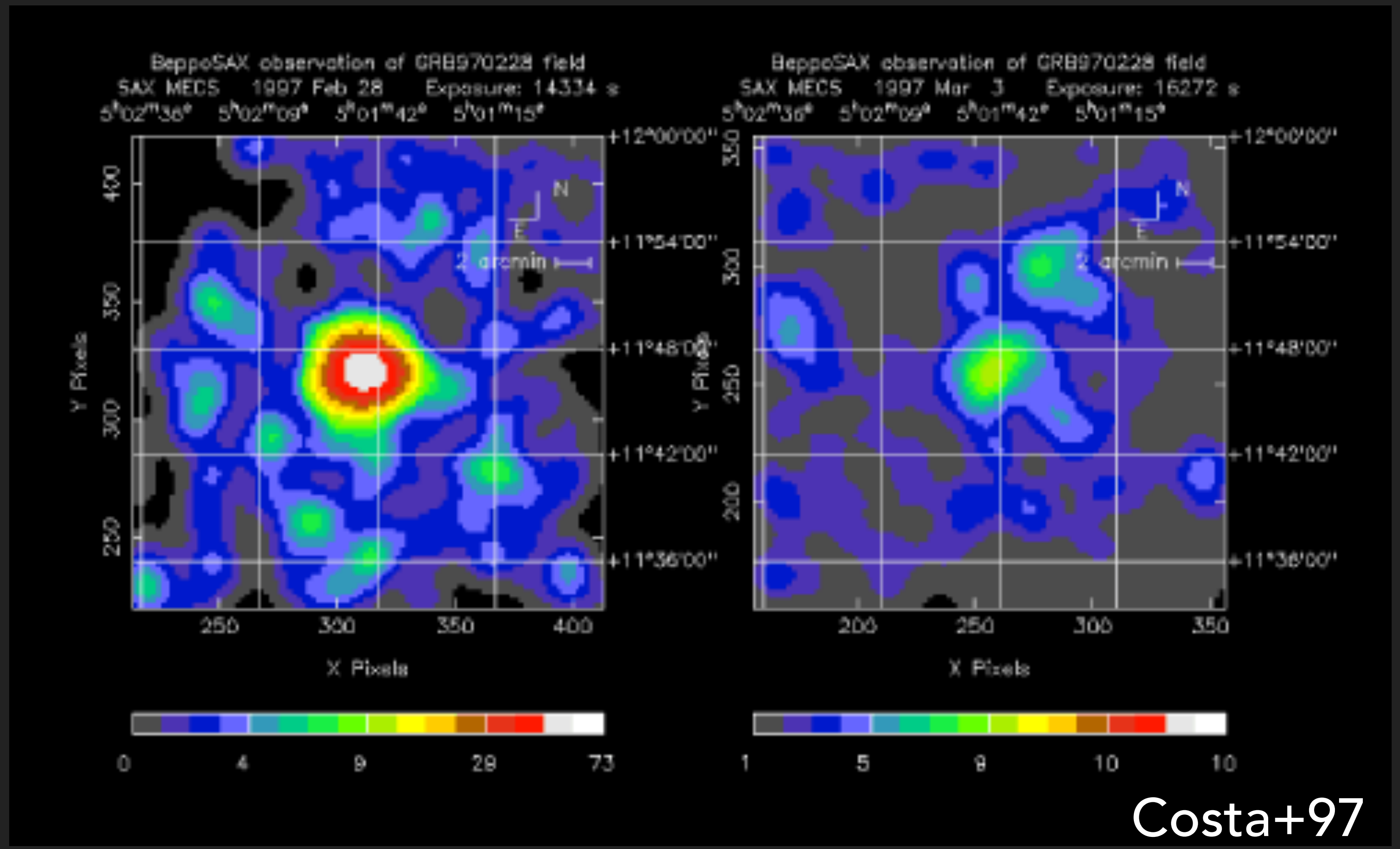

Costa+97


BeppoSAX

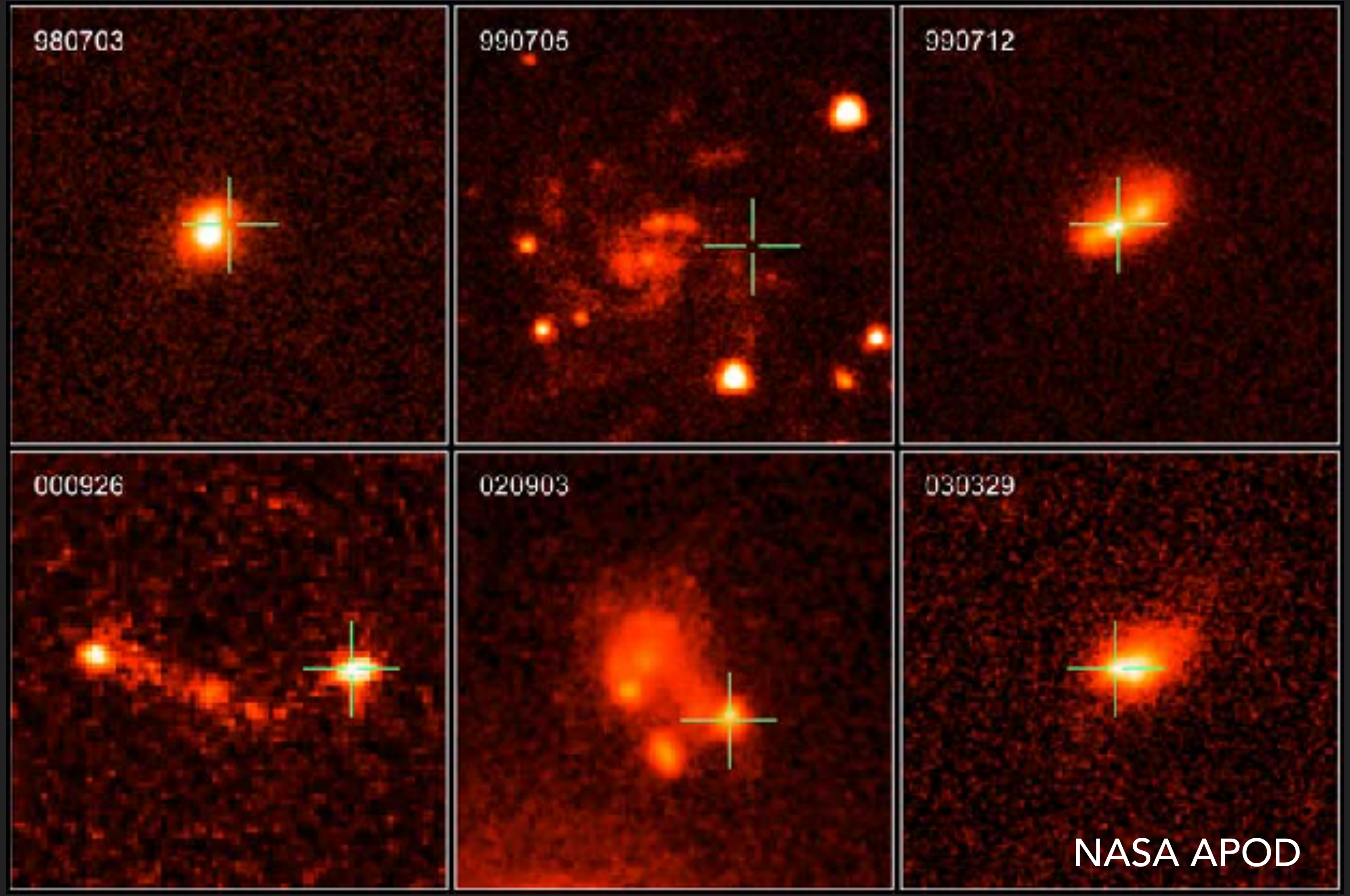

NASA APOD

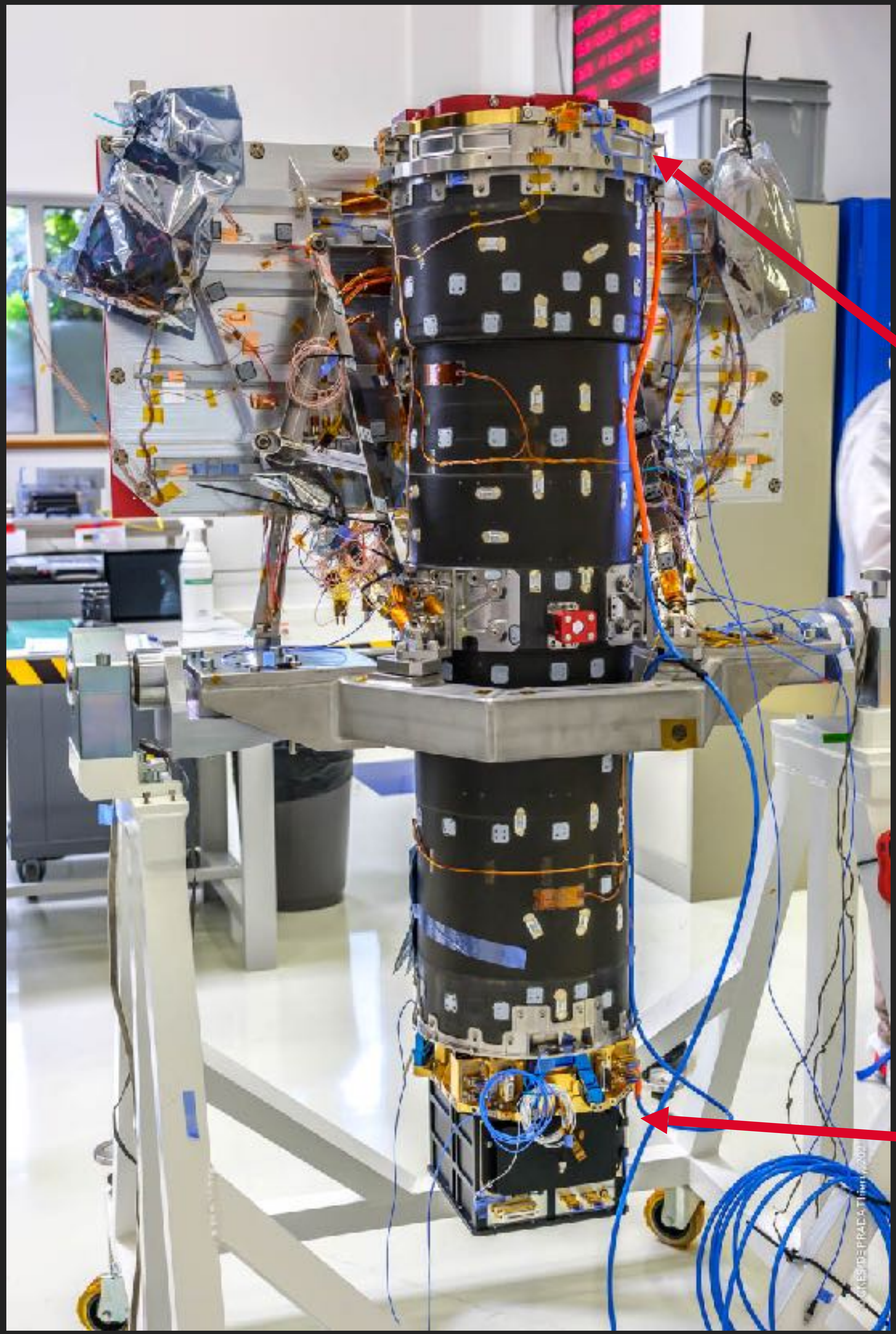

MXT

MXT Optics

| | |
|---|---|
| Energy range | 0.2 – 10 keV |
| Field of View | 58 × 58 arcmin |
| Angular resolution | 10 arcmin at 1.5 keV |
| Source location accuracy | < 120 arcsec for 80 % GRBs |
| Effective area | $\sim 35$ cm$^2$ at 1.5 keV |
| Sensitivity ($5\sigma$) | 10 mCrab in 10 s |
| | 150 $\mu$Crab in 10 ks |
| Energy resolution | < 80 eV at 1.5 keV |
| Time resolution | 100 ms |

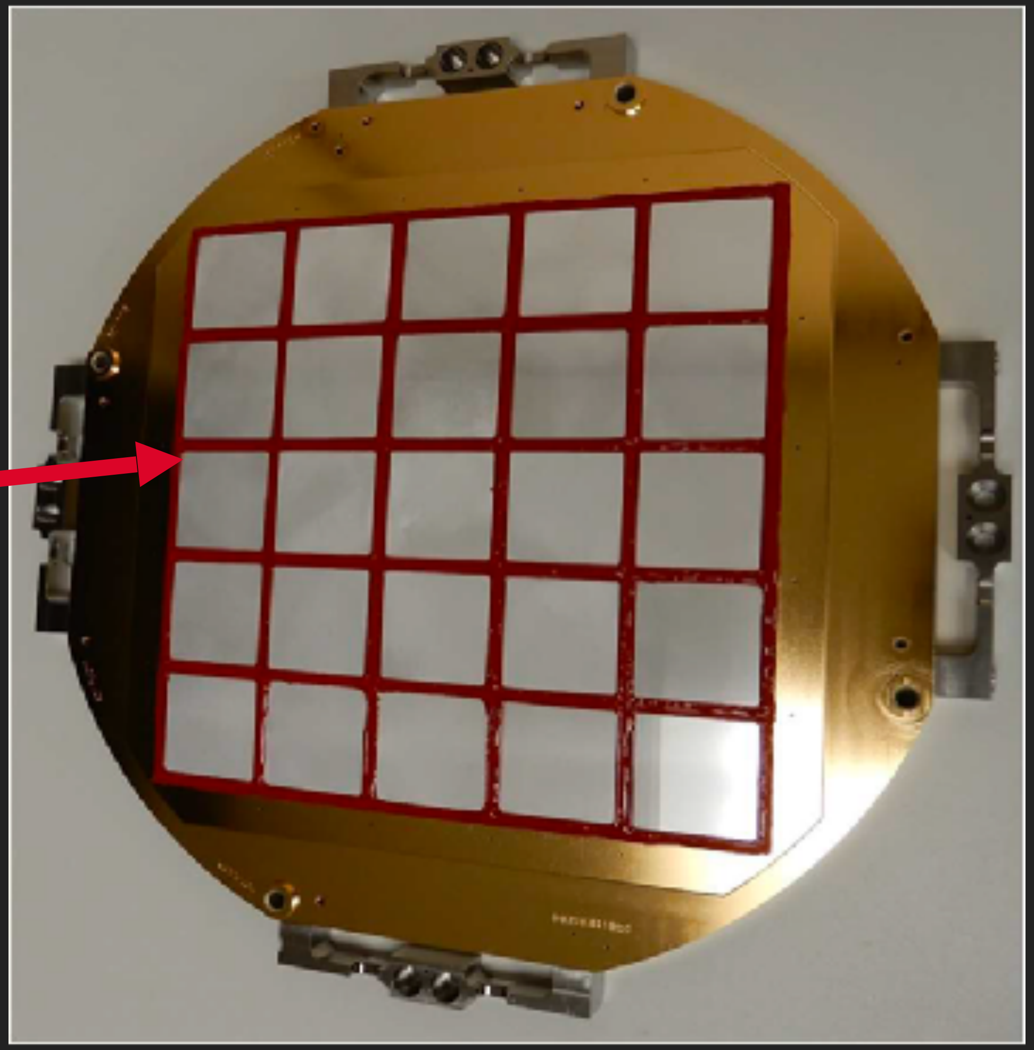

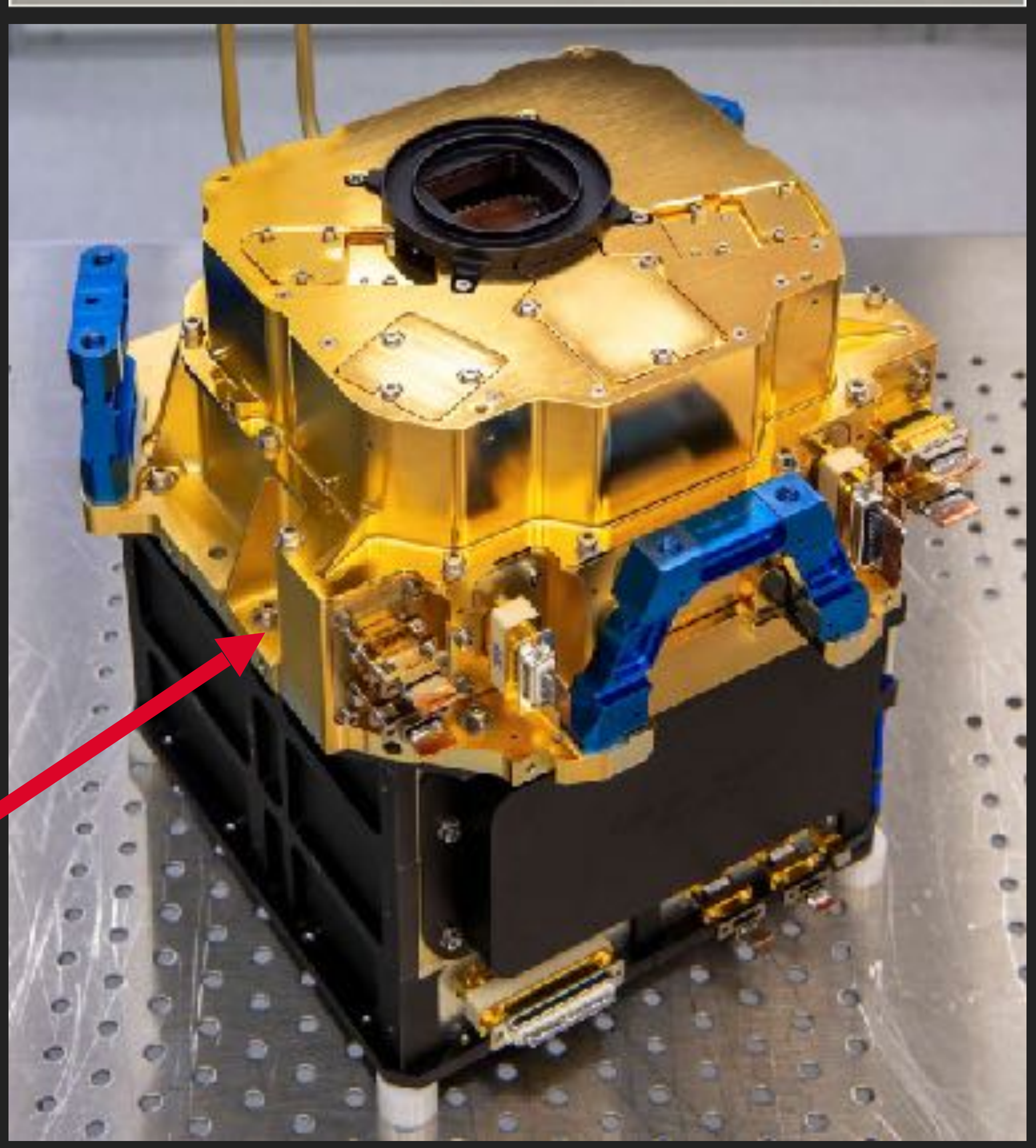

MXT Camera & FEE

cnes CENTRE NATIONAL D'ÉTUDES SPATIALES

cea irfu

MPE Max-Planck-Institut für extraterrestrische Physik

University of Leicester

Observatoire astronomique de Strasbourg

IJCLab Irène Joliot-Curie

EBERHARD KARLS UNIVERSITÄT TÜBINGEN

MXT Data Processing Unit(s): implement the MXT control and scientific OBSW

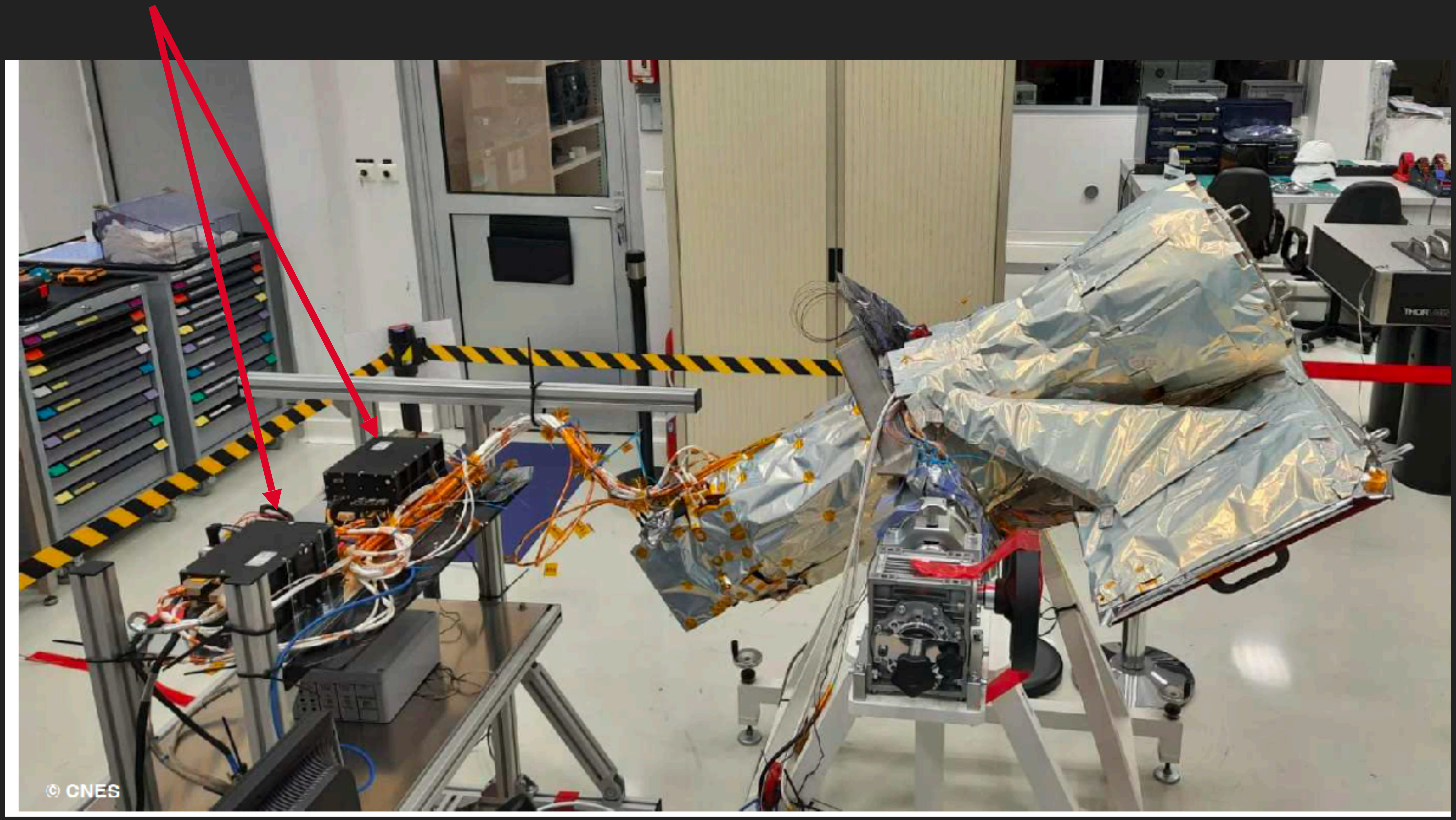


MXT Status - 2023/05/09

# MXT SENSITIVITY



- More information about the MXT performance can be found here
  - https://arxiv.org/abs/2211.13489

- Using the MXT effective area derived during on ground end-to-end testing at the MPE Panter facility, one can estimate the expected counts for an astrophysical source in the MXT

- For example, if we consider a Crab-like spectrum with a photon index $\Gamma$ =2.1, a normalization of 9 photons/cm$^2$/s/keV at 1 keV and an $N_H$ equivalent column density of $0.45\times10^{22}$ atoms/cm$^2$, we obtain an expected count rate of 121 cts/s in the MXT detector over the entire energy range in 1 ks.

- The 5$\sigma$ MXT sensitivity is hence
  - 1 mCrab in this case (1ks), 13 mCrab in 10 s, and 400 μCrab for a 10 ks observations.

- However, these values can are based on the simple comparison of the expected counts over the entire the detector and they do not consider the advantage of the imaging properties of the MXT, where> 50% of the counts are concentrated in the center of the PSF.
  - The latter is spread over an area of about 100×100 pixels$^2$, and the expected background within this area is about a 0.15 fraction of the one expected on the whole detector (~ 1 cts/ s).
  - Taking this into account, the final sensitivity value is improved by a factor 30%.

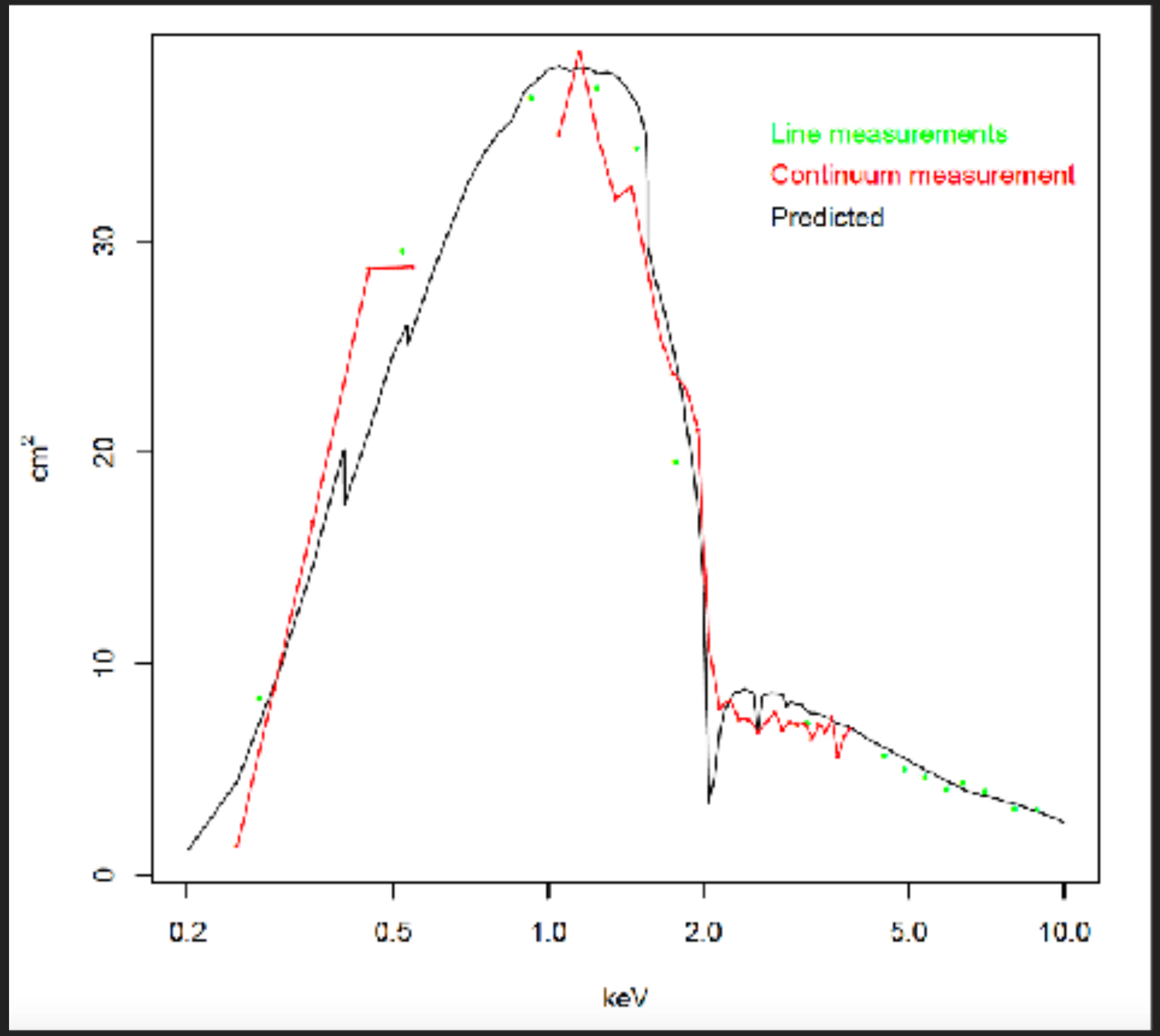


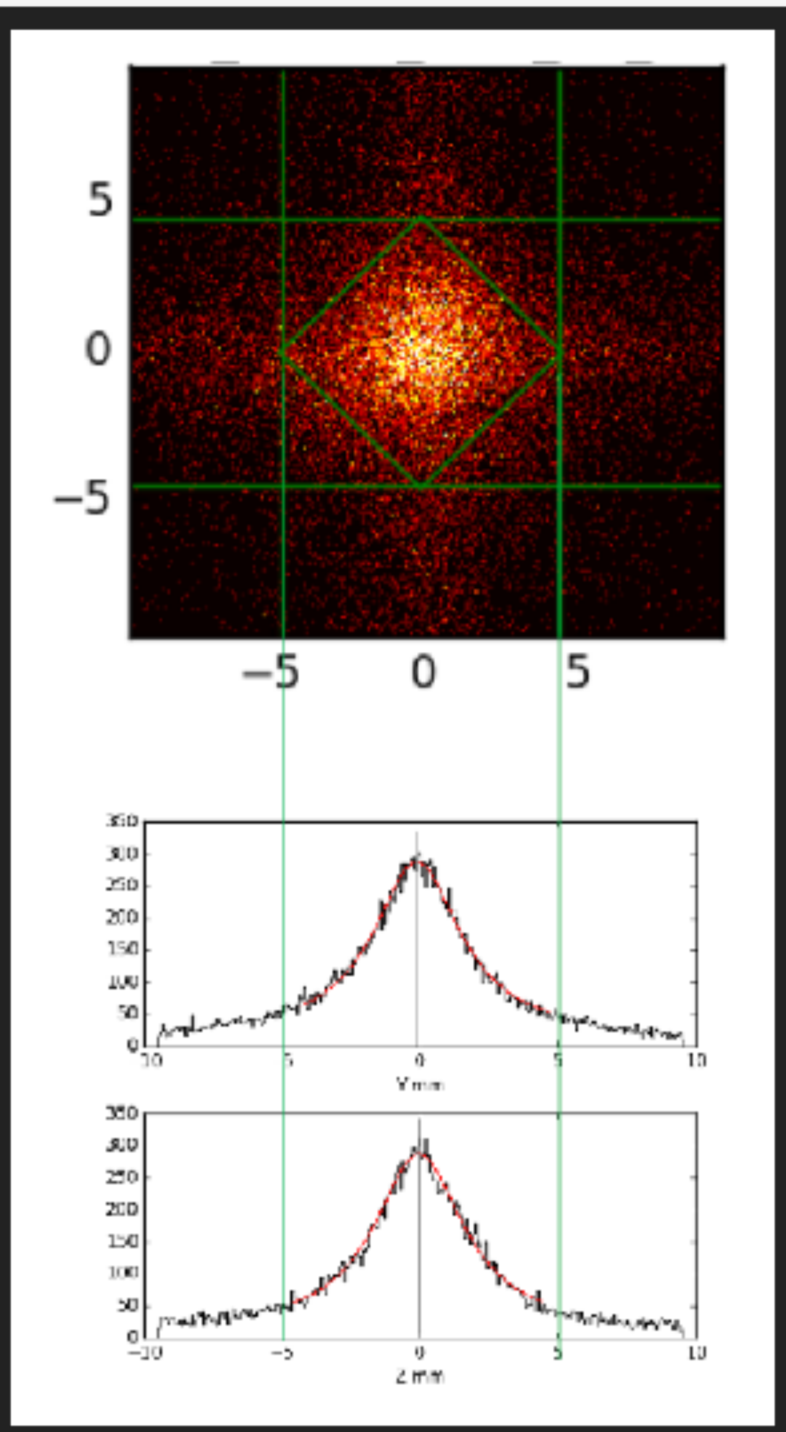

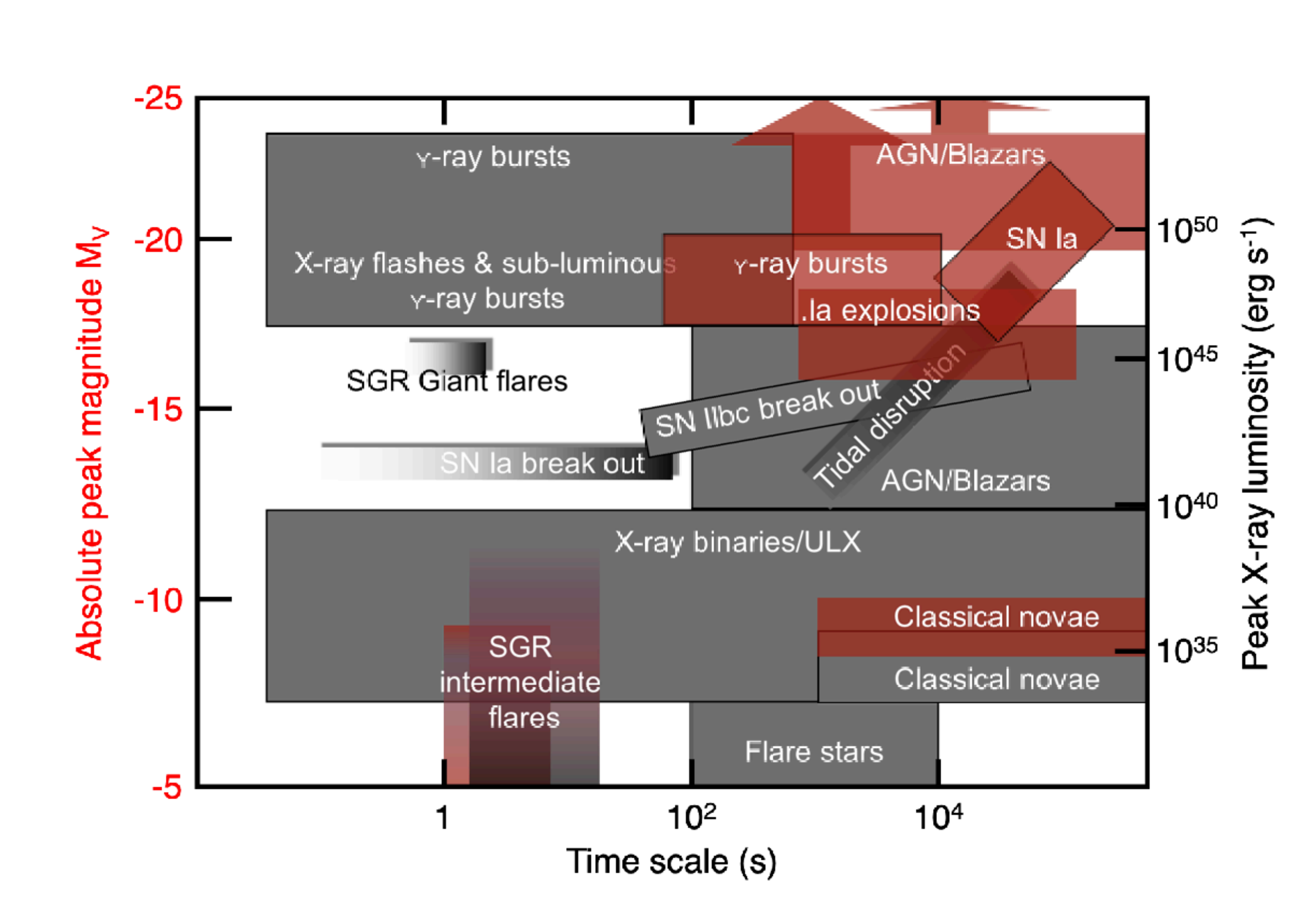
-25
-20
-15
-10
-5
Absolute peak magnitude M_V
γ-ray bursts
X-ray flashes & sub-luminous
γ-ray bursts
AGN/Blazars
SN Ia
γ-ray bursts
.Ia explosions
SGR Giant flares
SN IIbc break out
Tidal disruption
SN Ia break out
AGN/Blazars
X-ray binaries/ULX
Classical novae
SGR
intermediate
flares
Classical novae
Flare stars
1
10²
10⁴
Time scale (s)
10⁵⁰
10⁴⁵
10⁴⁰
10³⁵
Peak X-ray luminosity (erg s⁻¹)

- One of the main goals of MXT is to **significantly reduce the GRB error region** produced by ECLAIRs
  - The typical search regions will shrink from a ~10 arc min radius to a ~1-2 arc min radius, implying a 96-99% reduction in the sky area to search for optical telescopes
- In addition, being MXT a spectro-imager, it will provide spectra, images and light curves (minimum time resolution of 100 ms) built from the individual photon lists recorded on board. -> multi-wavelength light curves, SED, $N_H$ vs $A_V$

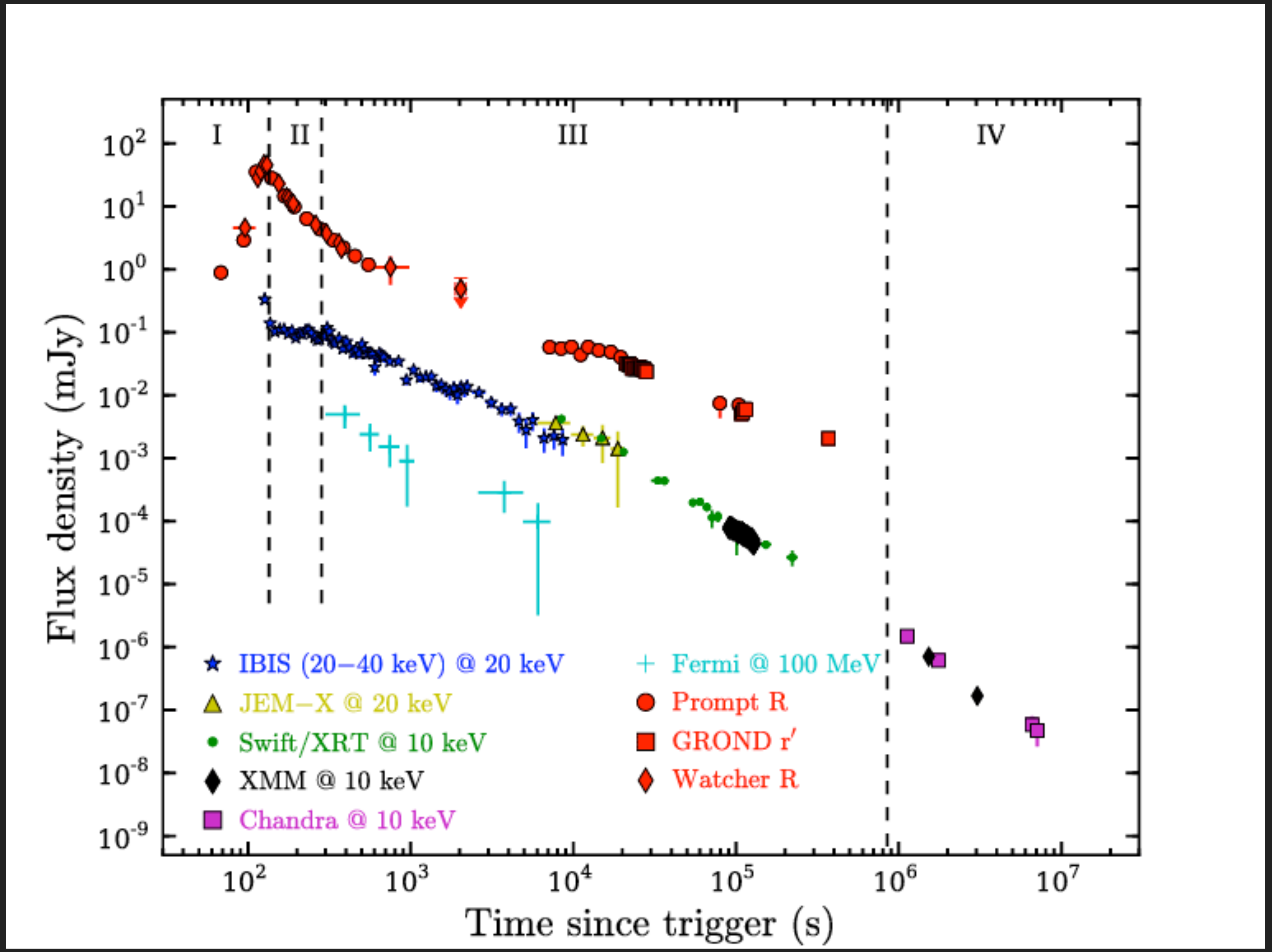


*GRB 121107A; Martin-Carrillo+14*

- Some of the GRB afterglow characteristics will be derived in (near) real-time by the MDPU on board
    - More specifically, after the satellite slew the MPDU will start to build an image accumulating the X-ray events, registered by the focal plane, on a first ~30 s long exposure.
    - This image is searched for significant excesses (up to three) and their coordinates and integrated fluxes are sent to ground through the VHF network.
    - This process is repeated every ~30 s in order to increase the statistics and improve the positional accuracy. 10 minutes after the observation start, the best MXT position is transmitted to the VT, which will use this information to adjust its observing window (see later)
- The FSC (SVOM French Science Centre) will process these messages, filter the derived positions against known X-ray sources, send the MXT positions to to scientific community (including SVOM GFTs) and built a « live » light curve of the afterglow using the integrated flux information

- SVOM will follow-up GW alerts provided by LIGO/Virgo/Kagra interferometers (see M. Branchesi lecture)
- Some models predict that in case of binary NS (BNS) mergers the optical kilonova may be associated to intense X-ray emission, in case the end product of the merger is a (transient) ms magnetar (see Clara Plasse's talk)
- Typical error regions for BNS merger can span tens to hundreds of square degrees on the sky (depending on the number of involved interferometers)
- Thanks to its wide FOV of about one square degree,svom GW error regions can be tiled efficiently especially it the tiles are biased against nearby galaxies
- Also in this case, X-ray sources are searched for on board at the end of each tile (5-10 minutes), and the results is sent to ground through the VHF network

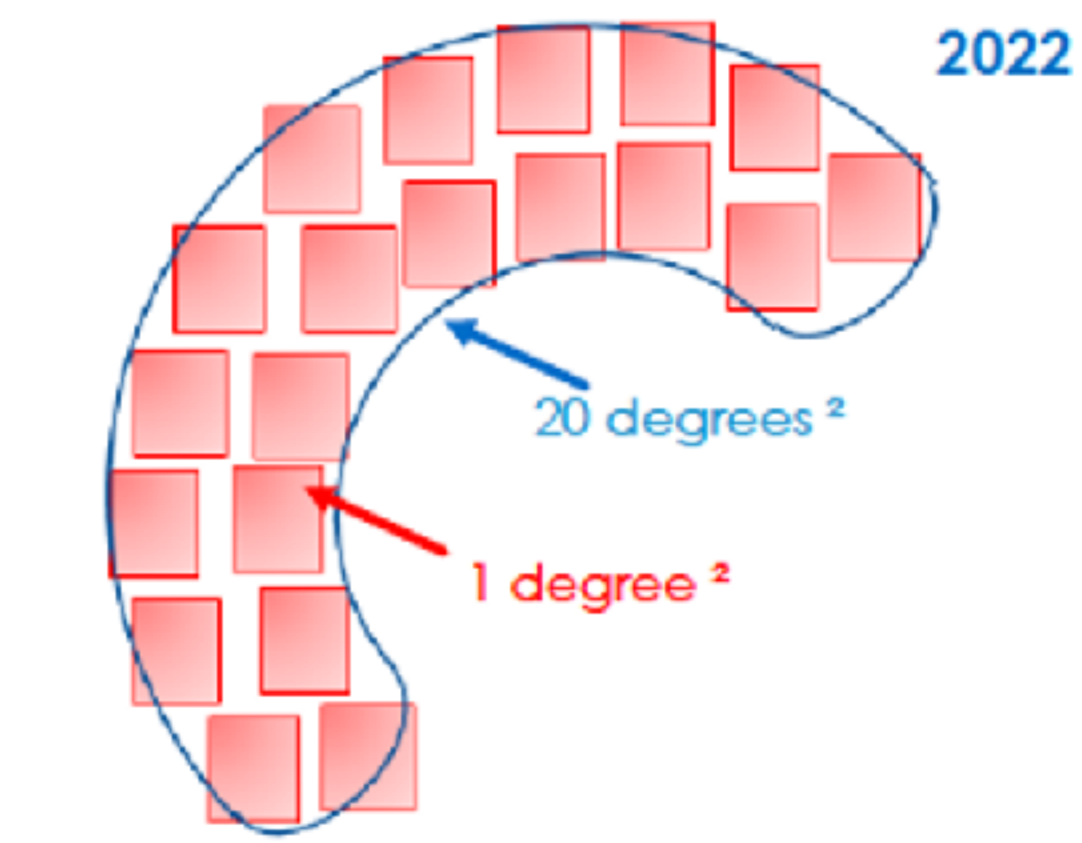


***Svom tiling strategy :***
Simulations :
5 observations / orbit of 500 sec for 4 orbits (~6h) = 20 tiles

# GRB FOLLOW-UP WITH THE VT

**S**pace
**V**ariable
**O**bject
**M**onitor



SPACE

ECLAIRS

MXT

VT

GRM

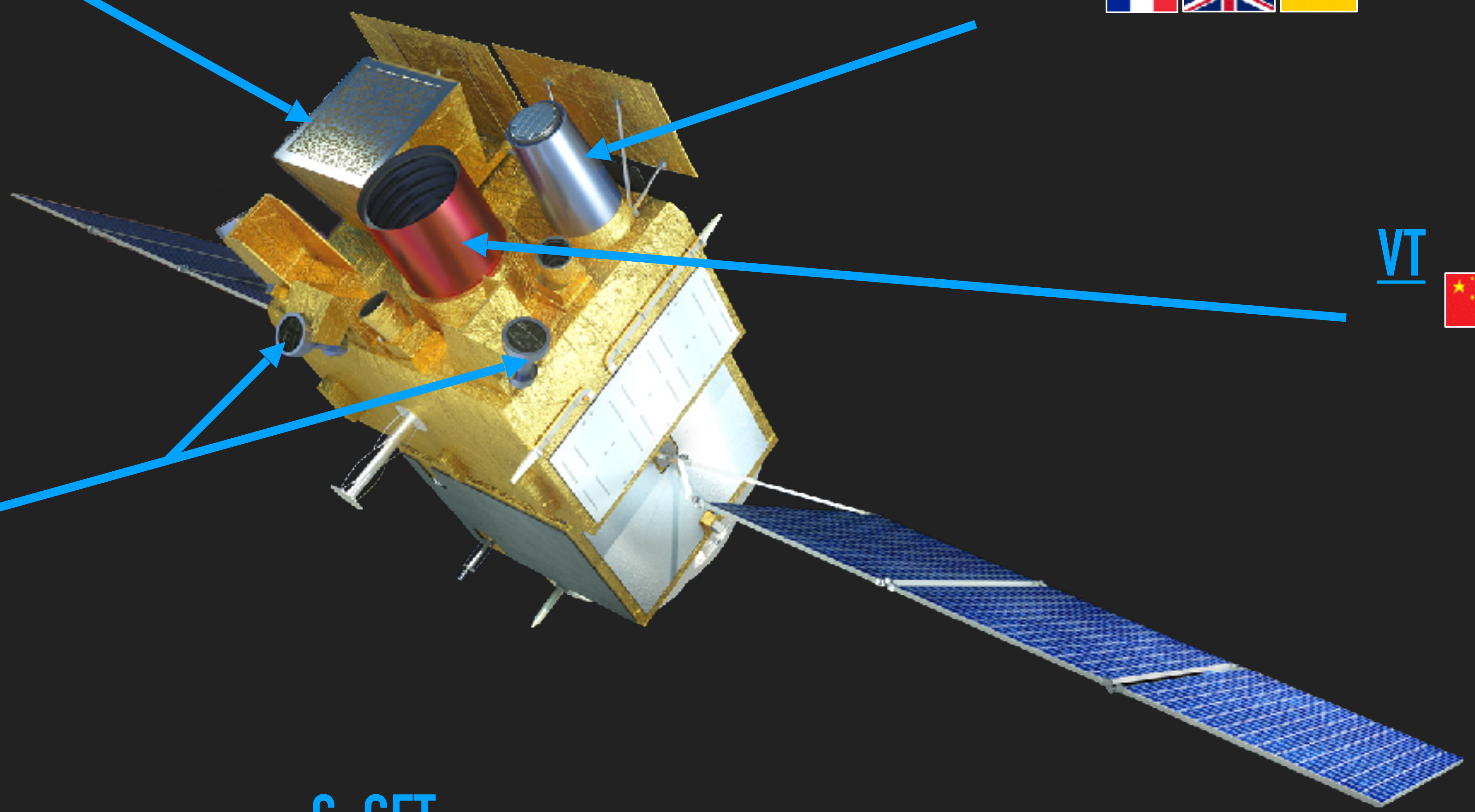

GROUND

GWAC

C-GFT

F-GFT (COLIBRI)

- **Rapidly identify** optical afterglow of GRBs detected by SVOM
- Provide **arc second localization** of candidate afterglow
- **Early optical/NIR information** (temporal evolution, extinguished GRBs, high redshift…)
- Crucial step to **allow for further ground-based follow-up** such as **spectroscopy** (for redshift)

- Ritchey-Chretien telescope
- Aperture: 440 mm
- Magnitude limit in V : ~22.5 after 300s
- Field of View : ~ 26′ x 26′
- RON: < 6e-/pix (rms) in 100s

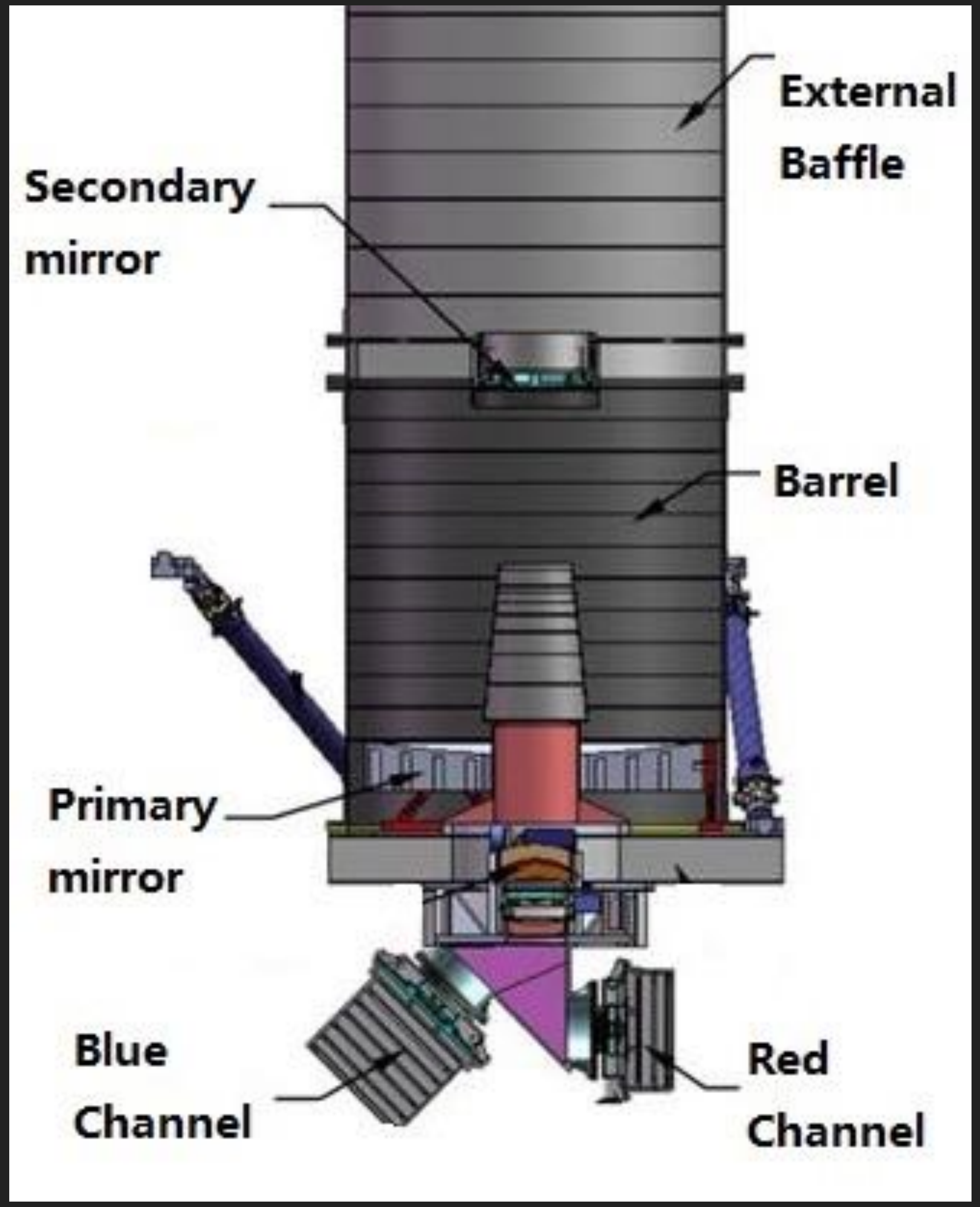

- Two **simultaneous** channels split by a dichroic:
  - Blue channel:
    - 4000 to 6500 Å
    - 2K×2K normal back-illuminated CCD detector
    - PSF: 2.9" (diameter of 80% energy)
  - Red channel:
    - 6500 Å to 1 μm
    - 2K×2K deep-depleted CCD detector for sensitivity at longer wavelengths
    - PSF: 1.9" (diameter of 70% energy)

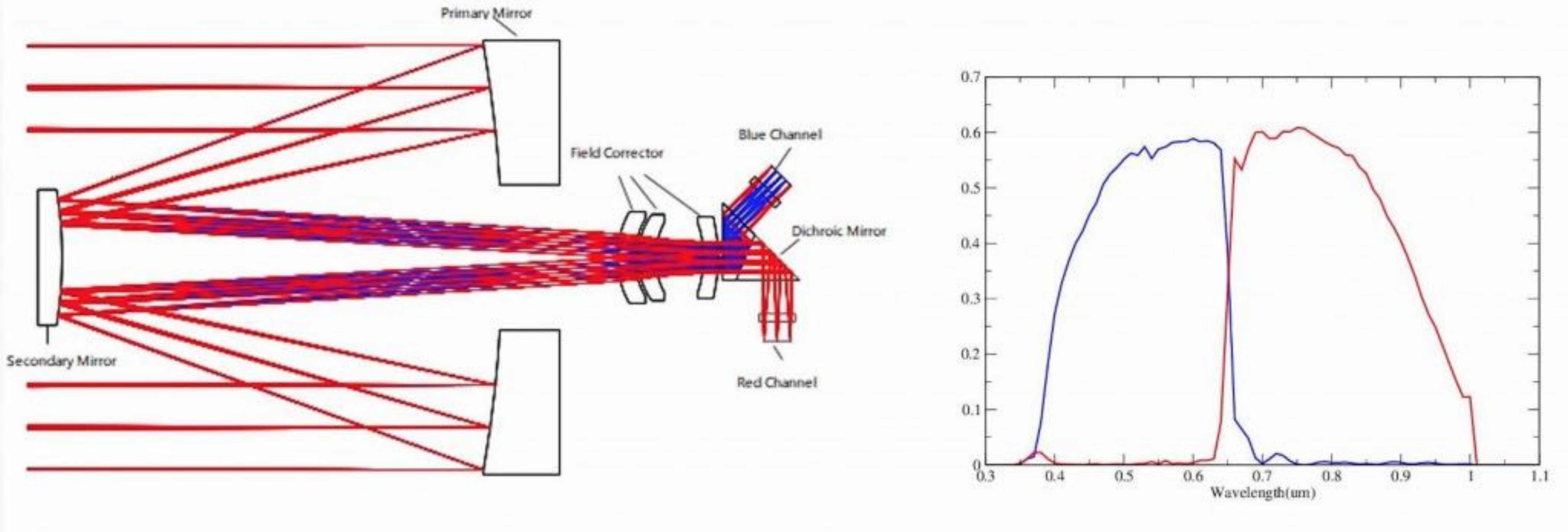

# VT DESIGN FOR GRBS

- **VT FoV** covers **ECLAIRs error region**

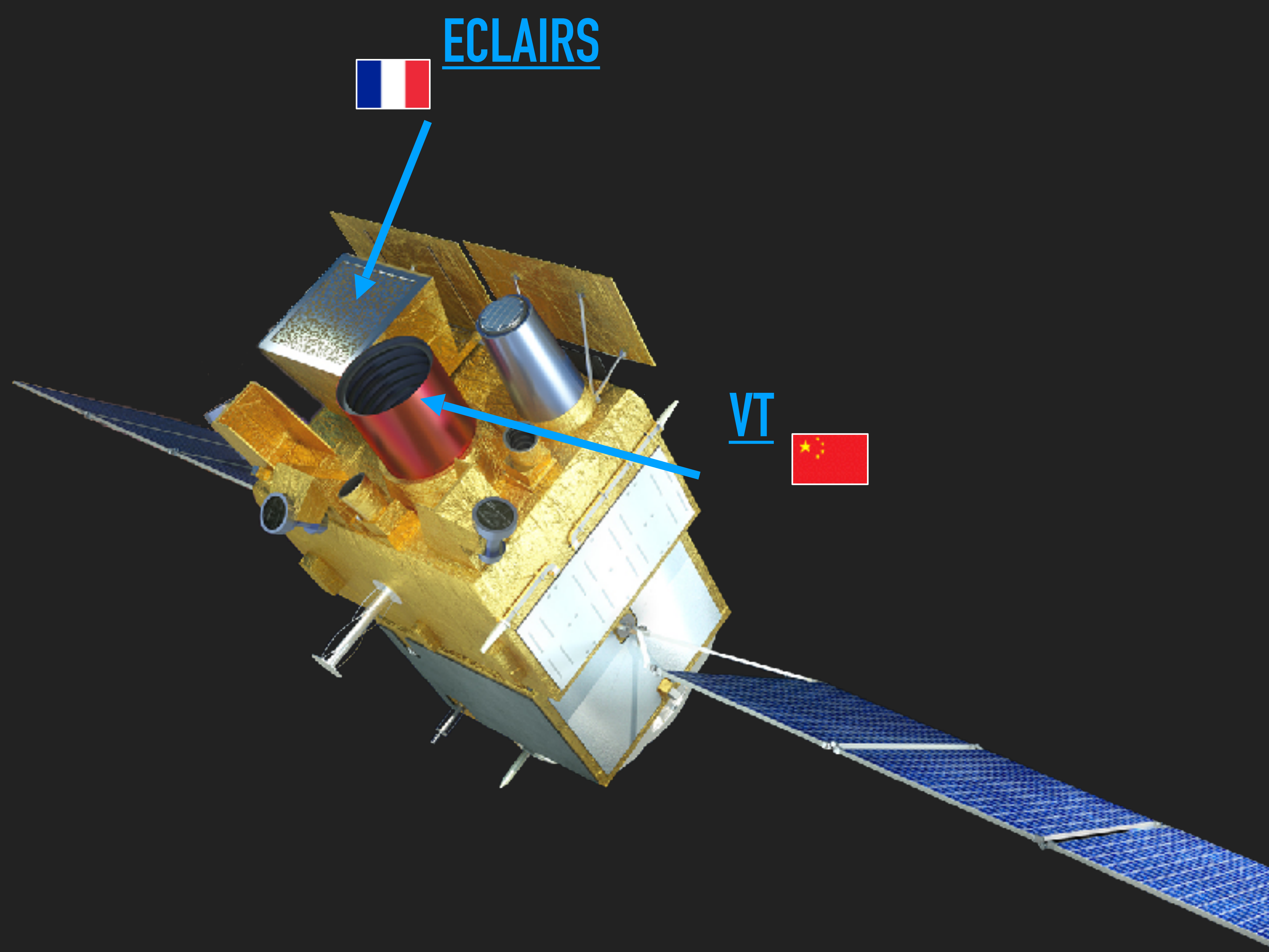

# VT DESIGN FOR GRBS

- **VT FoV** covers **ECLAIRs error region**
- VT **co-aligned** with MXT -> cross calibration for improved MXT accuracy

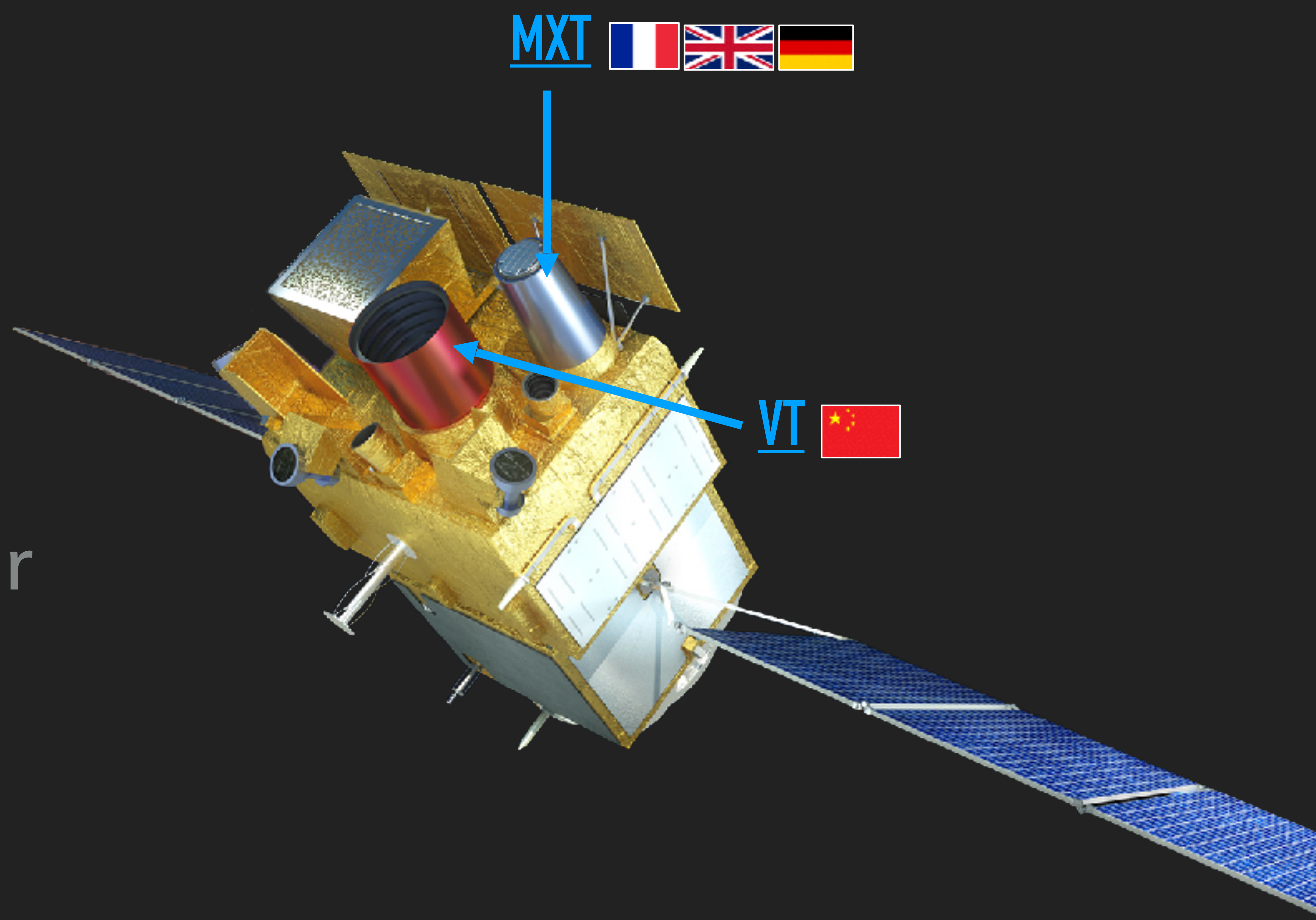

# VT DESIGN FOR GRBS

- **VT FoV** covers **ECLAIRs error region**
- VT **co-aligned** with MXT -> cross calibration for improved MXT accuracy
- Red and Blue channels for early hints of **high-z** or **dusty** GRBs
- Red channel extends to 1 µm for **high-z** GRBs

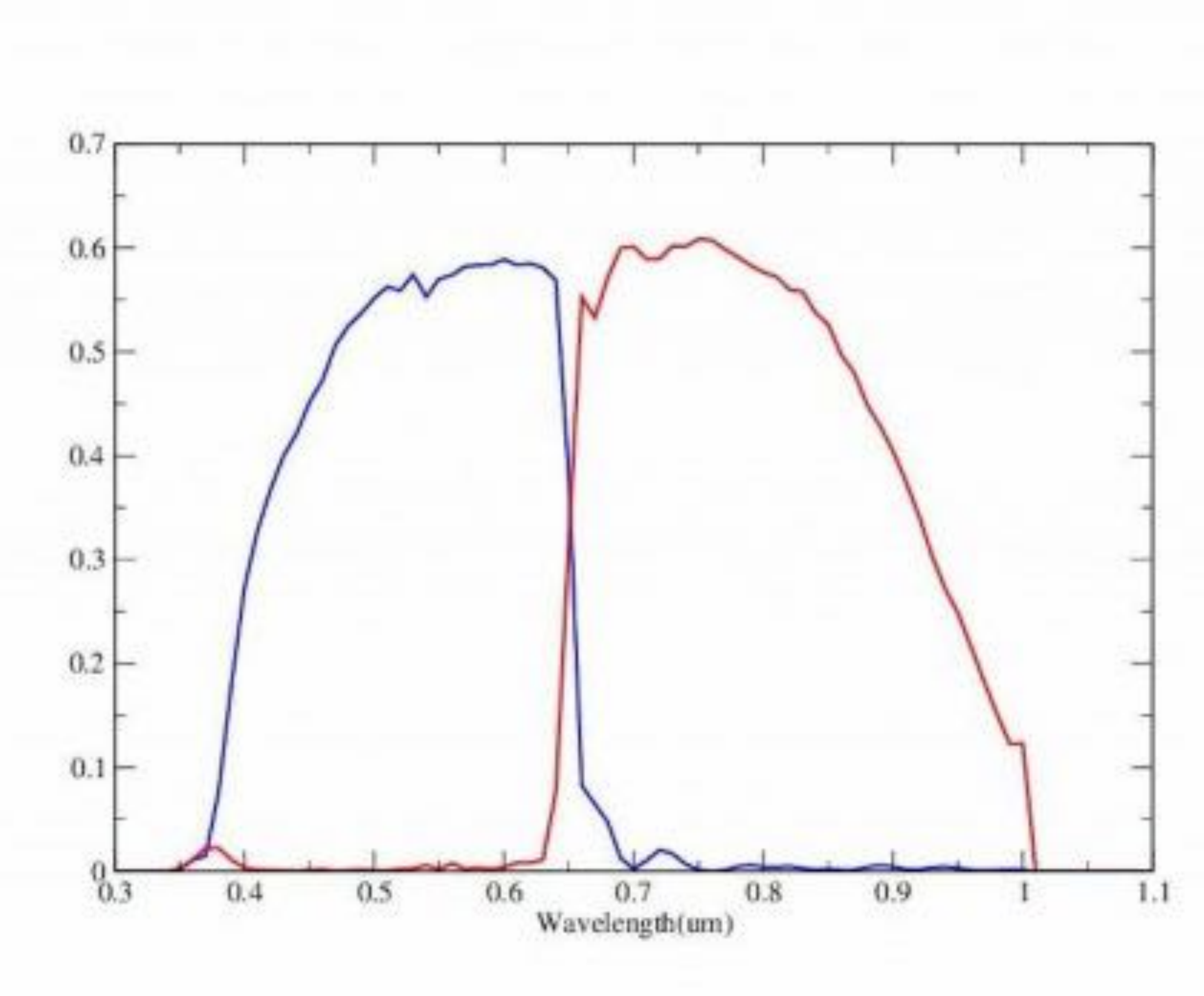

- **Core Program** (up to 4 sequences after a GRB detection):
  - 1st sequence: short **5 min** exposition (3 x 100s combined into one image)
  - 2nd-4th sequence: deeper **10 min** image
- Basic on-board processing on 6′ x 6′ arc min subimage, centered on MXT position if available
- Specific data is **downlinked** in near **real time** to Earth via **VHF network** (low bandwidth) and covered by Beidou redundancy in case of VHF failure
- VHF data include **1bit subimage** and **list of detected sources** which are processed immediately to disseminate information to wider community

- **Multiple modules** running in **real time** at French Science Center (FSC) which processes VT VHF data as it arrives

- Algorithm identifies afterglow candidates:
  - **New sources** not in catalogs
  - Existing sources having **varied**
  - Within/close to **MXT position**

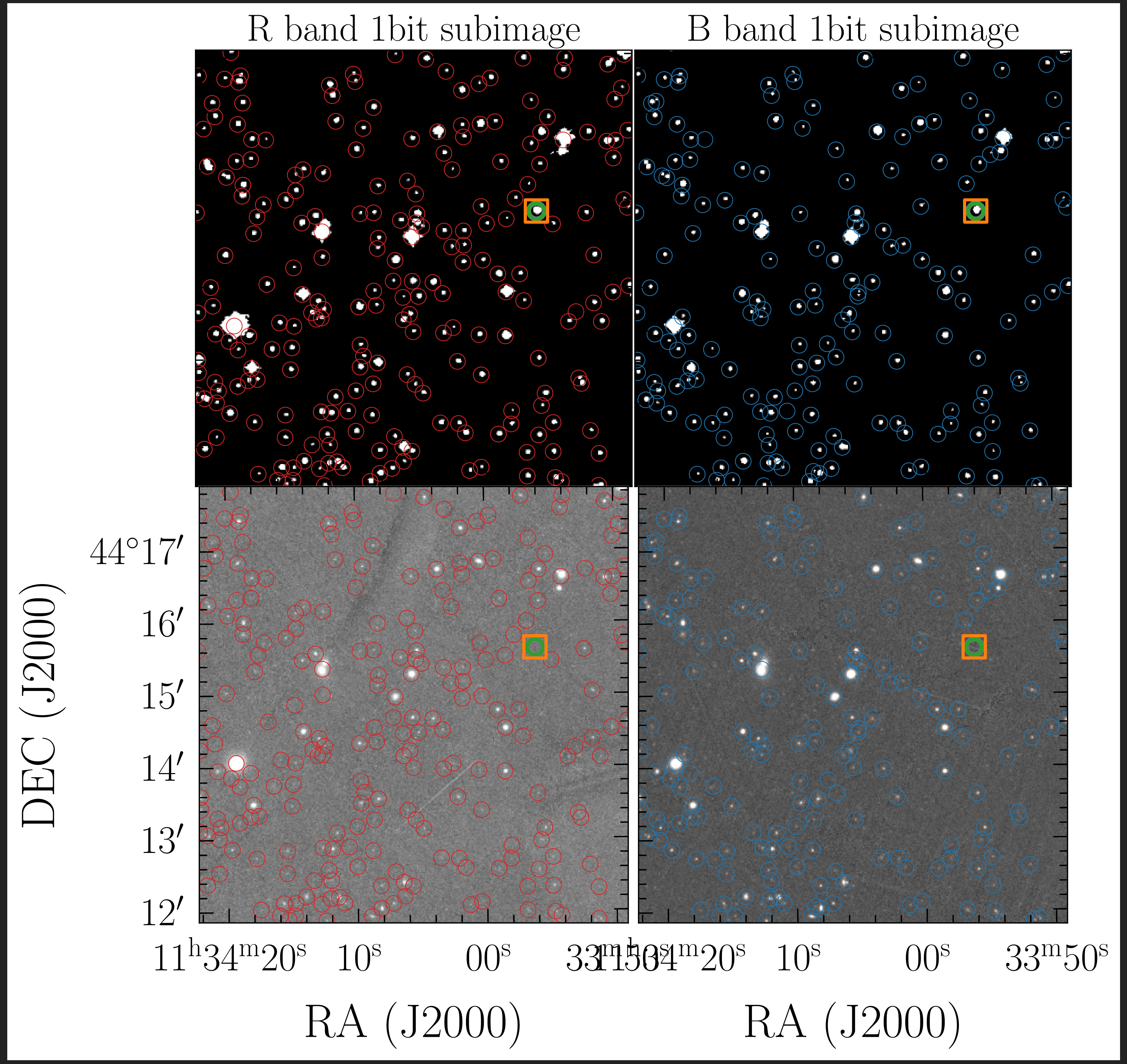

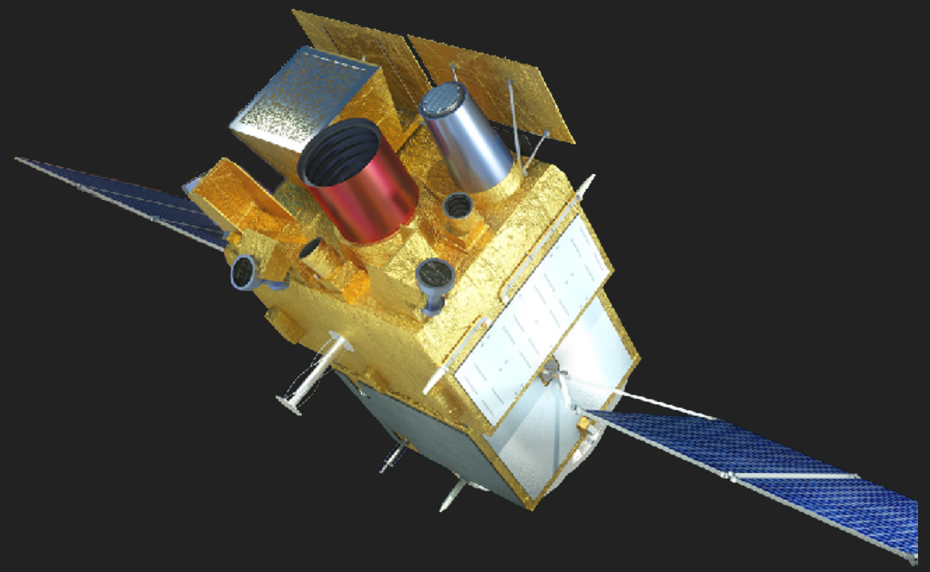

**S**pace
**V**ariable
**O**bject
**M**onitor

- VT is onboard Visible Telescope of SVOM
- It is key to get an early optical detection and localize the GRB afterglow enabling the use of GRBs as probes of the Universe
- Designed for optimal follow-up of GRBs detected by ECLAIRs, in particular high-z and dusty GRBs thanks to two bands, extending up to 1 micron
- Already integrated on flight model in Shanghai!

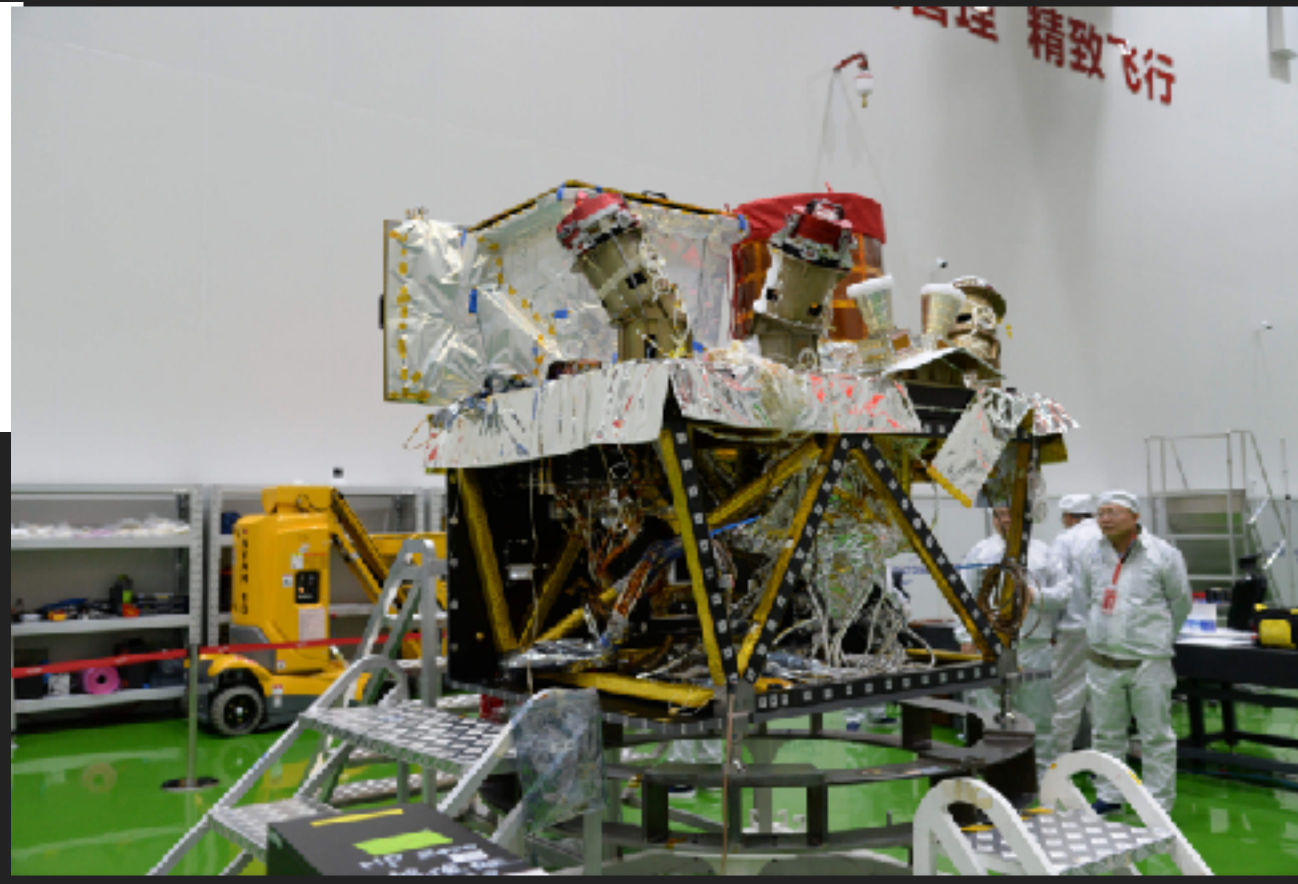

# CONCLUSIONS

- The rapid SVOM follow-up from space will provide a series of crucial information on GRBs (and other transients)
  - MXT will provide ~arcmin localization for the majority of SVOM GRBs largely enhancing the chances of identifying the counterpart at other wavelengths
    - It will also provide spectral and temporal X-ray characteristics for each GRB, enabling the study of GRB afterglows physical parameters
  - The VT is able pinpoint the GRBs at arcsec level, implying a potential rapid follow-up by large ground based telescopes (spectroscopy!)
    - It will also provide a first indication of the distance (moderately high redshift, if non-detection in the blue channel) or the environment (« dusty ») of the GRBs.

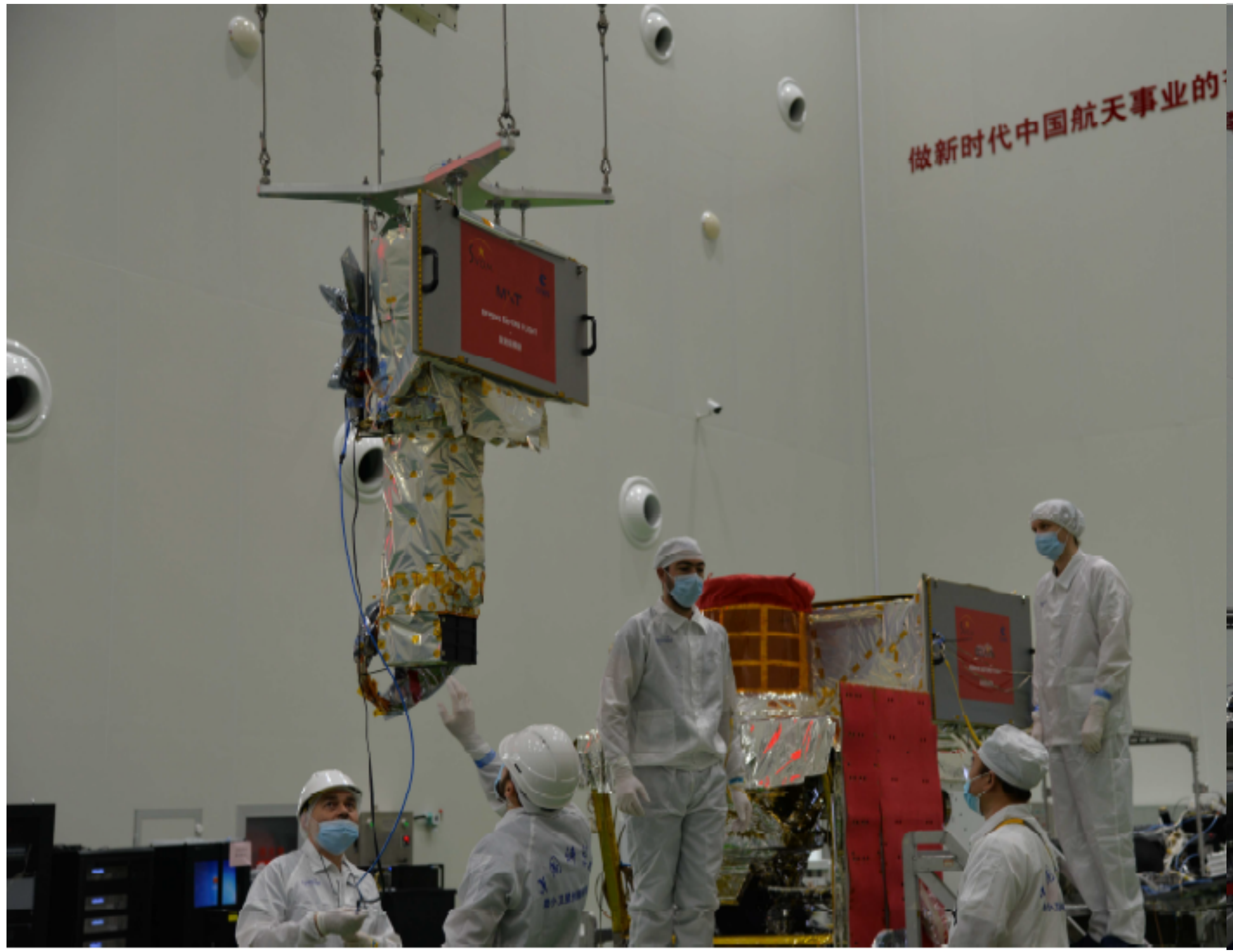


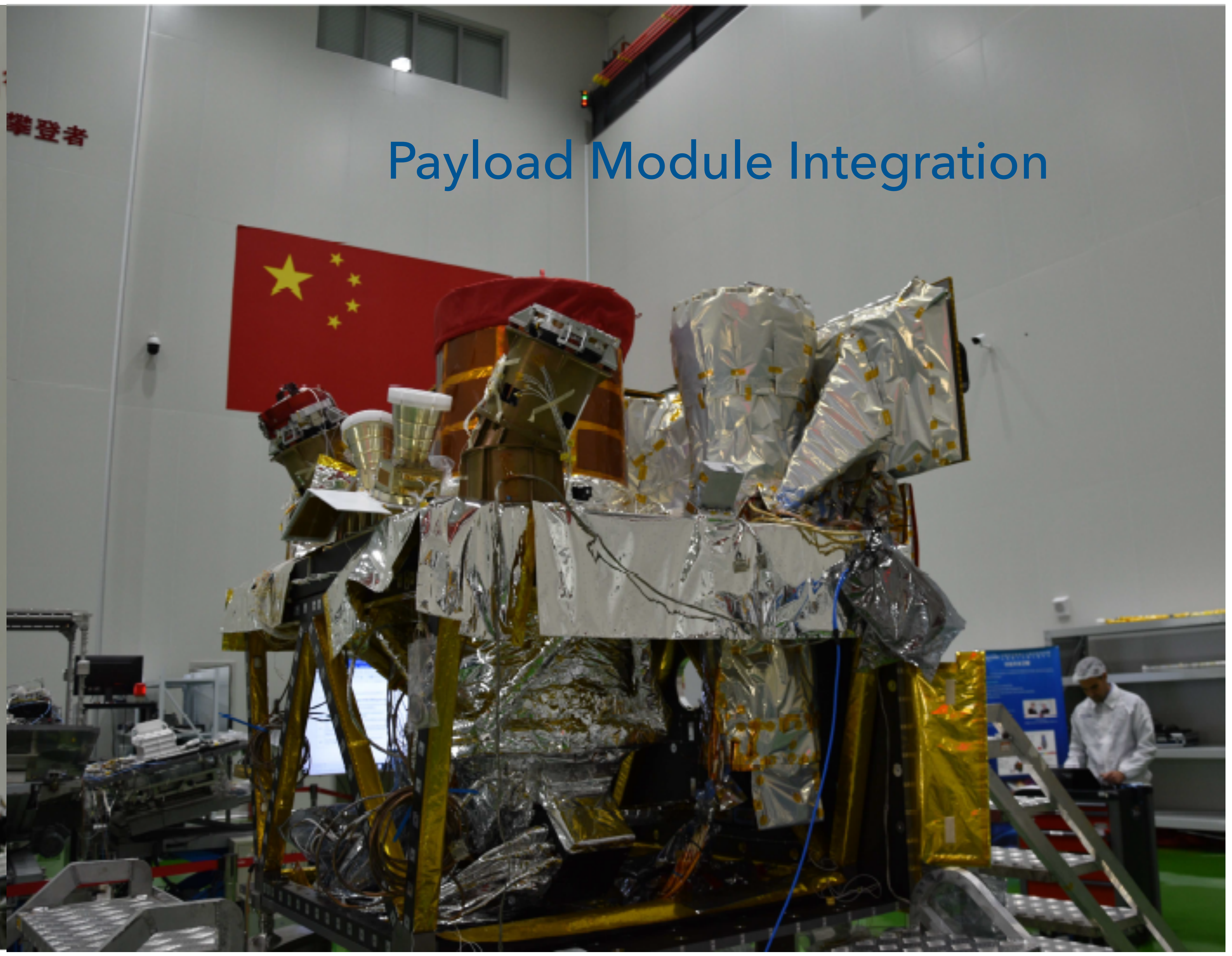


Payload Module Integration

Matching with the service module

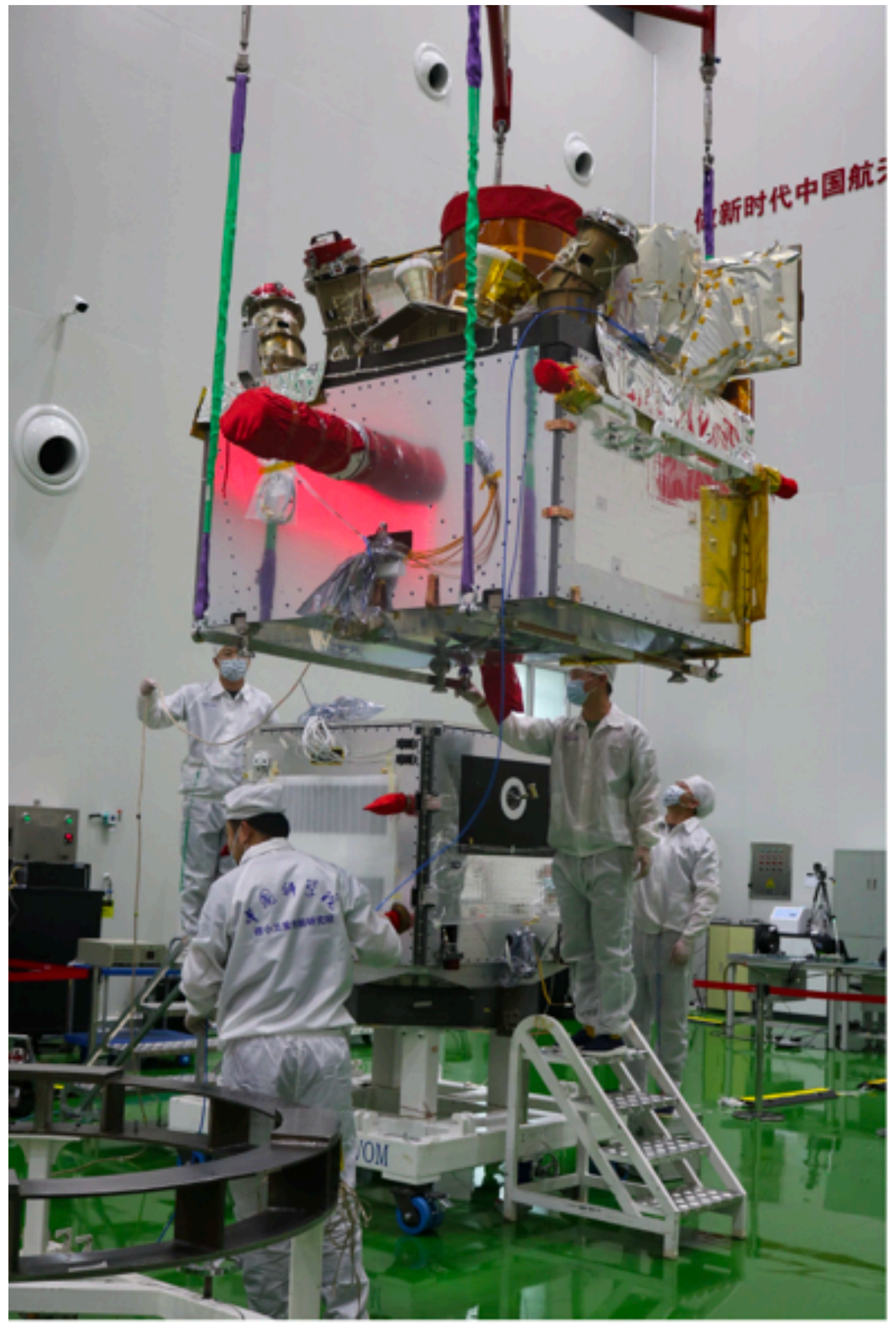

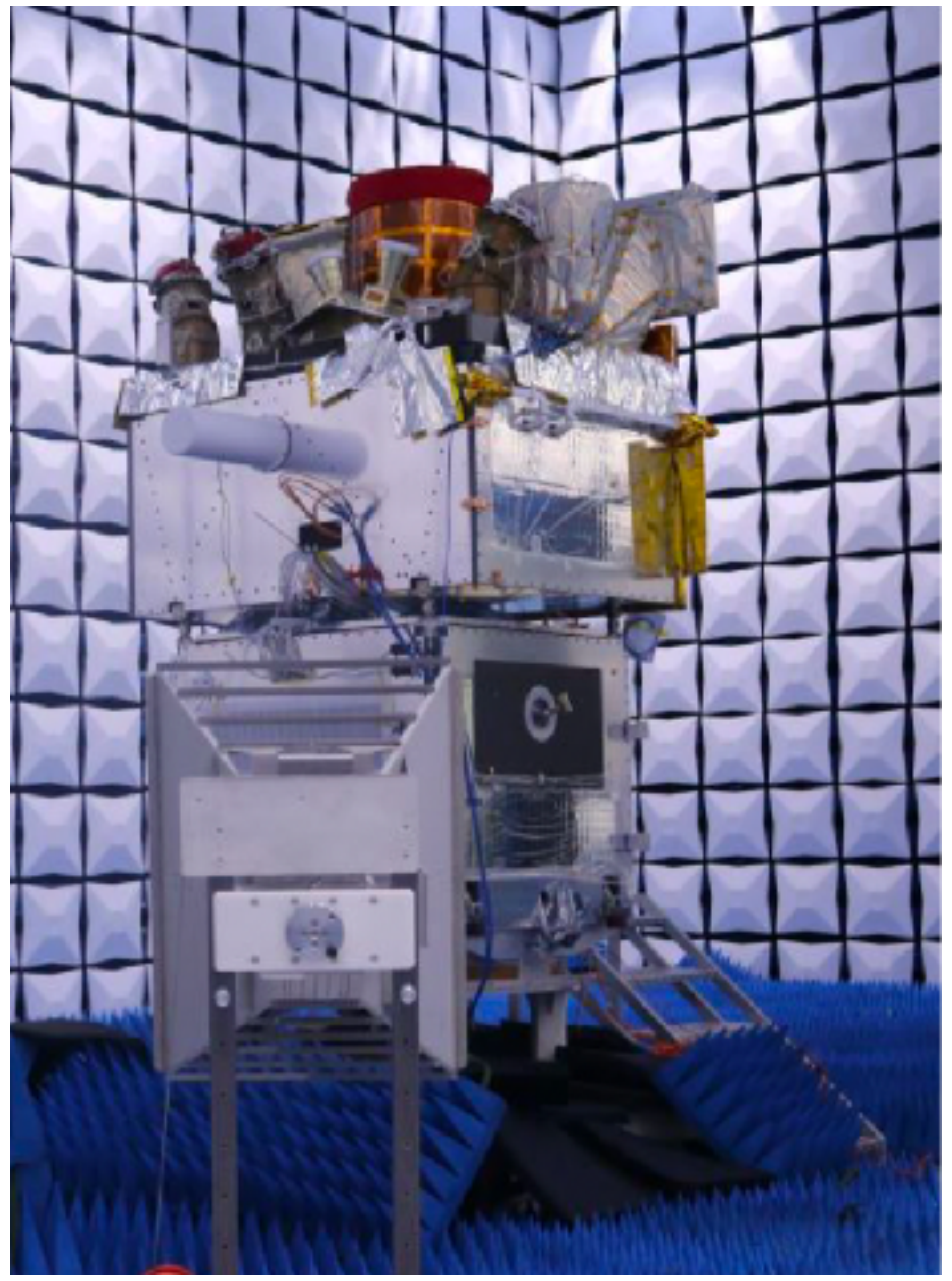

SVOM in the anechoic chamber for EMC tests